Schweizerische Eidgenossenschaft
Confédération suisse
Confederazione Svizzera
Confederaziun svizra

Federal Department of the Environment, Transport, Energy and Communications DETEC

Swiss Federal Office of Energy SFOE
Energy Research and Cleantech Division

Final report dated 31.03.2025

DEPLOI the HEAT - CH

DEmonstrate Production enhancement through LOw cost dIrectional steel shot drilling for district HEATing - CH

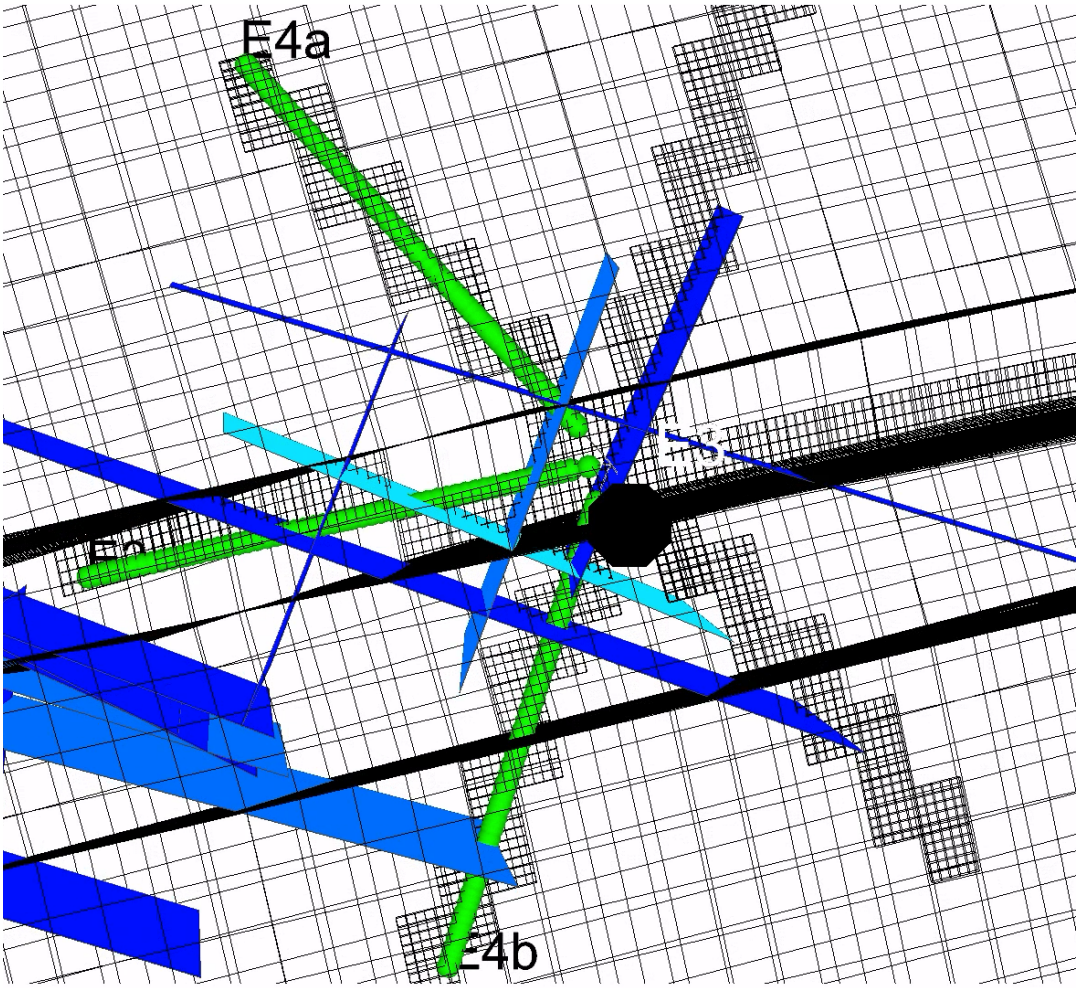

Zoom out of intersection of lateral wells (in green) with the fracture corridors (in blue)

Date: 31.03.2025

Location: Bern

Publisher:
Swiss Federal Office of Energy SFOE
Energy Research and Cleantech
CH-3003 Bern
www.bfe.admin.ch

Subsidy recipients:
ETH Zürich
Sonneggstrasse 5, 8092 Zurich
https://ethz.ch/en.html

VersuchsStollen Hagerbach AG (VSH)
Polistrasse 1, 8893 Flums Hochwiese
https://hagerbach.ch/

Services Industriels de Genève (SIG)
2, Château-Bloch – 1219 Le Lignon
https://ww2.sig-ge.ch/

Services industriels de Lausanne (SIL)
Place Chauderon 23, CP7416, 1002 Lausanne
https://www.lausanne.ch/vie-pratique/energies-et-eau/services-industriels.html

Grob Gemüse (GROB)
Bodenacker, 8255 Schlattingen
https://www.grob-gemuese.ch/

Authors:

Paromita Deb, ETH Zürich, paromita.deb@eaps.ethz.ch
Andreas Reinicke, TNO, andreas.reinicke@tno.nl
Jan Jette Blangé, Canopus Drilling B.V., jjblange@canopusdrillingsolutions.com
Morteza Esmaeilpour, ETH Zürich, morteza.esmaeilpour@eaps.ethz.ch
Dirk Alfermann, ETH Zürich, dalfermann@eaps.ethz.ch
Michel Meyer, michel.meyer@sig-ge.ch
Martin Saar, martin.saar@eaps.ethz.ch

SFOE project coordinators:
Men Wirz, Men.Wirz@bfe.admin.ch
Florence Bégué, Florence.Begue@bfe.admin.ch
Stefano Benato, Stefano.Benato@bfe.admin.ch

SFOE contract number: SI/502488-01
The authors bear the entire responsibility for the content of this report and for the conclusions drawn therefrom.

Zusammenfassung

Directional Steel Shot Drilling (DSSD), eine neuartige, von Canopus Drilling Solutions B.V. entwickelte Richtbohrtechnologie, bietet eine innovative Lösung zur Steigerung der Produktivität und Kosteneffizienz von Geothermiebohrungen. Die DSSD-Technologie ermöglicht den kosteneffizienten Bau von Multilateral-Bohrungen, um den Kontakt zum Reservoir zu erhöhen. Hierdurch können die Herausforderungen geringer Reservoirqualität minimiert werden, vor allem wenn diese auf größere Heterogenität und geringe Durchlässigkeit des Reservoirs zurückzuführen sind.

Die DSSD-Technologie kombiniert das konventionelle mechanische Bohren mit der erosiven Wirkung von Stahkugeln, die im Bohrmeissel beschleunigt werden. Die Wirkung der Stahlkugeln kann in Abhängigkeit von der Ausrichtung des Bohrmeißels gesteuert werden, wodurch ein neuartiges Richtbohrsystem entsteht, dass die Herstellung komplexer Bohrlochgeometrien vereinfacht.

Im Rahmen des EU-GEOTHERMICA-Projekts DEPLOI the HEAT wurde die DSSD-Technologie von Canopus umfangreichen Labortests unterzogen, ein Prototyp wurde gebaut und in einem Feldversuch in der Schweiz eingesetzt. Darüber hinaus wurde im Rahmen des Schweizer Beitrags zum GEOTHERMICA-Projekt eine Modellierungsstudie durchgeführt, um die Auswirkungen dieser Technologie auf geothermische Projekte mit mittlerer Tiefe in der Schweiz für Fernwärmeanwendungen zu bewerten.

Nachfolgend sind die wichtigsten Ergebnisse des Feldversuchs im VersuchsStollen Hagerbach aufgeführt:

1. Ein sicherer Betrieb (mit hohem Druck) konnte realisiert werden; weder Zwischenfälle noch Schäden sind aufgetreten.
2. Das DSSD-System wurde erfolgreich in den normalen Bohrbetrieb integriert.
3. Mit dem DSSD-System wurden zwei Horizontalbohrungen mit einer Länge von ~125 m erbohrt.
4. Mit der Stahlkugel-Bohrtechnik konnte eine ROP-Verbesserung um den Faktor 3 erzielt werden.
5. Tangentiale Abschnitte ohne Steuerung wurden mit minimaler Abweichung gebohrt. Die Abweichung lag innerhalb von 0,3deg/30m (DLS).
6. Insgesamt wurden vier beabsichtigte Richtungsänderungen durch Einsatz der Stahlkugel-Bohrtechnik mit einer DLS von 4-7 Grad/30m realisiert. Dies entspricht der maximalen Richtungsänderung, die die Steifigkeit des Bohrsystems zulässt.
7. Mit einer Spülungsrate von 600 l/min wurde eine ausreichende Bohrlochreinigung erzielt. Bei diesen Spülungsraten besteht die Gefahr von Auswaschungen, wenn der Bohrvortrieb unterbrochen wird, um Bohrgestänge hinzuzufügen.
8. Die Betriebsdrücke konnten für das gebohrte Gestein (Schiefer) auf 150-200 bar reduziert werden. Das System war für höhere Drücke bis zu 300 bar einsatzfähig.
9. Mit der Stahlkugelinjektionseinheit (SIU) konnte eine stabile Injektion realisiert werden. Die SIU erforderte einen Pulsationsdämpfer und einen Strömungsbypass, um voll funktionsfähig zu sein.
10. Die Richtbohrung arbeitete mit einer Stahlkugelkonzentration von 0,5 %, was der Kapazität der SIU entspricht. Für den nächsten Feldversuch mit einer 6-Zoll-Bohrung ist keine Aufrüstung der SIU erforderlich. In harten Gesteinen oder bei großer Tiefe wäre eine höhere Konzentration interessant, um die Bohrgeschwindigkeit und Lebensdauer des Meißels zu erhöhen.
11. Der Stellmotor, die Sensoren, die Kommunikation im Bohrloch und die Steuereinheit des Steuermoduls funktionierten wie gewünscht. Die Konzentrationsimpulse der Stahlkugeln im Bohrfluid entsprachen den Erwartungen. Allerdings muss der Verschleiß eines Kommunikationskabels im Bohrsystem in Zukunft verhindert werden.

12. Die elektromagnetische Telemetrie mit dem Bohrsystem von der Oberfläche aus funktionierte nicht aufgrund von unerwarteten elektromagnetischen Störungen. Für zukünftige Anwendungen sollte ein anderes Telemetriesystem eingesetzt werden. Für den geplante 6-Zoll-Feldversuch können Standard-Spülungsimpulssysteme integriert werden.Die numerische Modellierungsstudie verwendet einen prädiktiven Ansatz zur Modellierung des Lagerstättenverhaltens und zur Untersuchung der Produktivität und der wirtschaftlichen Machbarkeit des Einsatzes der DSSD-Technologie für mehrseitige Bohrungen in Karbonatlagerstätten mit mittlerer Tiefe (< 1500 m), die geklüftet sind. Das geologische Modell von Genf diente aufgrund der verfügbaren Daten als struktureller Rahmen für diese Studie. Der stochastische Ansatz, bei dem ein Ensemble von Bruchmodellen mit unterschiedlichen Parametern verwendet wird, die die Unsicherheit und Variabilität der Lagerstätteneigenschaften erfassen, gewährleistet jedoch, dass die Ergebnisse auch auf andere bruchdominierte Karbonatlagerstätten übertragbar sind. Die Studie konzentrierte sich auf die Formationen der Unterkreide (LC) und des Oberen Jura (UJ) im Genfer Becken und erstellte über 1.000 statische Reservoirmodelle und 1.200 dynamische Simulationen, um die Auswirkungen von DSSD-Multilateralen auf die Durchflussraten, die thermische Leistung und die wichtigsten wirtschaftlichen Kennzahlen, einschließlich der Wärmegestehungskosten (LCOH) und der spezifischen Kapitalkosten (SCC), zu bewerten.

Die Ergebnisse der Modellierungsstudie zeigen, dass im Oberjura (Malm) die Hinzufügung einer zweiten seitlichen Bohrung die Produktion um 45-50 % erhöht, während eine dritte seitliche Bohrung die Produktion fast verdoppelt (95-100 %). Die Anwendung von DSSD verbessert auch die Wirtschaftlichkeit, da die Wärmegestehungskosten (LCOH) im Vergleich zu konventionellen Methoden erheblich gesenkt werden, wobei die dreiseitige Konfiguration das günstigste Kosten-Nutzen-Verhältnis aufweist. Trotz eines Anstiegs der Kapitalkosten um 12 % bei der Bohrung mit einer einzigen Bohrung senkt der Einsatz von DSSD die Kosten für Oberflächenanlagen (SCC) und die LCOH um etwa 17 %. Im Vergleich zu konventionellen Bohrungen senkt DSSD die Bohrkosten um ~25 % bei einer einzelnen Lateralbohrung, ~37 % bei zwei Lateralen und ~44 % bei drei Lateralen. Diese Ergebnisse bestätigen, dass DSSD ein vielversprechender Ansatz zur Verbesserung der Leistung und der wirtschaftlichen Effizienz von geothermischen Bohrungen ist, insbesondere für direkte Wärmeversorgungssysteme im Genfer Becken.

Résumé

Le forage directionnel à la grenaille d'acier (DSSD), une nouvelle technologie de forage directionnel mise au point par Canopus Drilling Solutions B.V., offre une solution innovante pour améliorer la productivité et la rentabilité des forages géothermiques. La technologie DSSD permet la construction rentable de puits multilatéraux afin d'augmenter les surfaces de contact avec le réservoir et de surmonter ainsi les défis liés à la qualité de ce dernier, principalement en raison de son hétérogénéité et de sa faible perméabilité du réservoir.

La technologie DSSD combine l'action mécanique conventionnelle du forage avec l'action érosive des grenailles d'acier accélérées par la pression. L'action de la grenaille d'acier peut être contrôlée en fonction de l'orientation du trépan, ce qui permet d'obtenir un nouveau système de forage directionnel rotatif qui simplifie la création de géométries de forage complexes.

Dans le cadre du projet européen GEOTHERMICA DEPLOI the HEAT, la technologie DSSD de Canopus a fait l'objet d'essais approfondis en laboratoire et un prototype a été construit et déployé dans le cadre d'un essai de terrain pleinement opérationnel en Suisse.

En outre, une étude de modélisation a été réalisée dans le cadre de la contribution suisse au projet GEOTHERMICA afin d'évaluer l'impact de cette technologie sur les projets géothermiques de moyenne profondeur en Suisse pour les applications de chauffage urbain.

Voici les principaux résultats de l'essai sur le terrain à VersuchsStollen Hagerbach:

1. Des opérations sûres (à haute pression) ont pu être réalisées, sans incident ni dommage.
2. Le système DSSD a été intégré avec succès dans les opérations de forage standard.
3. Deux puits horizontaux ont été forés avec le système DSSD, chacun d'une longueur de 125 mètres.
4. Une amélioration du ROP d'un facteur 3 a pu être réalisée grâce à l’impact des billes d'acier.
5. Des sections tangentes sans direction ont été forées avec une déviation minimale par rapport à la trajectoire droite ; DLS dans les 0,3deg/30m.
6. Quatre virages intentionnels au total avec une DLS de 4-7 deg/30m ont été réalisés en faisant circuler de la grenaille d'acier, ce qui est cohérent avec la rigidité de l'assemblage de forage.
7. Le nettoyage du trou a été suffisant à 600 l/min, alors que ces débits présentent un risque d'érosion lorsque la progression se fait en position penchée pour effectuer des raccordements ou pendant les mouvements de va-et-vient.
8. Les pressions de fonctionnement ont pu être réduites à 150-200 bars pour le type de roche forée (ardoise). Le système était opérationnel pour des pressions plus élevées, jusqu'à 300 bars.
9. Une injection stable avec l'unité d'injection de grenaille d'acier (SIU) a pu être réalisée. Le SIU a nécessité un amortisseur de pulsations et un by-pass de débit pour être pleinement opérationnel.
10. Le forage directionnel a fonctionné à une concentration de grenaille d'acier de 0,5 %, ce qui correspond à la capacité d'injection de l'unité d'injection de grenaille d'acier existante. Aucune amélioration du SIU n'est nécessaire pour l'essai de forage de 6 pouces prévu. Dans les formations de roches dures ou à grande profondeur, une concentration plus élevée serait intéressante pour augmenter le taux de pénétration et la longévité du trépan.
11. L'actionneur, les capteurs, la communication en fond de trou et l'unité de commande du module de pilotage ont fonctionné comme prévu. Le module d'orientation a créé des impulsions de concentration et la manipulation des solides s'est déroulée comme prévu. Toutefois, l'usure d'un câble de communication devra être évitée à l'avenir.
12. La télémétrie électromagnétique avec l'assemblage de fond de puits depuis la surface n'était pas opérationnelle en raison d'un bruit inattendu. Pour les applications futures, un système de

télémétrie différent devrait être utilisé.L'étude de modélisation numérique utilise une approche prédictive pour modéliser le comportement du réservoir et étudier la productivité et la faisabilité économique de l'utilisation de la technologie DSSD pour le forage de puits multilatéraux dans des réservoirs carbonatés fracturés de moyenne profondeur (<1500 m). Le modèle géologique genevois a servi de cadre structurel à cette étude en raison des données disponibles. Cependant, l'approche stochastique, qui utilise un ensemble de modèles de fractures avec des paramètres variables qui saisissent l'incertitude et la variabilité des propriétés du réservoir, garantit que les résultats sont applicables à d'autres réservoirs carbonatés dominés par des fractures. En se concentrant sur les formations du Crétacé inférieur (LC) et du Jurassique supérieur (UJ) dans le bassin de Genève, l'étude a généré plus de 1 000 modèles statiques de réservoirs et 1 200 simulations dynamiques pour évaluer l'impact des multilatérales DSSD sur les débits, la production thermique et les mesures économiques clés, y compris le coût de la chaleur nivelé (LCOH) et les coûts d'investissement spécifiques (SCC).

Les résultats de l'étude de modélisation indiquent que dans le Jurassique supérieur (Malm), l'ajout d'un deuxième puits latéral pourrait augmenter la productivité de 45 à 50 %, tandis qu'un troisième puits latéral doublerait pratiquement la production (95 à 100 %). L'application de la DSSD améliore également la viabilité économique en réduisant de manière significative le coût de la chaleur (LCOH) par rapport aux méthodes conventionnelles, la configuration à trois latéraux offrant le rapport coût-bénéfice le plus favorable. Malgré une augmentation de 12 % des coûts d'investissement pour le forage d'un seul latéral, l'utilisation du DSSD réduit les coûts des installations de surface (SCC) et le LCOH d'environ 17 %. Par rapport au forage conventionnel, la DSSD réduit les coûts de forage d'environ 25 % pour les latéraux simples, d'environ 37 % pour les latéraux doubles et d'environ 44 % pour les latéraux triples. Ces résultats confirment que le DSSD est une approche prometteuse pour améliorer la performance et l'efficacité économique des puits géothermiques, en particulier pour les systèmes d'approvisionnement direct en chaleur dans le bassin genevois.

Summary

Directional Steel Shot Drilling (DSSD), a novel directional drilling technology developed by Canopus Drilling Solutions B.V., offers an innovative solution to enhance the productivity and cost-effectiveness of geothermal drilling. The DSSD technology allows for the cost-effective construction of multilateral wells to increase the reservoir contact, thereby overcoming challenges of reservoir quality, primarily due to heterogeneity and low permeability of the reservoir.

The DSSD technology combines conventional mechanical drilling action with the erosive action of pressure accelerated steel shots. The steel shot action can be controlled with respect to the orientation of the drilling bit resulting in a novel rotating directional drilling system that simplifies the creation of complex borehole geometries. As part of the EU GEOTHERMICA project DEPLOI the HEAT, Canopus' DSSD technology underwent extensive lab testing and a prototype has been constructed and deployed in a full operational field trial in Switzerland. Additionally, a modeling study was conducted as part of the Swiss contribution to the GEOTHERMICA project to assess the impact of this technology on medium-depth geothermal projects in Switzerland for district heating applications.

Below are the key results of the field trial in VersuchsStollen Hagerbach:

1. Safe operations (with high pressure) could be realized, no incidents, no damage.
2. Integration DSSD system was successfully integrated in standard drilling operations.
3. Two horizontal wellbores have been drilled with the DSSD system, each 125 m long.
4. ROP enhancement of factor 3 could be realized with steel shots.
5. Tangent sections without steering have been drilled with minimum deviation from the straight trajectory; DLS within 0.3deg/30m.
6. Four intended turns in total with DLS of 4-7 deg/30m have been realized while circulating steel shot, consistent with stiffness of the drilling assembly.
7. Hole cleaning was sufficient at 600 l/min while these flow rates pose a risk of wash-outs when progression is stooped for making connections or while reciprocating.
8. operating pressures could be reduced to 150-200 bar range for the drilled rock type (slate). System was operational for higher pressures up to 300bar.
9. Stable injection with the steel shot injection unit (SIU) could be realized. The SIU required a pulsation dampener and a flow by-pass to be fully functional.
10. The directional drilling action worked at a steel shot concentration of 0.5%, which is the injection capacity of the existing SIU. No SIU upgrade is required for the planned for 6 inch wellbore trial. In hard rock formations or at large depth, a higher concentration would be attractive for increasing the rate of penetration and the bit longevity.
11. The actuator, sensors, down hole communication, and control unit of the steering module worked as desired. The steering sub created concentration pulses and the solids handling was as expected. However, the wear on a communication cable must be prevented in future.
12. The electro-magnetic telemetry with the downhole assembly from surface wasn't operational due to unexpected noise. For future application a different telemetry system should be deployed. For 6 inch applications standard mud-pulse systems can be integrated.

The numerical modeling study utilizes a predictive approach to model reservoir behavior and investigate the productivity and economic feasibility of using the DSSD technology for drilling multi-lateral wells in medium-depth (<1500 m) fractured carbonate reservoirs. The Geneva geological model served as the structural framework for this study due to its available data. However, the stochastic approach, utilizing an ensemble of fracture models with varying parameters that captures the uncertainty and variability in reservoir properties, ensures that the findings are applicable to other fracture-dominated carbonate

reservoirs. Focusing on the Lower Cretaceous (LC) and Upper Jurassic (UJ) formations in the Geneva Basin, the study generated over 1,000 static reservoir models and 1,200 dynamic simulations to evaluate the impact of DSSD multi-laterals on flow rates, thermal output, and key economic metrics, including Levelized Cost of Heat (LCOH) and Specific Capital Costs (SCC).

Results from the modeling study indicate that in the Upper Jurassic (Malm), the addition of a second lateral well increases production by 45-50%, while a third lateral well nearly doubles production (95-100%). The application of DSSD also improves economic viability by significantly reducing the Levelized Cost of Heat (LCOH) compared to conventional methods, with the three-lateral configuration providing the most favorable cost-benefit ratio. Despite a 12% increase in capital costs for drilling with a single lateral, the use of DSSD reduces surface facility costs (SCC) and LCOH by approximately 17%. Compared to conventional drilling, DSSD lowers drilling costs by ~25% for single laterals, ~37% for dual laterals, and ~44% for three laterals. These findings confirm that DSSD is a promising approach for enhancing the performance and economic efficiency of geothermal wells, particularly for direct heat supply systems in the Geneva Basin.

Contents

List of figures

Abbreviations

Abbreviation	Organization
ETHZ	Eidgenössische Technische Hochschule Zürich
GEG	Geothermal Energy and Geofluids (group)
GROB	Grob Gemüse
RCSG	Rijswijk Centre for Sustainable Geo-energy
SIG	Services Industriels de Genève
SIL	Services Industriels de Lausanne
TNO	Nederlandse Organisatie voor Toegepast Natuurwetenschappelijk Onderzoek
VSH	VersuchsStollen Hagerbach

Abbreviation	Name
ABI	Acoustic Borehole Imager
BHA	Bottom Hole Assembly
CAL	Caliper
CMG	Computer Modeling Group
EM	Electro-Magnetic
FAT	Factory Acceptance Test
DDP	Detailed Drilling Plan
DFM	Discrete Fracture Model
DM	Directional Module
DP-DK	Dual Porosity - Dual Permeability
DPM	Dual Porosity Model
DSSD	Directional Steel Shot Drilling
DWOP	Drilling Well On Paper

OBI	Optical Borehole Imager
PDC	Polycrystalline Diamond Cutter
PIF	Productivity Improvement Factor
SIU	Steel shot Injection Unit
RSS	Rotary Steerable System
TANGO	Techno-economic Analysis of Geo-energy Operations

Abbreviation	**Parameter**	**Unit**
DLS	DogLeg Severity	[deg/30m]
kh	horizontal permeability	m^2
kv	vertical permeability	m^2
ROP	Rate Of Penetration	[m/h]
WOB	Weight On Bit	[kdaN]
RPM	Rotation Per Minute	[1/min]

0 Executive summary

Derived from the earth's natural heat, geothermal energy is a reliable, sustainable and baseload energy source, which can play a critical role towards achieving a net-zero future. Yet, geothermal energy accounts for less than 1 % of the total renewable-based installed energy generation capacity worldwide (IRENA, 2023). One of the major factors hindering its development is related to the large capital costs involved in drilling into the uncertain subsurface structures and reservoir fluid conditions. Drilling can account for up to 50 % - 75 % of total geothermal project costs (Tester, 2006; Petty et al., 2009). Hence, technological development for drilling cheaper and efficient geothermal wells is one of the major research questions, which is actively investigated in both industry and academic sectors. Within the framework of the project DEPLOI the HEAT-CH, a novel drilling technology - Directional Steel Shot Drilling (DSSD) is investigated by performing field trials and numerical studies. DEPLOI the HEAT stands for DEmonstrate Production enhancement with LOw cost sIde-track drilling for HEAT production. The technology is developed by Canopus Geothermal BV and is expected to drill cost-effective multiple slim holes from one main hole in any desired direction, thereby boosting reservoir contact and well productivity.

DSSD underwent extensive lab testing, prototype development, and a full-scale field trial in Switzerland. The Swiss contribution to the project includes technology trials, evaluations, and modeling studies to assess DSSD's impact on medium-depth geothermal projects. Additionally, a new trial in the Netherlands in Ede is set to begin in Q4/ 2025 to further evaluate its performance.

The modeling study explores the potential of DSSD technology to improve the economics of geothermal district heating projects in the Geneva basin, focusing on medium-depth fractured carbonate reservoirs (Lower Cretaceous and Upper Jurassic). Using stochastic static modeling and dynamic simulations, it evaluates reservoir characteristics, production rates, and economic feasibility resulting in estimates of Levelized Cost of Heat (LCOH) and Specific Capital Costs (SCC). Results favor the Upper Jurassic (UJ) reservoir for its superior thermal and petrophysical properties. Multilateral wells, especially triple-lateral configurations, significantly boost production and reduce costs when drilled with DSSD technology. The findings highlight the efficiency of multilaterals for geothermal development and their suitability for high-volume, stable energy output.

1 Introduction

1.1 Background information

Reliable delivery of economic well performance of deep geothermal projects is significantly influenced by uncertain reservoir quality, such as matrix and fracture conductivity heterogeneity, compartmentalization, and fracture density and spacing. Horizontal and multi-lateral wells are known to enhance productivity by increasing connectivity with the reservoir, as demonstrated by various lateral configurations (Peters et al., 2015). However, due to high drilling costs, multi-lateral structures are often not a viable option, underscoring the need for cost-effective directional drilling solutions.

Simpler, low-cost, clean water jet-based systems for lateral drilling, such as those provided by Radial Drilling Services (https://www.radialdrilling.com/), have been available for many years. A schematic of potential lateral structures from a vertical main wellbore is shown in Figure 1a, and the productivity improvement factor (PIF) scaling with lateral length is presented in Figure 1b (Peters et al., 2015). The study highlighted that PIF is influenced by vertical-to-horizontal permeability ratios (kv/kh) and reservoir thickness, with PIFs up to three achieved using multi-lateral structures. However, commercial jet drilling systems have limitations: they are only suitable for softer, high-porosity rocks, produce a maximum lateral length of about 100 meters with one-inch diameters, and lack directional control, resulting in tortuous drill paths (Reinsch et al., 2018). The applicability and limitations of un-steered jet drilling systems were comprehensively studied in the EU HORIZON 2020 project SURE (https://www.sure-h2020.eu/). The study concluded that directional solutions with greater control and capability in harder rocks are necessary for enhanced geothermal well performance.

Canopus Drilling Solutions Geothermal BV (http://canopusdrillingsolutions.com/) has developed a novel directional steel shot drilling system (DSSD) to Technology Readiness Level (TRL) 6/7 under the EU GEOTHERMICA project DEPLOI. The DSSD system offers a promising solution by combining mechanical drilling with the erosive action of steel shots accelerated in drilling fluid to erode rock, enabling the drilling of slim hole diameters (4-1/8 to 6 inches) with high rates of penetration (ROP) even in hard rocks like sandstones, limestones, and granites. The DSSD system's ability to drill very tight radii facilitates the creation of laterals within the reservoir section (Figure 2Figure 2a), significantly reducing wellbore integrity and zonal isolation issues (Figure 2b). This technology enables precise directional control and complex borehole geometries, enhancing reservoir contact and productivity in heterogeneous and low-permeability reservoirs. This capability positions DSSD as a cost-effective alternative for drilling multi-lateral structures.

DSSD Technology Trial and its potential for geothermal reservoir development in Switzerland

Switzerland relies heavily on fossil fuel for its heating needs. In 2021, about 80 % of the heating energy needs were provided by fossil fuel (Link & Minnig, 2022). The option of using geothermal energy for heating purposes has been under consideration since several decades. The GEothermie 2020 program was initiated in 2013 by the State of Geneva with the aim to develop geothermal energy to substitute at least 20% of fossil energy used for heating purposes (Nawratil de Bono, 2020). SIG conducted exploration studies to access the main reservoir candidates for geothermal development in the Greater Geneva Basin. The first exploration well GEo-01 was completed in April 2018, while the second well, GEo-02 was completed in June 2020 (Nawratil de Bono, 2020; SIG, 2019) (see Figure 11 for location of wells). The primary target reservoirs for medium-depth (<1500 m) geothermal exploration, particularly for district heating, are the fractured carbonates of the Lower Cretaceous (LC) and the Upper Jurassic (UJ).

The directional steel shot drilling (DSSD) system holds the potential to become a transformative technology for medium-deep geothermal applications by enabling scalable well performance, reducing project economic risks, and expanding the accessible geothermal resource base. Its application and impact within the Swiss market is explored in close collaboration with industry partners within the follow-up project DEPLOI the HEAT-CH.

As part of the EU GEOTHERMICA project DEPLOI THE HEAT, a full-scale operational trial of the DSSD technology is conducted at the VersuchsStollen Hagerbach (VSH) test site in Switzerland. The trial, part of WP2, involved extensive lab testing and prototype construction to demonstrate system capabilities before scaling up to a field trial in Ede, the Netherlands.

Services Industriels de Genève (SIG), the public utility company of Geneva and its counterpart in Lausanne, Services Industriels de Lausanne (SIL) participated in DEPLOI the HEAT- CH as future users of the DSSD technology that is developed and tested in the project. If the comprehensive evaluation yields positive results, the operators plan to incorporate DSSD technology into their geothermal development projects for further trials and potential commercial deployment. Hence, in agreement with both the operating utilities SIG and SIL, impact of deployment of DSSD technology in LC and UJ reservoirs are investigated in WP 3 of this project. The main contribution of SIG and SIL in this WP is to support this study with data and information from their exploration geothermal fields. The Geneva geological model served as the structural framework for this study due to its available data as there was no geological data from Lausanne available during the duration of the project.

As Geneva basin is an exploration field, geological uncertainties exist related to fluid and structural conditions in the Geneva basin, which presents a substantial financial risk for drilling and production. Horizontal wells have in general proven highly effective in fractured formations, as their trajectory can intersect multiple fractures, increasing the likelihood of productive zones while reducing costs and risks. However, as in any exploratory fractured reservoir, the occurrence and distribution of the fracture driven permeability pathways are highly uncertain in the study area. From a reservoir modeling perspective, the nature and distribution of these features are random, heterogeneous, and localized, leading to varying flow capabilities across different parts of the geological units. Consequently, stochastic method is adopted to model the random distributions of fractures in the target formations. In this work, 1000 stochastically generated static models with varying fracture network properties is used to account for the uncertainty in permeability distribution in the fractured carbonates. Following this, numerical simulations and techno-economic calculations are performed to evaluate the efficiency of DSSD multi-lateral wells in terms of production enhancement and economics in these reservoirs.

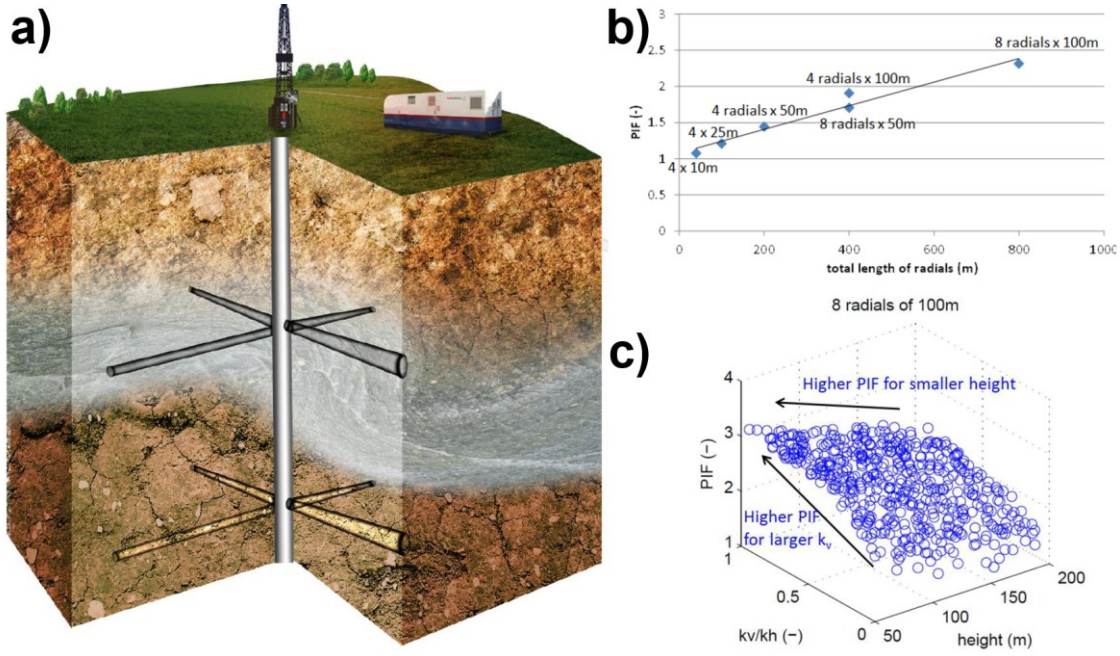

Figure 1: a) Schematics of lateral structure branching off from vertical main wellbore created by small, clean water jet drilling tools (http://www.radialdrilling.com b) Estimated Productivity Improvement Factor (PIF) for various lateral configurations for a sandstone reservoir case study. c) PIF as a function of permeability anisotropy (kv/kh) and reservoir height (Peters et al., 2015).

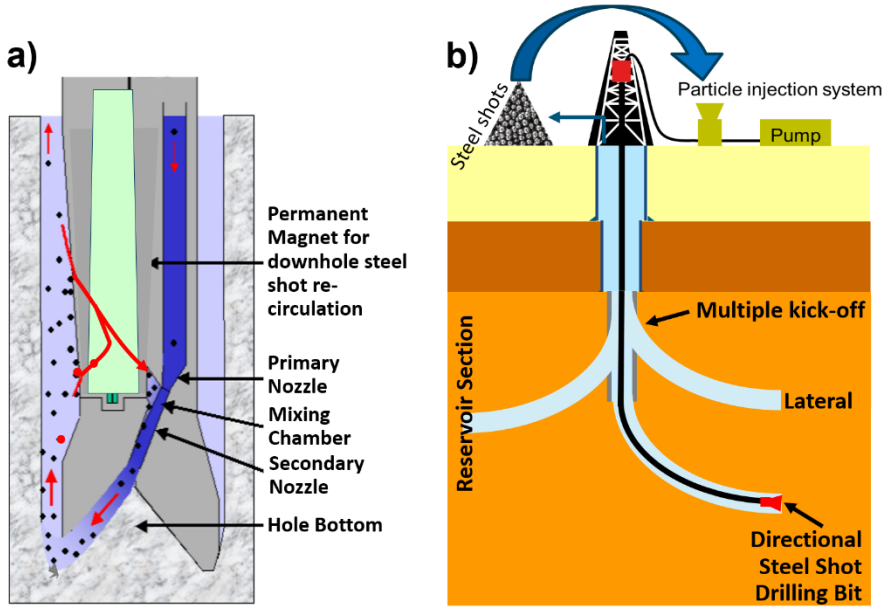

Figure 2: a) Schematic of Canopus' steel shot jet bit b) Construction of multi-lateral wells in the reservoir section by Canopus' directional steel shot drilling (DSSD) system

1.2 Objectives

The Canopus steel shot drilling technology claims to be able to drill deviated and horizontal multi-lateral boreholes with a short build section within the reservoir to stimulate the productivity of a geothermal asset, thereby de-risking the project. The costs of these lateral drilling operations are expected to be considerably lower, compared to standard directional drilling methods. Within this project, we investigate the above claims through field trials in WP2 and productivity and technoeconomic analysis in WP3.

Objective WP2: to test the commercial readiness of the DSSD technology through field trials in two geologically complex environments – tight limestone formation at the underground research facility in VersuchsStollen Hagerbach (VSH), Switzerland and a sandstone reservoir in Ede, Netherlands

The first field trial in VSH has been completed in summer 2023 and the results are reported in detail in a mid-term report. Following research questions are addressed by the technology trial at VSH, performing a full-scale test of the system and drilling two wellbores. Performance measures are the rate of penetration (ROP), wellbore curvature ("dogleg" severity), stability of the trajectory, hole cleaning efficiency, system pressure losses, bottom hole time, non-productive time, as well as many operational aspects like well completion, mud / steel shot handling and integration of the steel shot drilling in a full-scale, standard drilling system. The results of the technology trial at VSH are presented in 2.3:

1. Is the novel, directional steel shot drilling technology capable of drilling a defined wellbore trajectory?
2. Is the launch system to kick-off the lateral wellbores effectively functioning?
3. Is the current technology capable of geo-steering?
4. What is the system performance with respect to the rate of penetration (ROP), build radius, and hole cleaning?
5. What is the operational performance with respect to tool handling, tool control and technology integration into a standard drilling system?
6. Is the achieved wellbore quality sufficiently high?
7. Is it possible to complete the lateral structure with a standard well completion system?

8. What pressure losses are measured in a lateral structure during production simulation.

Objective WP3: to evaluate the potential (in terms of production improvement and economics) of using DSSD multi-lateral slim holes in medium depth (< 1500 m) fractured carbonate reservoirs (Lower Cretaceous and Upper Jurassic) that are typical targets for heating projects in Switzerland. This objective is to be achieved through statistical numerical modeling of reservoir performance and corresponding techno-economic calculations to deliver the specific capital costs or levelized costs of heat for the various realizations. This approach will deliver the economic de-risking potential of Canopus DSSD technology relevant for mid-depth geothermal heat projects in Switzerland.

1.3 Main activities and timelines

Main activities **WP2** and **WP3** during the project and their timelines are reported below:

(i) **September 2022 – January 2023**:

WP2/ WP3: Start of the project

WP2: FAT 1 DSSD; trial preparation

WP3: Meeting in Geneva to discuss about the geothermal field and available data; SIG and SIL decide on their geological reservoir of interest and geological model to be used for study, dissemination workshop during Connect Geothermal 2022 in Bern.

(ii) **October 2022 – April 2023**:

WP2/ WP3: Project Kick-off Meeting

WP2: Trial preparation

WP3: ETH begins data collection and analysis; conducts meetings with SIG and SIL operators (in-person meeting in Hagerbach, other online meetings) to understand available data and reservoir characteristics; literature study. Operators decide on the main reservoirs of interest – Lower Cretaceous and Upper Jurassic.

(iii) **May 2023 – December 2023**:

WP2/ WP3: 1st dissemination workshop, mid-term reporting and status review with BFE.

WP2: Trial execution, trial evaluation and reporting.

WP3: Development of conceptual models for characterization of fractured reservoirs, development of stochastic modeling approaches for generating static realizations of fractured reservoir, development of well designs for multi-laterals; preliminary numerical modeling studies to test developed workflows; workshops in Hagerbach and Lausanne with SIG and SIL to agree on the modeling approaches. In absence of other geological data, SIL agreed that stochastic investigation with varying fracture permeability is useful for them to have initial estimates of productivity from the reservoirs of interest.

(iv) **January 2024 – March 2024:**

WP2: Start FAT 2 DSSD

WP3: Stochastic modeling for static realizations of fractured reservoirs in Geneva basin; dynamic simulations of reservoir production in the various stochastically generated static realizations for evaluating the potential increase in production capacity because of multi-lateral slim holes intersecting the fractured zones; simultaneous report writing.

(v) **August 2024 – November 2024:**

WP2/ WP3: 2nd dissemination workshop at ETH Zurich; Geothermica project midterm review meeting

WP3: Techno-economic assessment using outputs of dynamic simulations to quantify the increase in production in terms of Levelized Cost of Heat (LCOH) and Specific Capital Costs (SCC), final reporting.

2 WP2: Technology Trial at VersuchsStollen Hagerbach Test Site

2.1 Equipment of the Directional Steel Shot Drilling system

Canopus' Directional Steel Shot Drilling (DSSD) system is an innovative combination of an alternative rock erosion mechanism and a novel rotary steerable system (RSS) for directional control. The DSSD system combines a mechanical polycrystalline diamond cutter (PDC) with the erosive action of small steel shots accelerated transported in the drilling fluid and in the bit nozzles. Each steel shot is expelled at high speed from the nozzles of the modified PDC drill bit, (see Figure 3 below) and impacts on the rock surface to fracture the rock.

Figure 3: Overview of key operational equipment deployed during the trial at VSH test site.

The steering action is controlled by the steering sub which is part of the downhole equipment integrated in the bottom hole assembly (BHA). The steering sub internals (see Figure 4) orient the abrasive jet erosion for direction changes by controlling the timing at which higher concentrations of the steel shot particles exit the drill bit synchronized with the orientation of the drill bit (tool face). Thereby, the erosive action is enhanced at one site of the wellbore bottom resulting in the direction of drilling.

Figure 4: Internals of the steering sub showing centralizers (top), sensors pack (middle), and the rotor (bottom)

At the surface, the steel shot injection unit (SIU) provides the steel shot concentration to the drill bit by continuous, rate-controlled steel shot injection into the drilling fluid stream coming from the rig pump (Figure 3). Thereby, the SIU impacts the rate of penetration (ROP) as well as the maximum built rate towards a defined direction that can be archived.

From the returning drilling fluid, the cuttings and steel shots are removed by a conventional shaker and a magnetic drum separator, respectively (Figure 3). The cleaned drilling fluid is stored on the mud tank and re-circulated to the well by the high-pressure rig pump. Likewise, the steel shots are reinjected by the SIU. This surface system including steel shot separator and SIU enables that the drilling fluid and the steel shot circulate in a closed loop. These two units are the main equipment that is required to extend the functionality of existing drilling surface equipment for steel shot drilling. For the trial, a Vermeer 55 horizontal rig was utilized (Figure 3). A schematic view of the surface setup showing the line-up of all equipment for the trial is given in Figure 6.

A detailed explanation of the technology's operation can be found in Jan Jette Blangé, et al 2022.

2.2 VersuchsStollen Hagerbach (VSH) Test Site

The location of the VSH test site was selected to enables access to a fractured, hard, silicious limestone formation with slate layer overburden. This specific geological setting is important to assess the performance of the DSSD system at conditions relevant for the fractured / karstified Mesozoic units targeted by the Swiss project partners for future geothermal applications.

Downhole conditions (e.g. pore-fluid pressure, rock stress) may affect the performance of the drilling system incl. the rate of penetration (ROP). Tests at the surface or in laboratory environment without pore-fluid pressure or rock overburden often overestimate drilling performance. Hence, the VSH location with its overburden rock, that includes pore fluids (water), i.e. a water column, results in conditions to investigate the novel drilling technology under a (more) realistic scenario.

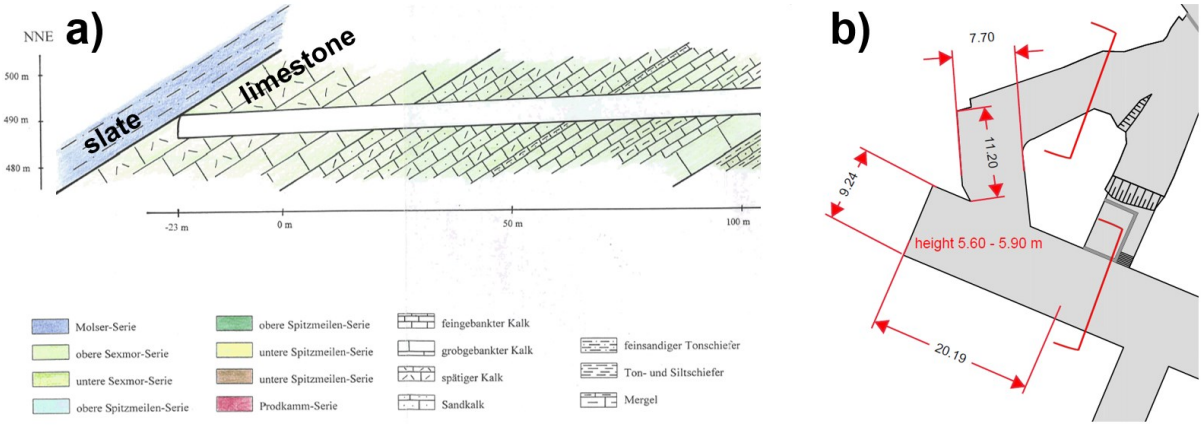

Figure 5: Schematic cross section (not to scale) of the VSH main gallery intersecting silicious limestone towards the slate overburden. b) Site dimension at the drilling location at the end of the main gallery.

A schematic cross section of the rock formations intersected by the main gallery of VSH test site is displayed in Figure 5. The exact distance from end of gallery to the interface between limestone and slate was not known. From another gallery nearby crossing the interface, it was expected that the drilling operation will take place in limestone for ~100m before intersecting the slate layer. During actual drilling operations a different lithology has been encountered, black slate with quartzite layers. The gallery dimensions at the drilling location are given in Figure 5.

2.3 WP2: Technology trial at VersuchsStollen Hagerbach (VSH) test site

Within several month of collaboration of the core trial execution team, the Detailed Drilling Plan (DDP) has been produced. The DDP covers all phases of the operations, comprises the risk register, the time plan and the responsibilities of the project execution. The DDP was used as basis for the Drilling Well On Paper (DWOP) meeting that has been facilitated prior to the trial kick-off in collaboration with all involved parties. The DDP and DWOP are standard documents and procedures for a well construction project.

Preceded by several months of preparation, the equipment for the VSH-trial arrived on location on Monday June 12. The Bottom Hole Assemblies (BHAs) were unpacked, the drill unit positioned, the flow line set-up, and cables, wiring, hoses and tubing placed. Figure 6 shows a schematic layout of all surface component of the drilling system as well as their line-up. Also three cameras were installed to monitor the high-pressure pump area, the shaker and for a time lapse recording of the trial. From that Monday onwards, the trial operations assessing various settings and drilling configurations lasted 4 weeks followed by some days for demobilization and wellbore logging. On Wednesday, July 12 the trial was finalized. In the following a weekly summary of the key operations and learnings is given.

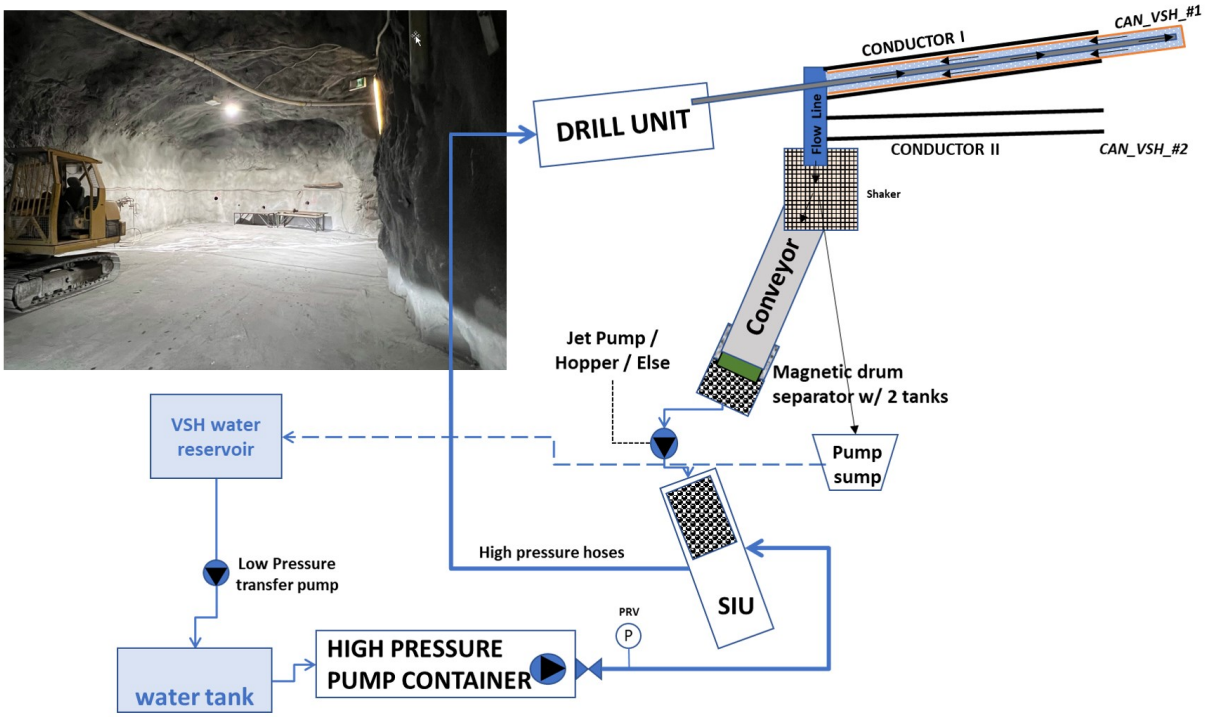

Figure 6: Schematic layout of all VSH-trial system components placed and operated in the shown niche of VSH underground facility.

Week 1

The first week has been used to position all components, connect the data acquisition system to rig up and get the various components of the system running.

- Drill unit and data-acquisition of push/pull forces is operational. Torque left/right, string RPM (rotation per minute) and ROP (rate of penetration) can be sampled at 10 Hz. The data is life recorded on Canopus system. Rotating head position (to derive the hole depth) is missing. Issue will be resolved with direct matching of setting changes with depth and formation logging with depth.
- Drilling assembly make up and break out in horizontal position has been trained and optimized some extend but it takes considerable time – about 3-4 h – including the move of the rig out and in. A team of 4 to 5 persons is required for drilling assembly make-up.
- Steel shot return system has been modified to resolve solids sticking to the conveyer belt and its ridges. A new, longer belt with reduced slope and without ridges has been placed.
- Pump pressure, flow rate and cumulative pumped volume are recorded in control cabin (1 Hz). The data is exported real time to the Canopus Laptop.
- The electro-magnetic telemetry for communication with the BHA has been tested and the electronics of the drilling assemblies have been prepared.
- The first 25 m of wellbore have been drilled out with a standard drill bit (no steel shots) to allow for installation and placement of the full steel shot BHA (about 25 m long). The rock within these first 25m of drilling seems to be primarily slate and not competent limestone as expected.
- Further drilling activities are reviewed for lower mechanical specific energy required for the drilling of slate. Hence, the flow rate will be reduced as well as the operating pressures. The reduced flow rate must be sufficient for hole cleaning purposes transporting cuttings and steel shots out of the wellbore.

At the end of the first week all equipment has been installed, procedures have been tested and the first drilling assembly has been placed in the wellbore.

Figure 7: Overview of the drill site (left) and making-up and running-in-hole the ‘empty’ DSSD drilling assembly without electronics (right) for test purposes.

Week 2

The second week has been used to transition from rigging up and getting the system running to learning how to drill effectively with the integrated system.

- The data acquisition system has been completed, now including the recording of the rotating head position and hence, the recording of the rate of penetration (ROP).
- The Steel Shot Injection Unit (SIU) requires flow rates of 200-350 l/min for controlled steel shot injection, at higher flow rate the injection became unstable. The hole cleaning to transport all steel shots out of the sub-horizontal well requires 600 l/min. Consequently, a flow bypass has been installed between the high-pressure pump and the SIU to comply with both requirements.
- The installation of the pulsation dampener was required to realize stable operation of the SIU. The dampener will also reduce any fatigue of the high-pressure conduits.
- Performance of the Canopus bit in the slate is very good and 80m/h ROPs can be reached with 3 kdaN pushing force (WOB). However, in the event of running at high ROP into a harder rock layers, in the specific case very component quartzite, the bit cutters can be damaged due to local overloading. The erosive jets may mitigate this damage to some extend if carefully positioned for this specific purpose. During the trial, the drilling preferably is to be done with max 1 kdaN pushing force to avoid bit damage.
- The quartzite layer at 54-56 m hole depth should probably better be avoided during future sidetracking operations and drilling through this layer must be done with lower WOB and RPM settings than in slate.
- There are indications of some wash-outs in the wellbore as well as some wellbore undulations. The flow rate of 600 l/min has been proven to be sufficient in cleaning out the wellbore but washing/jetting into the wall should be avoided.
- The long BHA handling (~ 25m) for horizontal drilling has posed some challenges. It remains a 4 - 5 person team-operation even after the team got skilled. Making up the drilling assembly including all electronics and connecting both the electronics, the internal housings and the external collars is the most challenging part of the BHA handling.
- The shaker had to be modified to avoid leaking of solids, in particular fine steel shots when separating the drilling fluids (water) from the returns. Additional steel plates have been mounted on the shaker screen to stop the solids leaking from the shaker.
- At the end of week 2, the wellbore was logged with an acoustic televiewer and directional tool to show the wellbore quality and wellbore trajectory. The logging sonde could only be lowered into the first 30m of the well due to very high friction when pushing the logging string in manually. No steel shot drilling had been performed up to this depth. It could be shown that the wellbore was dipping to fast and a stiffer wellbore assembly for better directional control should be used for further drilling in week 3.

Fig. 8: Control room with data acquisition and three cameras for trial surveillance

While the functionality of the steel shot drilling systems could be demonstrated in week 2, the full capability of the steering sub (actuator, sensors, communication, battery consumption, calibration of tool face control and steering effectiveness) has to be shown in week 3 including steered drilling by steel shot erosive action.

Week 3

During the third week the team drilled for the first time with the complete Directional Stell Shot Drilling (DSSD) assembly and retrieved the first evidence of the steering action of the steering sub. The complete DSSD system drilled to 120 m hole depth and 400 kg steel shot was circulated. The EM-telemetry with the assembly could not be realized due to an unexpected high electromagnetic noise level at the trial side. Hence, steering sub data could only be downloaded and analyses from the tool memory after pulling the assembly out of the hole.

- The communication with the EM-tool failed because of interference with 16.7 Hz power transmission lines of the Swiss railroad. Communication frequency has been modified to 6 Hz, but the issue could not be solved.
- The steel shot concentration sensors and actuator of the steering sub worked as well as the tool face orientation detection. Steel shot concentration pulses were created synchronized with the bit rotation.
- The steel shot concentration can be reduced to values as low as 0.5%vol while maintaining for sufficient hole making and steering action. Even at the reduced bit pressure setting of 120 bar (instead of 300 bar) the steel shot erosion at 0.5%vol seems to be sufficient to maintain ROP. With these new settings, washing out of the slate is avoided and damage of the bit can be mitigated.
- The down hole directional data of the first DSSD run indicates a steering action of the steering sub at 500 l/min and 60 RPM. The indicated effect of the steering sub default angle was up and to the left while the overall steering action was limited.

The steering effect with the DSSD assembly has been demonstrated within week 3 and a safe operating window to limit wash-outs (lower pressure, lower steel shot concentration) and avoid bit damage (limit of 1 kdaN WOB) has been defined. Since the communication with the BHA could not be realized, pre-

programmed changes in drilling direction are utilized in week 4 by drilling 20m of each direction at minimum to allow the directional module (behind the bit) to detect the change.

Week 4

The objective of the final week was to get experience with the complete DSSD system, to change down hole settings through two-way communication via the EM-telemetry tool and get information on various tool performance settings like power consumption, potential wear zones in the down hole hardware, directional response and identify design & interface improvements and effective operational practices.

- The drilling operations have been performed in the second borehole in week 4. Comparable to the first borehole, no limestone could be drilled. The drilled lithology comprises slate with interbedded competent quartzite layers. The bedding plane was at a very high incidence angle with the bore hole direction. Consequently, the operational settings with lower pressure and lower steel shot concentration could be maintained.
- The EM-tool communication could be realized to surface but the tool could not receive (steering) commands from surface. The data of the Directional (DM) Module was communicated fine with the steering sub. Consequently, the DSSD assembly has been programmed to change the steering azimuth (tool face angle) every hour by 90 degrees automatically.
- The second wellbore was drilled to a depth of 125 m deploying the stiff and the flexible steel shot BHA and a clear directional effect of the steering sub was observed with the flexible assemble while the stiff assemble has sown very good angle holding capability.
- The steering sub created - as expected - concentration pulses of steel shots synchronized with the tool face orientation for steering. The control electronics worked as expected. The construction connecting the motor controller and actuator (for steel shot concentration modulation) has been damaged and was replaced. The future construction must be improved to avoid break down.
- Overall wear of the drilling assembly was negligible apart from the impact damage of the bit cutters when a sudden competence contrast is seen by the bit at interbedded quartzite layers. The internal sensor cable at the height of the actuator and the actuator-motor connection must be improved for robustness.
- The total steel shot mass circulated during the pilot was about 2500 kg. No wear of surface equipment was identified, nor any problems with making up drill string connections.
- Without the two-way communication, there was no opportunity to test the open hole side-tracking operations as planned.

The drilling activities for the VSH-trial of the DSSD system have been finished on July 07, 2023. Subsequently to the disassembling of the equipment, transport back to their original locations and the completion of the logging of the wellbores has been executed.

Figure 10: Used bit (left) vs. an unused bit (right). The used bit had several cutters at medium radius heavily damaged.

3 WP3: Numerical Modeling of Reservoir Access and Fluid Circulation and Economical Assessment for Specific Reservoir Candidates

As a preamble to this work, SIG and SIL met several times in workshops in order to compare existing data and the resulting levels of knowledge. They were able to appreciate the fact that significant similarities (stratigraphic and structural in particular) existed in the geological contexts encountered but also in the targets aimed for hydrothermal geothermal exploitations. Indeed, in the Geneva area, where there are more data available, it was found that the differences in geological context, existing from one potential target to another, were certainly more significant than the differences expected between the Geneva and Lausanne targets.

During additional sessions with ETHZ, it turned out that despite the difference in the quantity of available information between Geneva and Lausanne, it was entirely possible to carry out generic modeling work, useful not only for the Geneva and Lausanne fractured geothermal reservoirs but also extend to the broader Swiss Plateau. This feasibility stems from the fact that, in fractured formations, heat recovery performance is primarily dictated by the connectivity and permeability of the fracture network. Sensitivity analyses in fractured formations have demonstrated that reservoir properties, such as specific heat capacity and thermal conductivity, have a relatively minor impact on performance (Yang et al., 2023) compared to fracture characteristics such as fracture permeability, fracture aperture, and fracture density. The primary focus was, therefore, placed on the different fracture properties, generated stochastically. Hence, it was decided to utilize the data from Geneva, leveraging an already existing model at the periphery of the GEo-01 well as a complementary modeling foundation. Indeed, the GEo-01 target corresponded completely to the future Geneva and Lausanne targets (but also to those on the Swiss Plateau), namely faulted and karstic Mesozoic calcareous units. Furthermore, this target, already explored and being productive, and therefore having well data in addition to adjacent geophysical data, showed a diversity of faults (densities and orientations) sufficiently large to be representative of the expected regional diversity. To represent the uncertainty in the geometry, location, and attributes of fractures and faults in the different regions, a novel stochastic approach is implemented in this study

that allows the generation of thousands of static realizations of fractured reservoirs with varying properties that are constrained by local and regional information of the western SMB. In the following sections, we provide a brief introduction to the geology, the geothermal and the hydrothermal situation of Geneva and how the concepts can be applied to the neighboring area of Lausanne.

3.1 Geology and available data description

The Greater Geneva basin extends over 2200 km^2 and is located in the westernmost sector of the Swiss Plateau confined by the Salève mountain to the SE and the folder Jura chain to the NW. Figure 11 shows the geological map of Western Switzerland with location of SIG's exploration wells GEo-1 and GEo-2 along with the outline of the current study area (in blue) and the lithostratigraphy of the Western Alpine Molasse Basin (Guglielmetti. et al., 2020; Chelle-Michou et al. 2017). For detail description of the geological formations and their characteristics, readers are referred to Chelle-Michou et al. 2017, which provides an extensive review of the different wells drilled in Switzerland and France and analysis of temperature anomalies in the entire stratigraphic section of the Western Alpine Molasse basin.

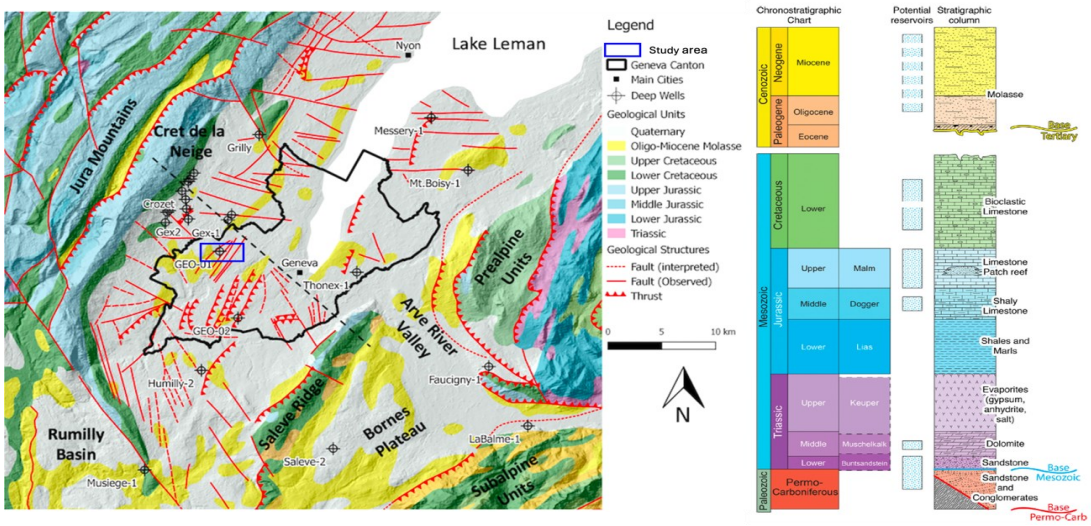

Figure 11: Left - Geologic map of Western Switzerland with locations of SIG exploration wells – GEo-1 and GEo-2 (modified from Guglielmetti. et al., 2020); Right - Stratigraphy of Western Alpine Molasse Basin (Source: Chelle-Michou et al. 2017).

3.2 Geothermal system and main structural trends

The geothermal resource in the Geneva basin is associated with deep aquifer systems which are heated by normal heat flow controlled by average geothermal gradient of ca. 25 – 30 °C/ km (Rybach, 1992; Chelle-Michou et al. 2017). Hence, the thermal anomalies are associated with heat advection related to fluid circulation along the faulted, fractured and karstified limestones of the Mesozoic formations (Moscariello et al. 2020; Nawratil de Bono et al., 2020). These faulted, fractured and karstified zones, if connected, enhance the intrinsic permeability of the reservoirs significantly. However, the high permeability connected fractured zones are sparse, spatially localized and distributed heterogeneously within a geothermal reservoir.

The geological and hydrogeological concepts shown in Figure 12 are completely identical in the Geneva (SIG) and Lausanne (SIL) regions. In fact, the expected water flows are exactly in equivalent environments, even if the stratigraphic units sometimes differ slightly in terms of the facies or thicknesses encountered.

To target these productive zones, it is important to identify the dominant structural trends, which are shaped by the regional and local tectonics over a long geologic period. The understanding of the dominant structural trends in the Geneva basin and the surrounding area has significantly improved over the last decade with the acquisition of 2D seismic data (discussed in Moscariello et al., 2020); borehole seismic surveys (Guglielmetti et al., 2020), GEo-1 borehole image surveys (SIG, 2019) and the recent acquisition of 3D seismic data by SIG in the canton of Geneva. The borehole images of the Lower Cretaceous unit acquired using an Acoustic Borehole Imager (ABI) and an Optical Borehole Imager (OBI) in well GEo-1 suggest the dominant direction of the open unmineralized fractures to be trending between N-S to NE-SW, indicating a preferential fluid flow direction oriented towards the NE-SW (SIG, 2019). Within the same interval, the mineralized fractures showed a significant dispersion of azimuths tending mostly towards ENE-WSW. While observations in a nearby borehole Thônex, located in the southwestern part of the Geneva basin, suggest the orientation of the open fractures in the Malm unit to be in N125ºE (Guglielmetti et al., 2020).

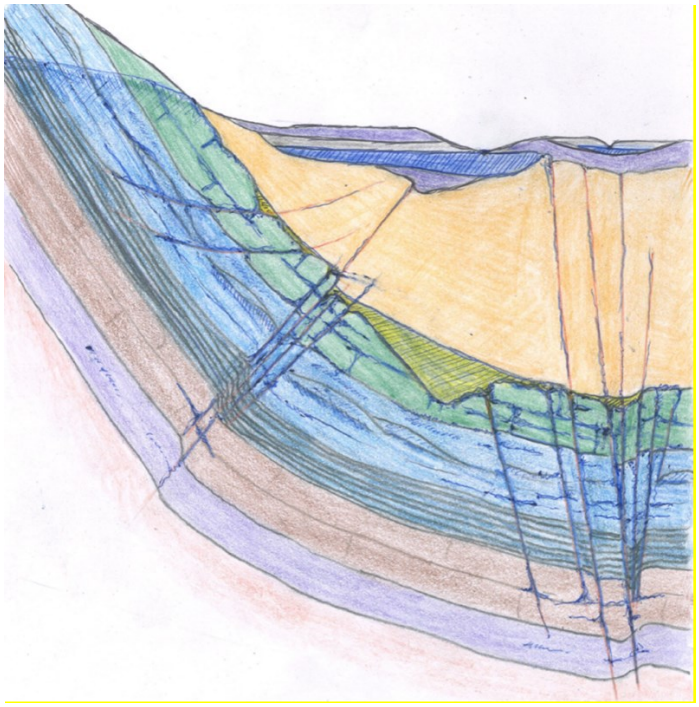

Figure 12: Conceptual geological model. With different fault typologies running through the entire Mesozoic series, incisions and karst in the Cretaceous units (green), karst inception levels in the Cretaceous and Malm units (blue), and still some geological units with possibly high matrix porosities (reef and dolomitic facies of the Upper Malm).

During the modeling phase, the results of recent 3D seismic acquisitions in Geneva were not yet fully known. Indeed, the processing and interpretation phases took some time and are still ongoing. Thus, at the start of the project, the data available for reflection and modeling were essentially those from previous 2D acquisitions and some well data. The methodology adopted therefore had to deal with information that was still relatively incomplete, and with the idea of conducting a study that would be valid for both the Geneva and Lausanne contexts. However, the results discovered in 3D in parallel with the modeling work carried out as part of this project only reinforced the approach decided and confirmed the interest in being able to work in models allowing to appreciate a diversity of distributions of fracturing in the geological massif (in terms of fracture densities and fracture orientations). The results showed that this variability of the distribution of fracturing did indeed exist, even on the scale of a small territory such as that of the Canton of Geneva. Indeed, in agreement with the above observations, the preliminary

interpretation of the recently acquired 3D seismic survey by SIG replaces the simplified view of the faulting system in the Geneva basin with a complex network of faults with two dominating trends: A family of faults with a generally east-west orientation and the locally outcropping strike-slip fault system oriented in the NW-SE direction. These orientations are supplemented by those of the main regional overlaps, which are rather NE-SW. These dominant regional structural orientations for faults and fractures are considered while generating the various static geological models.

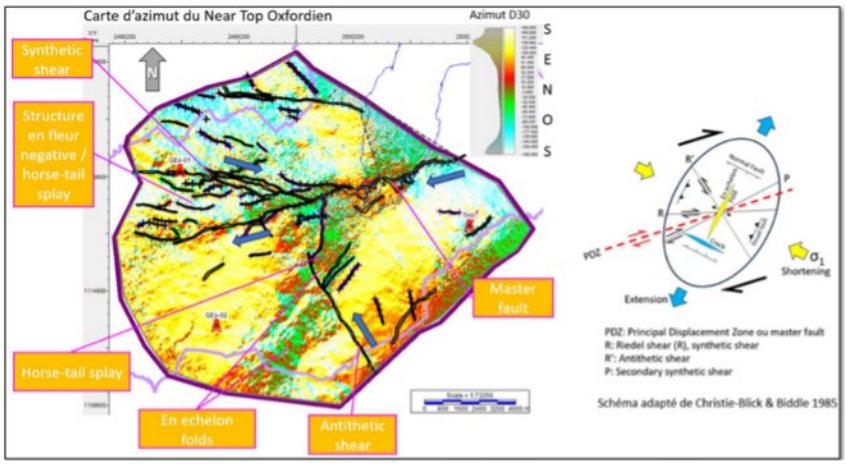

Figure 13: Distribution of faults on the extension of 3D in Geneva

3.3 Geological model

This geological model of the Geneva area, provided by SIG and established before 3D seismic results, is used as the structural framework for our study, and has dimensions of approximately 5 km × 3.5 km × 2.5 km. The model is developed integrating information from 2D seismic data and nearby wells in Switzerland and France. The total number of grid blocks is 98560, with 64, 35 and 44 grids in the I, J and K direction, respectively. Figure 14 shows the 3D geological model and a cross-section through it. The model is an export from the modeling software Petrel and consists of a non-uniform gridding structure. It consists of seven stratigraphic layers, which are further subdivided into several layers accounting for a total of 44 vertical layers.

Well GEo-1 was drilled by SIG with the objective to explore the shallow- to medium-depth geothermal reservoirs (< 1500 m) in the Geneva basin (Nawratil de Bono, 2020). It crossed the entire carbonate series reaching a total depth of 744.06 m and intersected the fractures and karstified formations of LC and UJ Malm (Twannbach) formations. The first three sections of the well (34.6'', 17.5'' and 12.25 '') are cased and cemented, whereas the last section (8.5'') between 411 m – 744 m is an open hole section, intersecting the Mesozoic reservoirs. Wireline log acquisitions performed in the different sections of the well (17.5'', 12.25'' and 8.5'') provided information about the stratigraphic formations and the associated thermo-physical and hydraulic properties. Preliminary reports from SIG, based on the analysis of well data from GEo-1, indicate that the Mesozoic reservoir units have very low matrix porosity and permeability and contain immobile water (Table 2), but the system as a whole, with these intense fracturing and especially the karst inception levels, is very productive with very high transmissivity.

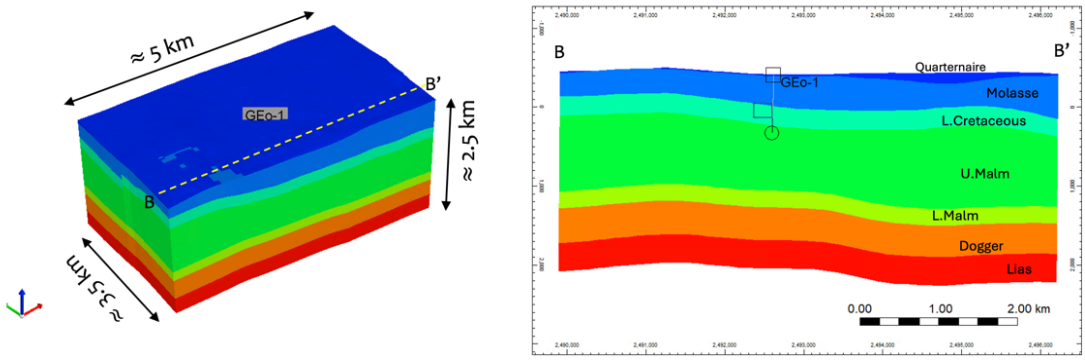

Figure 14: 3D geological model (left) and a cross section through it (right) showing the main lithological units and location of exploration well GEo-1 (Data Source – SIG)

The matrix porosity is reported to be between 3 % – 8 % in LC and UJ (Malm) respectively while matrix permeability was estimated to range from 1.26 – 10 mD from regional core data (SIG Report, 2019). These values are consistent with other studies performed on carbonate successions (Homuth and Saas, 2014; Rusillon, 2018; Moscariello et al., 2020). Well data from GEo-1 and publicly available literature are used for populating average matrix properties, such as porosity, permeability, thermal conductivity, and heat capacity in the geological model (see Table 2)

Well tests performed in GEo-1 encountered artesian pressure and produced up to 4000 m^3/day (50 l/s) from the Lower Cretaceous unit with a temperature of around 33 °C. The pressure reported in GEo-1 indicated an average hydrostatic pressure of around 10 bar (between 9.2 and 11.7 bar) at a depth of 515 m ± 20 m below sea level (SIG, 2019). The borehole images in GEo-1 indicated that the well intersected a high-permeability network consisting of dense fractures and karst features in the open-hole producing section. Analysis of the production tests in GEo-1 carried out in 2021 by a service provider reported a fracture permeability on the order of 6-7 Darcy for the densely fractured flow zones in the well. The second exploration well, GEo-2, located approximately 7 km south-east of Geo-1 (see Figure 11) produced less than 12 m^3/day (0.14 l/s) (SIG Internal communication), indicating a very tight and impermeable formation. No wellbore images were acquired in Geo-2. Similarly, another well, Thônex (see Figure 11 for location), intersected three fractured intervals identified in the borehole images, and produced 70° C warm water but with a very low flowrate of approximately 300 m^3/day) (3.8 l/s) (Moscariello et al., 2020). The drastic differences in the well flow rates within short distances provides evidence for the localized, disconnected, and heterogeneously distributed nature of the high-permeability zones.

3.4 Methodology

The work began with data collection and analysis, conducted by ETH, followed by meetings with SIG and SIL operators including an in-person meeting in Hagerbach, Geneva, and Lausanne and several additional online discussions to assess available data, reservoir characteristics and current hydrological and structural understanding. A literature review was performed by ETH to support the analysis. Meanwhile, SIG and SIL conducted several joint discussions to select their primary reservoirs of interest i.e., the Lower Cretaceous (LC) and Upper Jurassic (UC) units.

Once the conceptual model and the proposed methodology were agreed upon by all the partners, the development of the stochastic modeling approach, well designs, and preliminary numerical modeling studies were initiated. Section 3.4.1 provides a detailed description of the stochastic approach for

generating the static realizations of the fracture corridors. The various static models of fracture corridors (FCs) are then imported into the software CMG (Computer Modeling Group) and integrated with the geologic model (shown in Figure 14). Different multi-lateral well designs are then created in the model, which are used for dynamic simulations for a period of 20 years.

In Sections 3.4.2 and 3.4.3, a discussion of the different numerical constraints and well design scenarios are presented. For each target reservoir, around 6000 simulations are performed (1000 static models, two locations, three well designs). The massive number of simulations were performed using ETH's supercomputer, Euler. The final part of the work involves techno-economic calculation using the dynamic simulation results (production flow rates, temperature, and pressure) in our (GEG Group at ETHZ) in-house techno-economic simulator **TANGO** – **T**echno-economic **AN**alysis of **G**eo-energy **O**perations to perform the economic evaluation. Section 3.4.4 provides more information about TANGO.

3.4.1 Stochastic modeling of Fracture Corridors (FC)

In naturally fractured and karstified formations, faults, fractures, vugs and karst features enhance the formation's intrinsic permeability and porosity. Field-scale outcrop studies have shown that the fractured zones are generally characterized by a fault core and a damage zone, the latter associated with high-intensity fractures of varying lengths, apertures, and heights, forming fracture corridors (FCs) (de Joussineau and Petit, 2021, de Joussineau, 2023) (Figure 15). The individual fractures within the corridors can vary in dimensions (length, height, thicknesses) from cm to hundreds of meters (Kharrat and Ott, 2023), while the fracture corridors can vary from a few hundred meters to km long, creating high-permeability fluid pathways (Laubach, 1991).

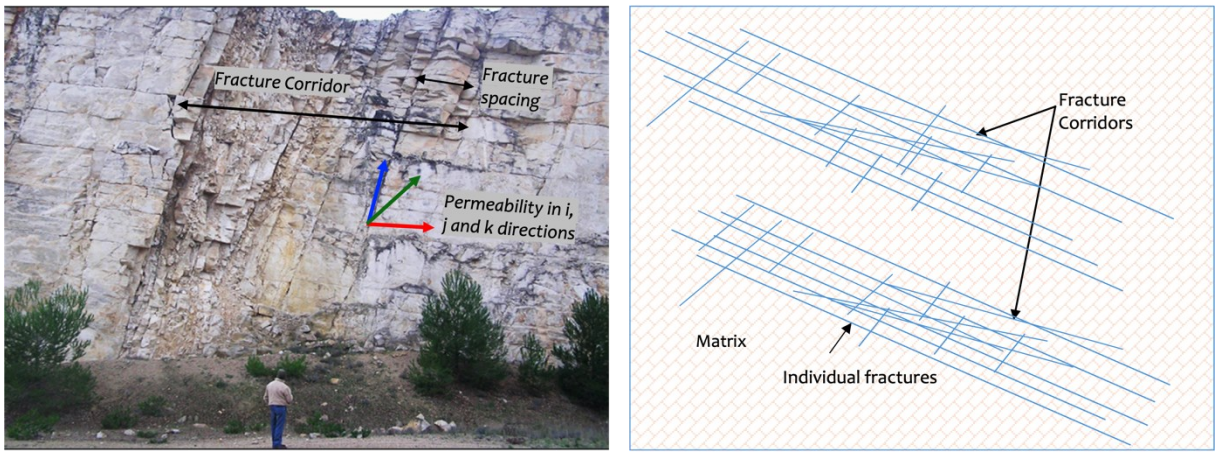

Figure 15: Left- Photo of a large-scale fracture corridor (Source – de Joussineau and Petit, 2021); Right - Conceptual sketch – top view of a fracture corridor in a fractured reservoir

Commonly used approaches for describing flow behavior in fractured media include (Smith & Schwartz, 1993; Li & Lee, 2008; Lee et al., 2001):

Different approaches are used to model fractured reservoirs, depending on the study's objectives, data availability, and computational resources. While some studies rely on continuum models for large-scale applications, others prefer discrete fracture network (DFN) models for detailed fracture representations. Our approach builds on the DFN concept but introduces fracture corridors (FCs), which are intensely fractured zones that drive the main fluid flow in addition to the rock matrix, whose permeability depends on formation type and is defined by the user. The approach allows the modeling of fracture-related intense damage zones, which might be localized and heterogeneously distributed in the rock formation. The algorithm, developed in MATLAB, generates FCs that are characterized by dense fracture network,

with stochastically assigned fracture properties, such as aperture, lengths, densities, orientation, and fracture permeability, which are constrained using available regional and local geological information. The code follows a recursive algorithm and is initiated at one point defined by the user, which is the center of the FC. Based on the input statistical parameters defined by the user (Table 1), the code generates fracture networks with the following constraints: (a) major parallel or subparallel fractures oriented in a user-defined dominant direction and (b) minor connecting fractures oriented perpendicular to the dominant direction randomly intersecting the major fractures. The only known deterministic fractures in the study area are within the LC and UJ formations in the location of the GEo-1 well. Hence, all the static realizations of FC consist of fractures that intersect well Geo-1.

The statistical moments for the parameters used for generating the FC realizations in the current case study are listed in Table 1. Geological information from boreholes, acoustic images, and structural maps are used for constraining the parameters of the probability distribution functions (PDFs). The height of the individual fractures within the FC is controlled by the thickness of the bounding stratigraphic formations. The fracture trace lengths are stochastically generated assuming a power-law distribution with minimum and maximum lengths compiled from literature values (Bonnet, 2001; de Joussineau, 2023).

From the discussions presented in Section 3.2, dominant structural trends were included in the stochastic model generations. A total of 500 realizations of FC models were generated with NW-SE as the main direction of open fractures. Within each ensemble, the individual fractures were allowed to disperse $\pm 5°$ from the primary direction to account for the dispersion of azimuths between WNW-ESE direction and NNW-SSE direction. This dispersion was observed in the borehole images of Geo-1 (SIG report, 2019). Similarly, another set of 500 realizations were created in the other dominant direction NE-SW with a dispersion angle of ± 5 ° set as a standard deviation.

A mean fracture frequency P10 (number of fractures per unit length) of 0.68 m^{-1} and mean aperture (width of single fractures) of 0.0006 m (calculated from minimum and maximum reported values) have been reported by SIG from the interpretation of borehole images. Considering the P10 value and the resolution of the numerical grid (approximately 100 m each in the x and the y direction), fracture frequency per grid cell and statistical moments for equivalent fracture aperture are calculated. Assuming that the fracture aperture follows a normal distribution, the algorithm randomly assigns aperture values to each fracture within the fracture corridor.

To obtain stochastic parameters for fracture permeability values relevant for the Geneva basin, information from dynamic data from well production tests and fracture characteristics from well bore images are used. Derivative analysis of the pumping tests in GEo-1 (March-2018) indicated a permeability of 1300 mD (millidarcy) for the major fracture network. In addition, fracture permeability evaluations are performed using data obtained from Acoustic Borehole Imager (ABI) images logged in GEo-1. Using Darcy's law for flow in porous media and the Cubic Law for flow in fractures, the fracture permeability, k_f, in a formation characterized by multiple fractures, spaced at distances, *s*, with aperture, *b*, is given by

$$k_f = \frac{b^3}{12s}$$

with a mean fracture number density of 0.68 m^{-1} and an aperture of 0.0006 m (calculated from minimum and maximum reported values), the fracture permeability is estimated to be $26 \times 10^{-12} (-12)$ m^2 or $26{,}000$ mD. Unlike porosity, permeability typically follows a lognormal distribution. Hence, permeability values obtained from dynamic analyses and the Cubic law for flow in fractures are in good agreement, since they are within the same order of magnitude, keeping in mind that permeability varies in nature by over 12 orders of magnitude. The above values, from the dynamic tests and from the Cubic law are used as minimum and maximum, values, respectively, to calculate the statistical moments, which are

then used in the stochastic algorithm. Each FC model is then integrated into the geological model by importing them into the reservoir simulator CMG. When fracture planes intercept the rock matrix grid, DFN segment control volumes are created, which contribute to fluid and pressure transfer between the FC and the reservoir matrix. Examples of realizations of FCs, integrated into geological models, along with the multi-lateral well designs, are presented in the next section (Figure 16).

Table 1: Parameters for generation of fracture networks (* compiled from field studies, source- Bonnet et al., 2001; de Joussineau, 2023; SIG Report, 2019)

Orientation		Aperture (m)		Permeability (mD)		Length* (m)		No. of realizations
μ	σ	μ	σ	min	max	min	max	
N 45º W	± 5 °	0.0006	0.0002	1300	26 000	1500	15000	500
N 45º E	± 5 °	0.0006	0.0002	1300	26 000	1500	15000	500

3.4.2 Numerical constraints

The average thermal gradient of the area is around 30 ℃/ km (Chelle-Michou et al. 2017; Rybach 1991). Considering steady-state conditions and conduction-dominated heat transfer, temperatures were calculated for all grid cells and assigned as initial conditions. The initial reservoir pressure was set to average hydrostatic conditions as indicated by the pressure monitoring data reported by SIG (approximately 10 bars at 515 m.a.s.l. $\pm$ 20 m). To reduce the boundary effects and correctly account for heat in the rock in proportion to the pore space, the reservoir simulator provides an option for applying a volume modifier value. A value of 100 is applied along the boundaries of the block volume that virtually increases the volume of the model region. It is assumed that the porous section of the reservoir is 100% saturated with water. Well data from exploration wells and internal SIG information are used for populating matrix properties, such as porosity, permeability, thermal conductivity, and heat capacity within the model (see Table 2)

Table 2- Average values of matrix properties (Source - SIG, 2019)

Formation	Thermal Conductivity (W/m/K)	Vol. Heat Capacity ($MJ/m^3/K$)	Matrix Porosity (%)	Matrix Permeability (mD)
Quaternary	2.25	2.3	0.15	10
Molasse	2.25	2.3	0.15	10

Lower Cretaceous	3	2.15	0.03	1
Upper Malm	3	2.2	0.08	1
Lower Malm	2.3	2.5	0.02	0.5
Dogger	2.5	2.2	0.02	1
Lias	1.8	2.5	0.02	0.5

CMG uses standard approaches from thermodynamics and fluid dynamics to solve for fluid flow, heat conduction and other physical processes. Due to the proprietary nature of the software, not all equations are explicitly provided in public documents. However, standard models, based on which CMG's equations are developed, are presented here.

Conservation of mass in a porous medium is expressed by the following continuity equation

$$\partial(\varphi \cdot \rho_f)/\partial t + \nabla \cdot (\rho_f \cdot \boldsymbol{v}) = 0$$

where φ is the rock's porosity (-) and ρ_f is the density of the fluid (kg/m^3); $\boldsymbol{v}$ is the Darcy velocity vector or specific discharge (m/s), defined by Darcy's law.

The wellbore fluid pressure at each layer is obtained by adding wellbore fluid pressure, P_{well1} (at layer =1) to the accumulated hydraulic head, h (m), which is the layer thickness in the well direction (CMG Manual)

$$P_{well} = P_{well1} + \int \rho_{av} \cdot g \cdot dh$$

The downhole volumetric fluid flow rate, q (m^3/s), from a production well at reservoir conditions is given by a radial inflow model that couples the pressure in the wellbore to the average grid block pressure (reservoir pressure)

$$q = \frac{2hk\lambda\,(P_{block} - P_{well})}{\mu\, ln\left(\frac{r_e}{r_w}\right)}$$

where k is the absolute (i.e. intrinsic) permeability (given in m^2) around the well bore, μ is the dynamic viscosity of the fluid (Pa s), λ is a geometric factor (-), which is a function of the size of the perforation and thickness of the grid block intersected by the well, P_{block} is the average grid block pressure or reservoir pressure (Pa) , P_{well} is the bottomhole fluid pressure (Pa) in the well, r_w is the radius of the wellbore (m), and r_e is the well pressure equivalent radius (m), calculated according to Peaceman (1983).

The steady-state heat transport equation defines the heat generation, H (W/m^3), composed of two terms

$$(\rho c)_f \boldsymbol{v}\, \nabla T - \nabla \cdot (\lambda_e \nabla T) = H.$$

An advective term with specific discharge, $\boldsymbol{v}$, where $(\rho c)_f$ is the thermal capacity of the fluid (J m $^{-3}$ K^{-1}) and T is the temperature (K), and a conductive term in which the effective thermal conductivity of the rock-fluid mixture λ_e (W m^{-1} K^{-1}) is assumed to be isotropic.

Thermal power and cumulative energy production are calculated to compare the thermal potential for the different well configurations. Thermal power P_{th} (W=J/s) is the rate at which heat energy is transferred in a thermal power plant, calculated using the following formulation

$$P_{th} = \dot{m}\, c_P\, \Delta T$$

where $\dot{m}$ is the fluid mass flow rate, c_P is the specific heat capacity at constant pressure and ΔT is the temperature difference between the fluid production temperature and the fluid reinjection temperature. Cumulative thermal energy production, E (J), is the total amount of thermal energy generated over a period of time (s), calculated by

$$E = \int P_{th}(t)\ dt$$

where $P_{th}(t)$ is the thermal power at time t and dt is a small-time interval.

It is to be noted that the gridding approach adopted in this study is based on the original corner-point gridding from the geological model, which was retained when importing the model into the CMG simulator via the Rescue File option. This ensures that the grid structure aligns with interpreted horizons and fault throws, preserving the integrity of the geological interpretations. No regridding was performed in CMG, except for local refinements of the grid cells intersecting the wells by 5 times in both x and y direction to capture the pressure variations close to the well with higher accuracy (can be seen in Figure 16b). The refined block has a resolution of 0.2 times the original x and y dimensions of the grid block (Peaceman, 1983). CMG provides a robust methodology for handling deviated well completions. The simulator calculates well indices based on geometric information, incorporating parameters such as the well angular fraction (wfrac), completion factor (ff), well radius (rw), skin, and perforation length (h).

3.4.3 Simplified multi-lateral well designs and modeling scenarios

Well design and geometry for optimized production from geothermal wells depend largely on the drilling technology and reservoir conditions. The technical aspects related to well designing and drilling are not within the scope of the present study. A simplified well design consisting of a main borehole with three laterals is created for comparative analyses of production increases with each lateral well (Figure 16a). It is assumed that a vertical well of standard sections will be drilled until the desired depth of interest is reached, following which the well is deviated, and slim holes with a diameter of 6 inches or less are drilled horizontally using the DEPLOI DSSD technology (Blangé et al., 2022), described elsewhere in this report. The lateral slim holes are not cased and hence the entire slim hole length will be in direct contact with the reservoir. Two production constraints are applied in all simulations: a maximum surface water rate of 25000 m^3 per day and a maximum fluid pressure drawdown (changes with reservoir depth). These limits ensure that the reservoir fluid pressure does not decline excessively relative to the initial or reference pressure, helping prevent rapid depletion and maintain long-term reservoir performance.

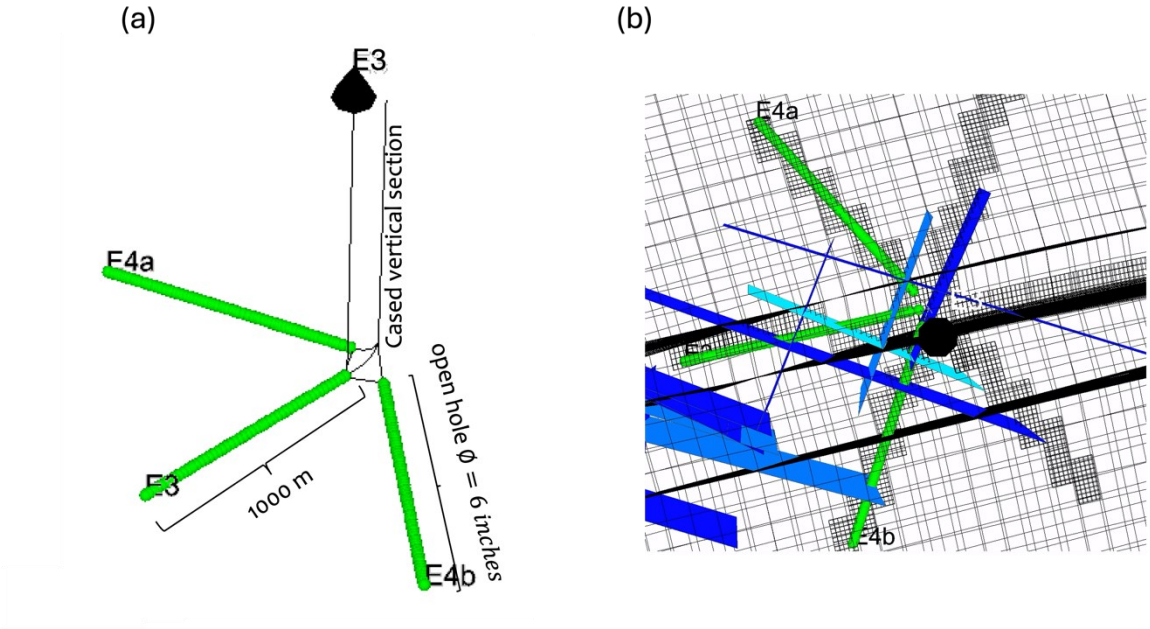

Figure 16 a) Example of a multi-lateral well design used for modeling in CMG, the green ends of the laterals (E3, E4a and E4b) indicate open hole section (b) Zoom out of intersection of wells with the fracture corridors (in blue)

Two different well depth scenarios are investigated to evaluate production from the LC and UJ, respectively. Additionally, within each reservoir, two locations are investigated: the western part of the model, where the well configuration is located around 1.5 km to the west of the GEo-1 well (Figure 17- left) and the eastern part of the model, where the well configuration is approximately 2 km to the east of GEo- 1 well (Figure 17- right). The wells in the western location start with the prefix 'W' while the ones in the east start with 'E'. In the LC reservoir, the vertical depth of the main borehole is 626 m. At this depth, it is assumed that the well is deviated and three lateral wells E1, E2a, and E2b, of length 1000 $\pm$ 50 m at angles of $\pm$ 60°, are drilled horizontally within the reservoir. Note that the optimum angle between multiple horizontal wells, drilled from a single main borehole, depends on the reservoir characteristics, operational goals, and stress orientations. A dedicated reservoir modeling study is encouraged to determine the most effective angle to maximize productivity. Within the deeper UJ reservoir, the main vertical borehole is 1500 m long and the three laterals E3, E4a, and E4b are of length 1000 $\pm$ 50 m. Figure 16a shows the multi-lateral design for the wells in the UJ reservoir (left), and Figure 16b provides a closer look at the intersection between the fractures and the wells (right). The trajectory and spacing between the wells are identical in both reservoirs, the only difference being the length of the vertically cased section of the borehole. A wellbore simulator is used for modeling changes in temperature and pressure inside the wellbores. The closed section of the well, i.e., from the first perforation to the land surface is vertical and hence the semi-analytical model (SAM) of the simulator CMG is used to account for the heat loss and pressure drop within the well bore.

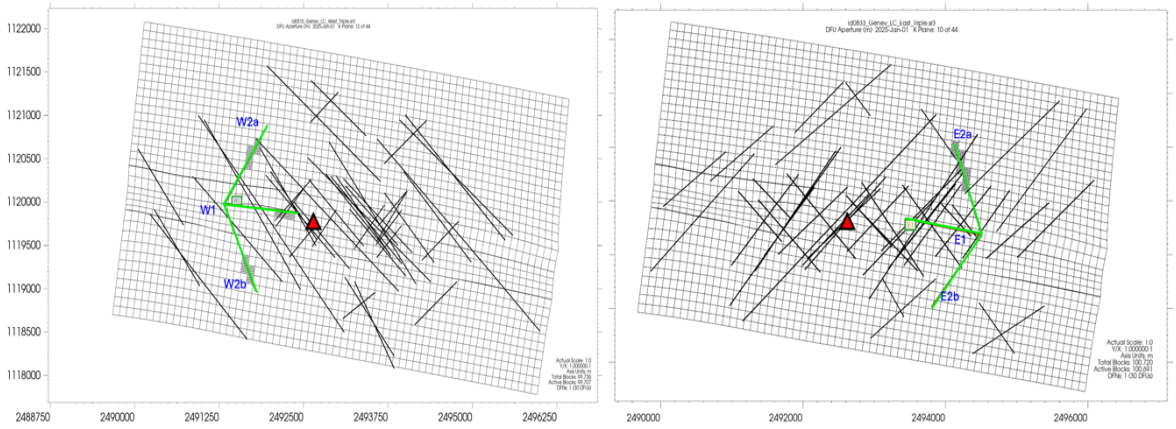

Figure 17: Top view of two random realizations of FC static models: left- with dominant fractures in the NW-SE direction and western multi-laterals, right –with dominant fractures in the NE-SW direction and eastern multi-laterals. The red triangle in both figures shows the location of well GEo-1.

Table 3: Conceptual well design parameters

	Lower Cretaceous (Eastern and Western configuration)	Upper Jurassic (Eastern and Western configuration)
Length of vertical	626 m	1500 m
Length of lateral	1000 m	1000 m
No. of laterals	3	3
Temperature gradient	~ 307 K	~ 329 K

3.4.4 Techno-economic model

Evaluating the economics of a geothermal field typically involves assessing a range of parameters, which can be broadly categorized into capital costs (CAPEX), operational costs (OPEX), energy production over time (temperature, flow rate), and efficiency metrics such as Levelized cost of Energy (LCOE). CAPEX includes costs of exploration (geological surveys, geophysical studies), permissions, drilling wells, infrastructure, and surface equipment that covers the cost of the power plant, heat exchangers, and other required facilities for extracting subsurface energy. OPEX includes parameters such as costs of well maintenance, surface facility upkeep, and other operation and maintenance costs. The techno-economic calculations in this study are performed using an in-house numerical simulator TANGO (Techno-economic ANalysis of Geo-energy Operations), developed by the GEG group at ETH Zurich. TANGO is built upon the open-source, python-based techno-economics calculator genGEO – generalizable GEOthermal simulator (Adams et al., 2021) that can estimate capital costs of geothermal power plants and provide LCOE values. The LCOE ($/kWh), calculated as the ratio of the present average capital cost of the energy generation to the total energy generated over the lifetime by a particular technology, is one of the fundamental parameters used to assess the economic value of a geothermal project. The LCOE is calculated using the following equation:

$$LCOE = \frac{C_{geothermal}}{\underline{W}} . \frac{CRF + F_{O\&M}}{CF * 8760}$$

where $C_{geothermal}$ is the geothermal plant capital cost, $\underline{W}$ is the capacity of the plant (in MW_{th}), CRF is the capital recovery factor, CF is the capacity factor and $F_{O\&M}$ is the fraction of operating and maintenance cost including the cost of electricity required to run the surface power plant . CRF is the factor by which a present capital sum is multiplied to find the future repayment series that will exactly recover it with interest. CF is the unitless ratio of actual electrical energy output over a given period to the theoretical maximum electrical energy output over that period. The ratio of the total geothermal capital costs to the capacity of the plant provides the specific capital cost,

$$SCC = \frac{C_{geothermal}}{\underline{W}}$$

SCC, measured in dollars per kilowatt ($/kW), refers to the upfront investment required to construct a power or heat generation facility. It includes the cost of drilling wells, installing infrastructure, and all initial expenses necessary to bring the geothermal field online. SCC can vary widely due to factors such a well depth, temperature, geology and technology. However, unlike $LCOE$, SCC does not depend on financing assumptions and hence is a more direct way to compare the economics of geothermal plants. In this work, LCOE will be referred to as LCOH (Levelized Cost of Heat) in further analyses.

The primary components of the capital cost model included in the calculation are the costs related to drilling wells, permissions, exploration, surface gathering system (surface piping system), and surface power plant. The total cost of the wells is the sum of the cost of the vertical section of the main boreholes, which is assumed to be drilled in a conventional manner, plus the cost of drilling the lateral sections using the DSSD technology plus the cost of a 500 m injection well. The average costs of drilling the vertical sections (including consumable rig costs, casing, mobilization/ demobilization and 20 % contingency) is approximated to be around 1300 €/m. For the lateral well sections, drilled using the DSSD technology, the cost estimate, assuming a low Rate of Penetration (ROP) of 10 m/hr is 355 €/m (estimates provided by Canopus Drilling Solutions). The cost includes rig, pumps, drill pipe, energy, consumables such as steel shots and bit, DSSD system, costs of mobilization/demobilization, and 20 % contingency. Since the laterals are to be in direct contact with the reservoir, casing is not included in this estimate. These costs are converted to USD for further calculations. Costs related to permission, exploration, surface gathering system, and surface power plant are calculated using models described in Adams et al. (2021). For calculating the LCOH, a discount rate of 9.6% for a system or financial lifetime of 20 years is considered. All results are in 2019 USD adjusted using producer price index multipliers reported by the U.S. bureau of Labor Statistics (BLS).

4 Results and discussion

The relevant aspects of the novel direction steel shot drilling (DSSD) technology have been assessed based on the information and expertise gained during the trial at Versuchstollen Hagerbach (VSH). The findings are presented and discussed in Section 4.1. The results of the modeling activities, focusing on the productivity and economic impact of the DSSD technology for medium-deep, fractured geothermal reservoirs in Switzerland are presented in Section 4.2.

4.1 WP2: DSSD Technology Trial at VersuchsStollen Hagerbach (VSH) Test Site

Lithology

The cuttings analysis and the optical borehole imager log confirmed that the wellbores have not been drilled in limestone formations as expected from the lithology information provided by VersuchsStollen Hagerbach. The lithology is dominated by black slate which is intersected by quartzite layers clearly visible as white bands in the log as well as in the collected cuttings. The gamma ray log confirmed the lithology change by a reduced gamma ray count when logging a quartzite layer (see Figure 19).

Impact of the steel shot erosion on rate of penetration (ROP)

The standard practice during the VSH-trial operations when started drilling after adding a new drill pipe joint to the drill string incorporated to first start the circulation to a modest flow rate, then rotate the bit to bottom, and then drill gently at a low weight on bit of about 1 kdaN. Then the flow rate was increased to the desired setting. After drilling operation was set to this stable mode, the steel shot injection was turned on. It took about 30 sec for the particles to arrive at the bit. The down hole arrival of the steel shot made the pump pressure increase by up to 14% which could be monitored well on surface.

Apart from the pump pressure increase, the arrival of steel shots at the bit was also directly observed by the driller. In order to keep the WOB settings constant, the driller had to increase the rate of penetration (ROP). The impact on the ROP was large during the initial drilling tests and resulted in ROPs above 80 m/h. These very high drill speeds requested an adjustment of bit settings to avoid bit damage.

The recorded data include ROP, WOB, string RPM, string torque, pump pressure, flow rate and injection rate. From this data the combined action of the PDC-bit cutters and the steel shot erosion can be investigated. The indication of the impact of the steel shot erosion action on ROP during the trial is as follows:

- At 60RPM, flow rate 500 l/min, pump pressure 117 bar, and WOB 1 kdaN, the circulation of 1.0% of steel shot made the ROP increase from 4 m/hr to 15 m/hr. An increase of the steel shot concentration to 1.2%. increase the ROP further to 20 m/hr.
- At flow rate 550 l/min, pump pressure 195 bar, WOB 1 kdaN and 40 RPM an increase of 10 m/hr to 20 m/hr ROP with lower steel shot concentration of 0.7% has been recorded.

The ROP data recorded during the field trial are plotted in Figure 18 next to the ROP performance data from laboratory tests conducted at TNO's Rijswijk center for Sustainable Geo-energy (RCSG). At the operational settings used during the trial, the steel shot erosion increases the ROP by a factor of two to four. This impact of the steel shot erosive action on the ROP is partly an effect of the low WOB setting resulting in a non-optimized mechanical drilling process and hence, a strong performance gain. While a realistic drilling operation in harder rock type would aim for higher WOB, the ability to drill at high ROB with reduced WOB has the advantages to limit mechanical load on the PDC cutters and can increase the bit life.

High ROP increases at low WOB settings (1 kdaN) have been demonstrated in laboratory tests executed at TNO's RCSG laboratory (see Figure 18). For competent concrete (UCS ~75 MPa) and hard limestone (UCS ~110 MPa) increases up to factor of 3 (concrete) and 15 (limestone) have been recorded with high steel shot concentrations. Likewise, the laboratory test of the VSH limestone resulted from 2 m/h to 16 m/h (factor 8) at comparable settings. The expectations for realistic drilling operations at depth in harder rock types is a factor of 2-3 in ROP gains. The test results reported from the VSH trial and laboratory work are often higher due to the unoptimized mechanical drilling. This effect is pronounced in hard rock like the Belgian limestone. For a reliable extrapolation to performance at larger depth, at higher WOB and higher bit pressure drop is required in future tests (filed and laboratory).

During the field tests the low strength slate type of rock requested reduced settings in terms of WOB, bit pressure, and steel shot concentration to mitigate extremely high ROPs. Initially. ROPs of more than 80 m/h have been achieved and resulted in a damaged bit when a very hard quartzite layer was intersected suddenly.

The VSH-trial confirms qualitatively the considerably ROP increase that can be realized when combine mechanical PDC drilling action with DSSD steel shot erosion. The results are in-line with the observations from the laboratory test campaign. The unexpected low strength of the drilled rock in this trial doesn't allow to operate at higher WOB settings due to the risks of bit damage when intersection hard fracture fillings (quartzite). In order to map the performance of the DSSD technology at realistic downhole, hard rock drilling conditions, further testing (i.e. at the RCSG laboratory) should be performed.

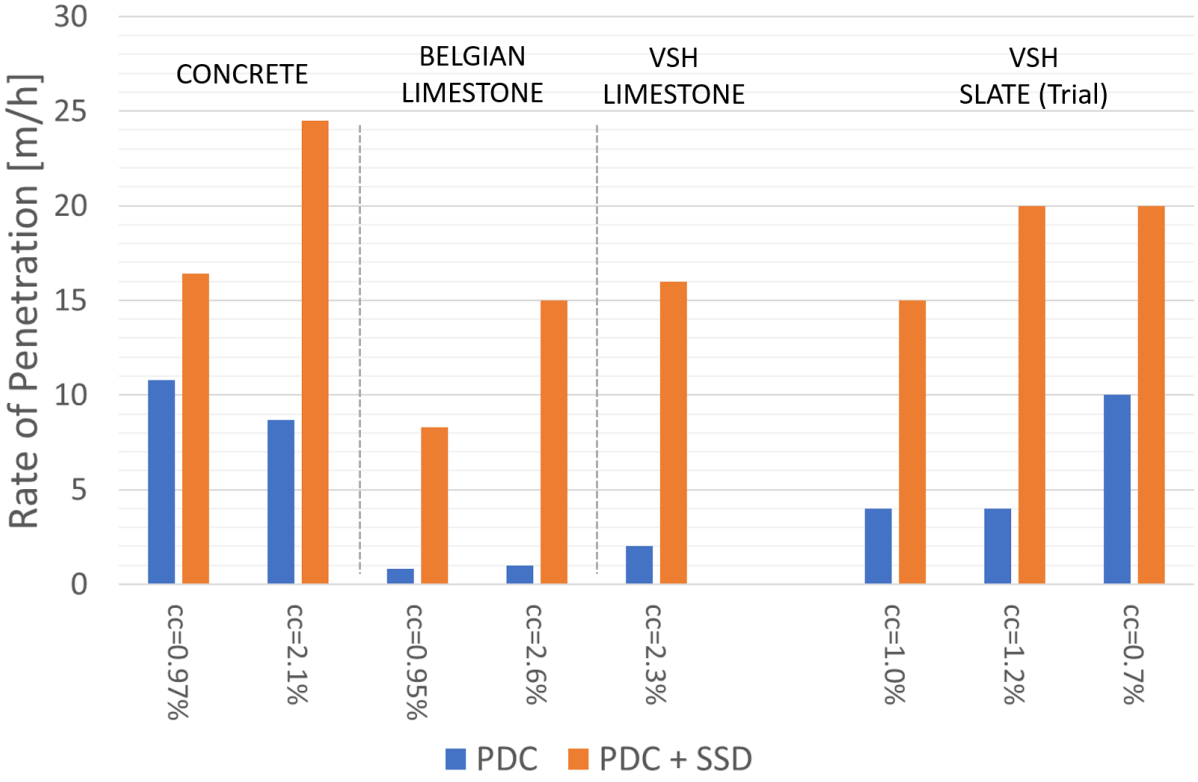

Figure 18: Comparison between PDC and steel shot drilling on ROP from laboratory tests (left) and the VSH trial (right)

Steel shot returns have been optimized during the second of the two drilled wellbores by means of better wellbore cleaning control. In the second wellbore no steel shots have been encountered during the logging campaign while the first wellbore had left steel shots in the well. The optimization of the steel shot returns is an important parameter during a drilling campaign. It has been demonstrated in previous work that the steel shot transport can be handled with standard hole cleaning calculations. Washouts and break-outs enlarging the wellbore diameter can results in settling and deposit of steel shots due to lower flow velocities. Likewise, loss zones like intersected fractures can result in flow velocity drop of losses of steel shots in fracture sets. These factors resulting in reduced returns of steel shots should be taken into account during a field campaign planning. The return of steel shots have not been quantified during the trial. Key factor beside the flow rate control was the separation of steel shots from cuttings. During the VSH trial, a single stage magnetic drum separator was used for this process (Figure 3) resulting in about 90 % of steel shot separation (estimate). An optimized separation

process (e.g. dual stage) can realize an efficiency of about 99 % steel shot reuse / recirculation during DSSD drilling operations.

Bore hole quality

The caliper run (CAL) and the acoustic borehole imager (ABI) run was utilized during logging to investigate the borehole quality. Changes in the radial extension of the arms (wellbore 2) are plotted in Figure 19 together with the nominal bit diameter of 104mm to visualize the deviation from a barrel type borehole.

In general, the wellbore is slightly overgaged with some pronounced groves / wash-out sections and short section with a very neat wellbore diameter. The neat wellbore diameter could be realized whenever the bit drilled through competent quartzite formations. Quartzite is in contrast to the slate not prone to wash-outs. The neat wellbore and presence of quartzite is confirmed in the gamma ray response (lower activity) as well as in the acoustic borehole imager which is plotted as computed borehole diameter.

Further down in the wellbore (56m onwards), the wellbore diameter is more controlled. At this stage, the pressures drop over the bit and the steel shot concentrations have been reduced to avoid washing out of slate formation.

At some depths levels distinct grooves were found in the caliper log. These groves correspond to a stop of drilling operation for adding a drill pipe. When making connections, the injection of steel shot was stopped temporarily. Hence, the clean water jets were powerful enough to remove rock by jetting of the slate formation. This might be an effect of the low hydrostatic pressure in the wellbore. At lower ambient pressures, a water jet can cavitate and the cavitation itself can have a damaging effect. Usually, this effect is suppressed at 10-20 bar hydrostatic head corresponding to a vertical depth of 100m – 200m.

The grooves seemed more pronounced at 600 l/min flow rate. At 500 l/min the grooves were minor. However, the hole cleaning required at least 550 l/min and preferably 600 l/min and some wash-outs due to the jetting action could not be avoided. To avoid cavitation, the bit pressure drop should not exceed 150 bar which is an important learning for future shallow demonstrations of deployments of the drilling tool. The nozzle size of the bit must be adapted in these situations to allow for sufficient flow rate while the maximum pressure is not exceeded.

The steel shot laden jets of the DSSD technology also created grooves when stopping ROP for a connection and circulating the steel shots out before stopping the drilling operations. It is therefore important to circulate steel shots out timed with the break of operations. An operational sequence reducing the flow rate just before lifting the bit from bottom and stopping the pumps and string rotation can have a supportive effect to limit the wash-outs.

For the directional control and the open hole side tracking, the capability of reaming a hole at the right moment and in the desired direction is important. The results above show that this desired reaming capability should be balanced by the suppression of the unwanted reaming. This balance is controlled by the magnitude of the desired steering action, the orientation and diameter of the nozzles in the bit, the hydraulics, the steel shot concentration in the drilling fluid / jets, and the best operational practices.

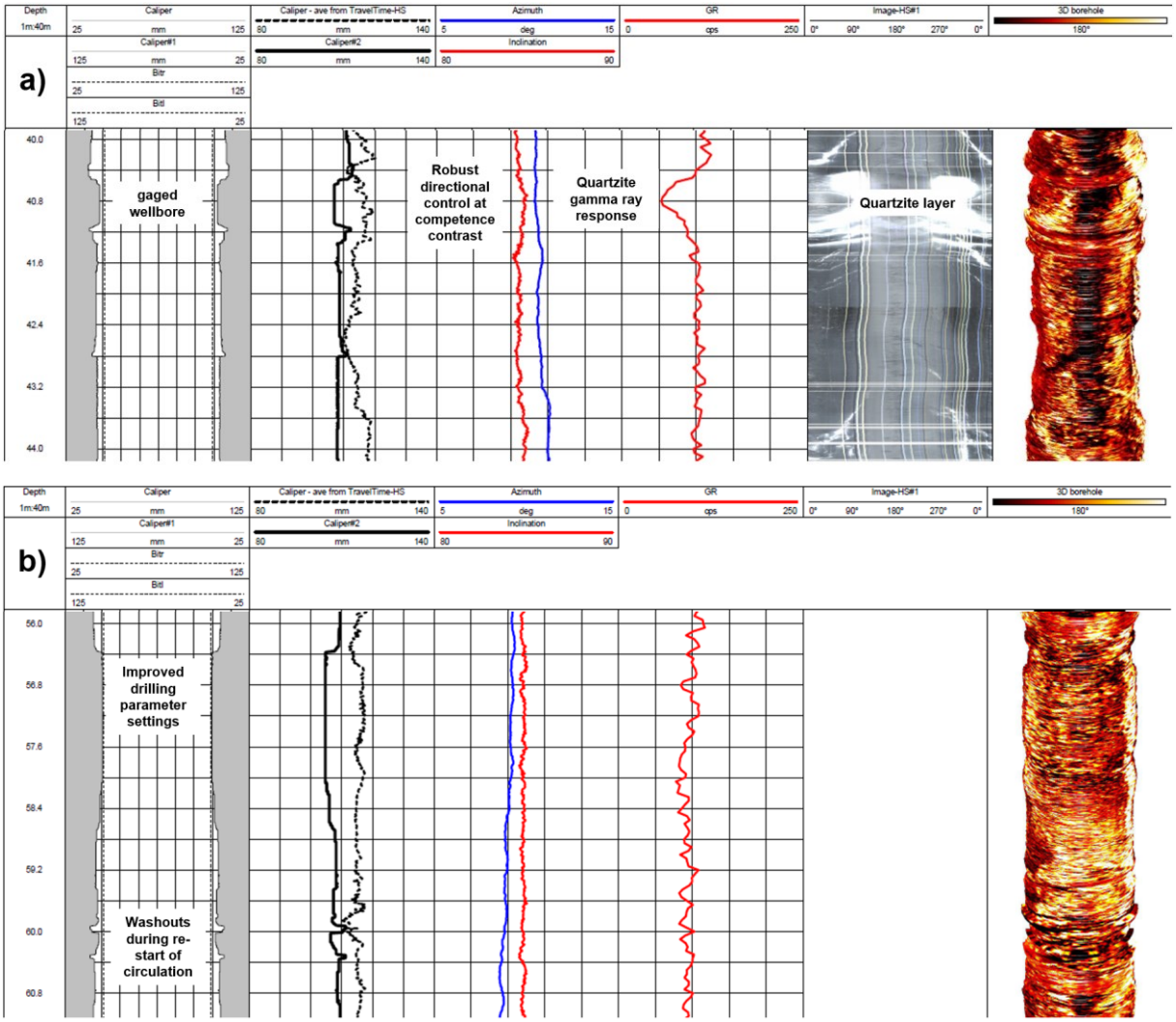

Figure 19: Selection of logging data from two depth intervals of the second wellbore (a) highlighting the presence and impact on wellbore quality of the competent quartzite layer and (b) demonstrating the improved drilling parameter settings adjusted for the softer slate drilling.

Bore hole trajectory

The bore hole trajectory was measured by the directional module (DM) in the EM-telemetry assembly, by a gyro run up to 50 m (along hole) depth through the drill pipe and by a surveying module in the logging suit deployed in open hole after demobilization of the rig.

The EM telemetry only recorded good surveys during string rotation breaks while adding a new joint. The reason for this limitation could not be fully clarified. The DM-measurements could have been hampered by a steel shot bed in the bore hole at the location of the sensors as the presence of steel impacts the magnetic field. The gyro run through the drill pipe could only reach the top of the drilling assembly and required some operational time. It was used in the beginning of wellbore 1 solely to independently confirm the wellbore trajectory without pulling pipe.

Running the open hole logging tool string produced a continuous log measuring the wellbore trajectory. The logging tool string had to be pushed manually through the horizontal open hole. Wellbore entry with the stiff centralized logging assembly was possible down to 89 m of wellbore 2. The wellbore irregularities and undulations and potential the curved trajectories hampered a deeper log.

All directional measurements together provided a reliable overview of the two wellbore trajectories. The gyro run confirmed the measurements of the DM in the drilling assembly while drilling wellbore 1. The potential presence of the steel shot on the low side of the horizontal wells apparently did not impact the magnetometer detection of the earth magnetic field.

The survey runs of the open hole logging were utilized in the first wellbore to cross-check the measurements of the DM and for the second wellbore a direct comparison between DM data and the logging survey could be made.

Due to the limited entry into the first wellbore with the logging equipment, no steel shot drilled sections could be logged and it was decided to focus on the second wellbore. It was found that the initial 30m of the first wellbore where dipping from 85° to 80° inclination and the standard drilling assembly used for this section had some drop tendency due to limited stiffness. Hence, Canopus stiffer drilling assembly was deployed without steel shots for drilling the initial 25m of the second wellbore.

A slight drop tendency from 88° to 83° has been observed and further in the drilling operation of the second wellbore, the wellbore has been drilled slightly upwards to compensate for the initial dip and then the inclination has been maintained at 85° inclination.

The direction data show an intentional turn in azimuth of the DSSD drilling assembly between 55m and 68m and then back to the original trajectory from 68m to 84m (along hole) depth. From the survey data the so-called dog leg severity (DLS) can be computed which expresses the change of azimuth or inclination per 100 ft (30m). The two dedicated steel shot steering actions that had been logged in wellbore 2 resulted in:

- ~2.0° to the left over 13m → 4.5 deg/30m DLS
- ~2.0° to the right over 16m → 3.8 deg/30m DLS

The measurements of the DM reported a somewhat stronger DLS of about 6.6 and 5.5 deg/30m in these sections. Both measurements, the DM and the open hole log show the same trend and the difference might be due to the accuracy of the magnetic field measurements or an influence of steel shots which might be present in the wellbore. Both surveys are based on the same measurement principle.

To determine the (limited) directional tendency of the bottom hole assembly without any steering action, a wellbore length was drilled without steering action. The inclination was found to be constant at 84° and the azimuth constant at 10°. The DLS is this section was less than 0.3 deg/30m confirming the very good angle holding capability of the assembly.

In advance to the drilling operations, the drilling assembly had been modelled by Canopus to be angle holding without steel shot steering action and to be able to turn with at least 5 deg/30m DLS. The modeling results could be confirmed with the field results reporting realized DLS between 3.8 deg/30m and 6.6 deg/30m (min. and max. of both measurements). A higher concentration of steel shots might result in even stronger steering action if the stiffness of the drilling assembly allows for this. The steel shot concentration has been limited during this phase of the trial drilling operations.

The logging run in wellbore 2 highlighted that intersecting of the competence contrast between quartzite layers and slate at pronounced incidence angle did not have an impact on the directional drilling trend (see Figure 19).

4.2 WP3: Statistical numerical modeling and techno-economic analysis of reservoir development with DSSD laterals

Dynamic simulations were performed in a total of 1000 static realizations of fractured carbonates to simulate the production behavior from different reservoir depths and well configurations, resulting in a total of around 12000 simulations. In this section, the results of the dynamic simulations will be discussed for the target reservoir candidates. To compare the increase in production related to the addition of

lateral wells, simulations were performed in three phases for each geological realization of a fractured reservoir: first producing only from a single lateral, later increasing the production from two laterals, and finally producing from all three laterals. Each of the simulations was run for a period of 20 years. The absolute value of different parameters, such as production rates and thermal energy are strongly driven by geological assumptions and production constraints used for dynamic modeling. Similarly, the values of LCOH are driven by financial assumptions. Hence, the reported numbers should be used cautiously with full knowledge of the applied boundary conditions. Absolute values are, therefore, only indicative, while the focus of this study is the relative difference in the values among different well configurations.

4.2.1 Lower Cretaceous (LC)

Reservoir Productivity and thermal energy output:

The histograms below (Figure 20 and Figure 21) show the distribution of production rate (in m3/day) and cumulative energy (in PJ) at the end of 20 years for three types of well configurations: single lateral (blue), dual lateral (red), and triple lateral (yellow) for 1000 geological scenarios in the eastern and western part of the lower cretaceous (LC) reservoir.

Location - 1: Eastern wells *(Figure 20)*

For the single well configuration, a high number of realizations has a production rate between 500 and 1800 m^3/ day, with the majority of the realizations producing around 800 m^3/day. The distribution is skewed towards lower values, with a few outliers producing rates higher than 1800 m^3/day, but they are rare. The 20-year cumulative thermal energy output varies accordingly between 0.1 PJ and 0.4 PJ, with the majority of the cases resulting in a cumulative energy production of 0.2 PJ. In the dual lateral well configuration, the majority of the simulations show a final production rate between 800 and 2400 m^3/day, with a most likely production rate of 1200 m^3/day. The cumulative energy production ranges between 0.2 and 0.7 PJ, with the majority of the cases producing around 0.35 PJ. In the case of triple laterals, most of the realizations result in the wells producing between 1400 and 3200 m^3/day, with some cases reaching close to 3500 m^3/day. The 20-year cumulative energy output varies from 0.3 to 1 PJ. The mode of the distribution is around 2200 m^3/day for the production rate and 0.5 PJ for the cumulative energy production.

Overall, for the single lateral scenarios, the outcomes are more tightly clustered than those of the dual and the triple lateral wells scenarios, suggesting higher predictability in the outcomes. With an increase in the number of lateral wells, the likelihood of intersection and connectivity with the fractures in the fracture corridor (FC) increases, resulting in more variability in permeability distributions across different geological scenarios. This condition is reflected in the histogram of the triple lateral scenarios, which show a wider variation in the production rates as well as in the cumulative energy distribution (Figure 20).

Location-2: Western wells *(Figure 21)*

Like the eastern single lateral wells, the distribution of production rate for single laterals in the western part of the reservoir is right-skewed, varying between 300 and 1800 m^3/day, with the most likely value of 800 m^3/day. A few outliers produce more than 2000 m^3/day. The cumulative 20-year thermal energy production also shows right-skewed distribution with values ranging between 0.1 and 0.5 PJ, while the

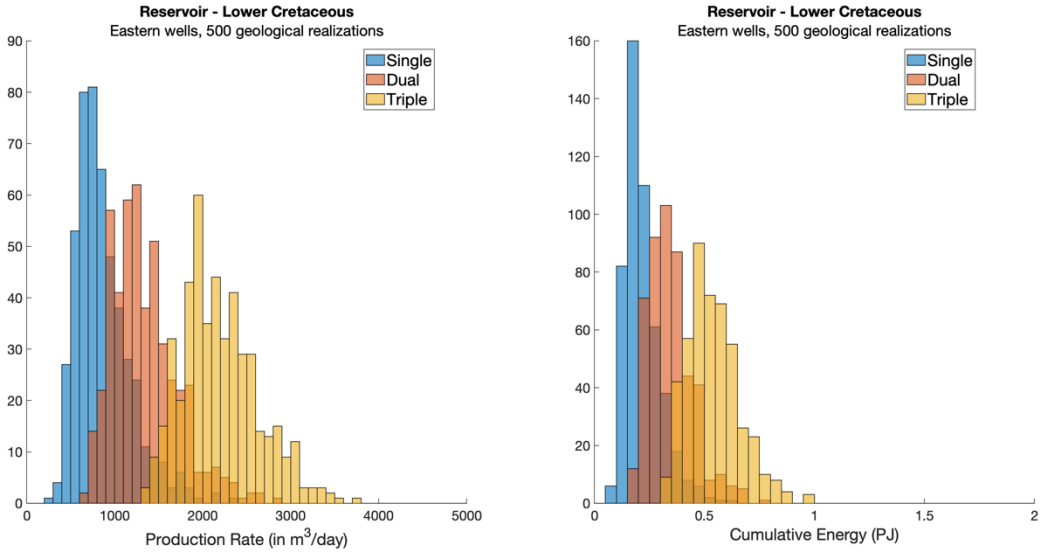

Figure 20: Eastern wells: Left – Production rate from 500 geological realizations at the end of 20 years from the eastern wells. Single lateral (in blue) indicates production only from E1; Dual lateral (in orange) includes production from E1 and E2a; Triple lateral (in yellow) includes production from E1, E2a and E2b. Right – Cumulative thermal energy production in petajoules (10^{15} joules) at the end of 20 years from different well configurations

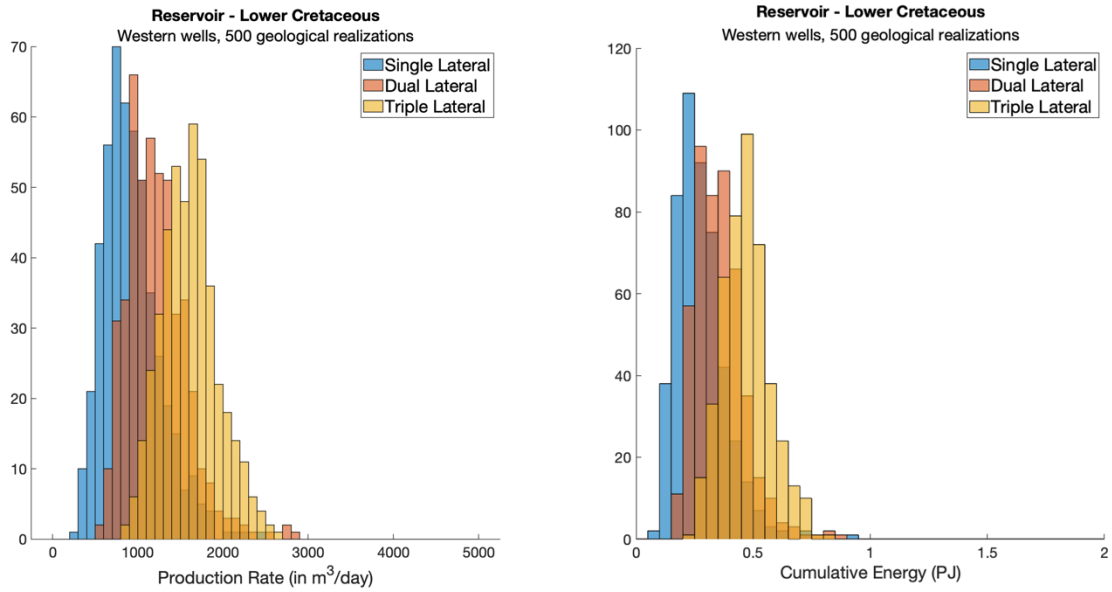

Figure 21: Western wells: Left – Production rate for 500 geological realizations at the end of 20 years from the western wells. Single lateral indicates production only from W1; Dual lateral includes production from W1 and W2a; Triple lateral includes production from W1, W2a and W2b. Right – Cumulative thermal energy in petajoules (10^{15} joules) at the end of 20 years from different well configurations

mode of the distribution is at 0.25 PJ. In the dual lateral well configuration, the majority of the simulations have the final production rate between 600 and 2200 m^3/day, with the most likely production rate of 1200 m^3/day. The cumulative 20-year energy production varies between 0.2 and 0.65 PJ. In case of triple laterals, most of the realizations result in the wells producing between 1000 and 3000 m^3/day. Corresponding cumulative energy production ranges between 0.25 and 0.75 PJ, with a few outliers

reaching 0.8 PJ. The most likely production rate is 1800 m^3/day, while the most likely value for cumulative energy production is 0.5 PJ.

Overall, the western wells have slightly lower production rates and cumulative thermal energy outputs than the eastern wells (compare Figure 20 and Figure 21). This is likely due to the increased thickness and depth of the stratigraphic units moving towards the east, which increase the overall volumetric heat capacity of the layer as well as the height of the fractures.

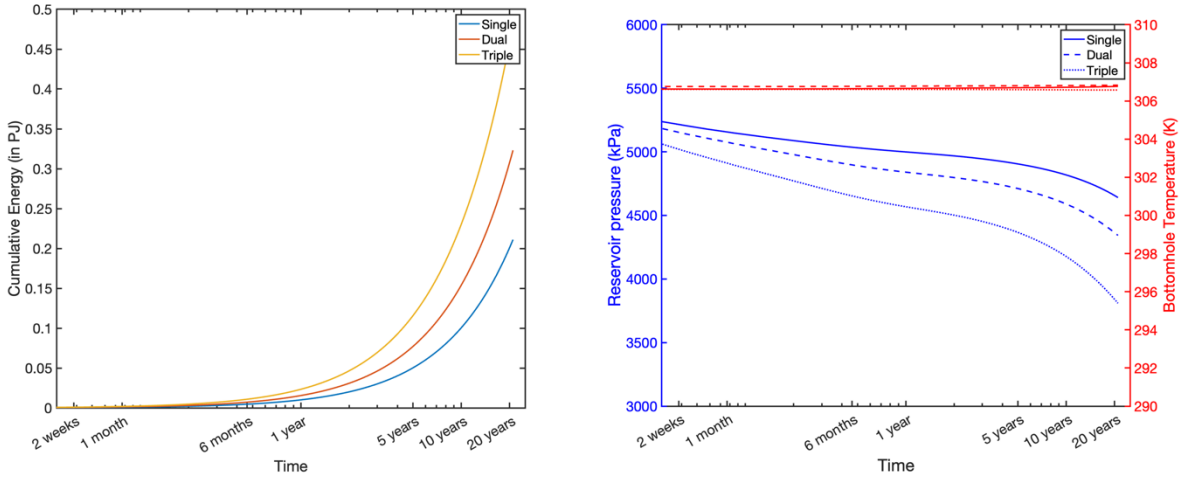

Figure 22: Most likely cumulative thermal energy production (left) and bottomhole temperature (BHT) and reservoir fluid pressure (right) from the LC for a production period of 20 years calculated from 1000 realizations for single, dual, and triple lateral well configurations (see legend).

In Figure 22 we examine the results from all simulations to evaluate the most likely values of cumulative energy production, bottomhole temperature (BHT), and average reservoir pressure over a period of 20 years for all geological realizations in the LC reservoir.

For single lateral well configurations, the most likely production rate is approximately 800 m^3/day for both eastern and western locations, increasing to approximately 1200 m^3/day with the addition of another lateral well (dual lateral wells). The corresponding most likely cumulative thermal energy production over a period of 20 years increases from 0.2 PJ (single lateral well) to around 0.3 PJ (dual lateral well), a productivity increase of ~ 50%. The addition of a third lateral well leads to a most likely production rate of up to 1800 m^3/day and a cumulative thermal energy output of 0.5 PJ (triple lateral well). Although not all triple laterals reach the highest possible thermal energy output, more than 50% of the cases lead to 150% higher production rates, compared to the single lateral well configurations.

For all well configurations, the production rates remain stable with a slight decline over a period of 20 years due to the imposed constraints of constant fluid pressure differentials. Similarly, the bottomhole temperature (BHT) of the fluid is maintained at 307 K (~34 ºC) for all well configurations for the entire production period. This thermal stability may be the result of the large reservoir size and slow heat extraction rates. As geothermal fluids are extracted, the heat stored in the surrounding rock mass slowly diffuses (i.e. conducts) back into the reservoir, stabilizing the temperature and balancing the heat loss from fluid extraction.

The fluid pressure decline (difference between the initial reservoir fluid pressure and the fluid pressure after 20 years) for all realizations is small for all three well patterns. As expected, the highest decline in fluid pressure is observed in the triple-lateral configuration (mean value ~1200 kPa), followed by the dual laterals (~800 kPa), and finally the single lateral (~600 kPa). It is possible that if the simulation

period was longer (50 years or more), a further pressure decline might be observed if the production continues with the same pressure differential (2500 kPa), which might necessitate pressure management strategies. On the other hand, if natural groundwater recharge is sufficient, and fluid production progresses sustainably, there might be enough natural fluid pressure to support continued fluid production for a longer period without the need to reinject produced fluids into the reservoir.

Economics

The net thermal power generated by each of the well configurations and the corresponding total capital costs (CAPEX) and LCOH values for all 1000 geological realizations are shown in Figure 23. The flow rate directly influences the generated thermal power.

As shown in Figure 23, the thermal power for the single lateral configuration varies widely, ranging from 200 kW to 1200 kW for different geological realizations, corresponding to the wide variation in the flow rate as seen in Figure 20 and Figure 21. The total capital costs for all realizations varies between $5.8 million to 6.1 million$, depending on the cost of the heat exchangers, which is a function of the thermal power. The LCOH values range from 0.1 $/kWh to as high as 0.5 $/kWh for the different realizations. As expected, with higher output of thermal energy, the LCOH exponentially reduces for each of the well configurations.

In case of dual lateral configurations, the net thermal power ranges from 300 kW to as high as 1400 kW, depending on the production rates. The total CAPEX ranges from $6.25 million to $6.65 million, a change of around 7-9%, compared to the single lateral well configurations. The corresponding LCOH decreases significantly and ranges between 0.1 $/kWh and 0.40 $/kWh (for some outliers).

In the case of triple lateral wells, there is a significant variability in the thermal power output as a result of the variability in the flow rates, varying between 600 kW and 1600 kW. The CAPEX increases by 15-16%, compared to the single lateral case, while the LCOH reduces significantly with the maximum value of around 0.25 $/kWh

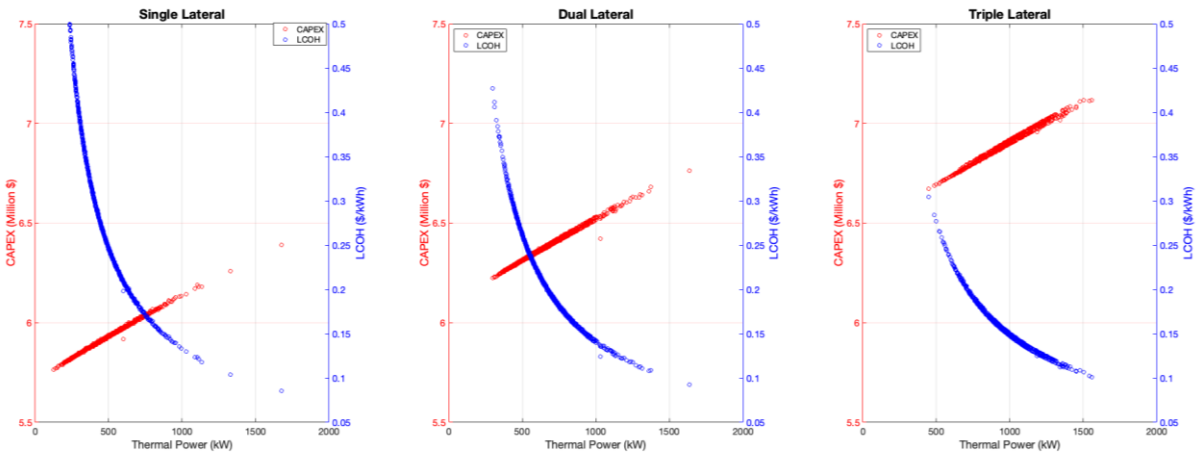

Figure 23: Thermal power (kW) versus total CAPEX ($) and LCOH ($/kWh) for single (left), dual (middle), and triple (right) lateral wells in the LC reservoir.

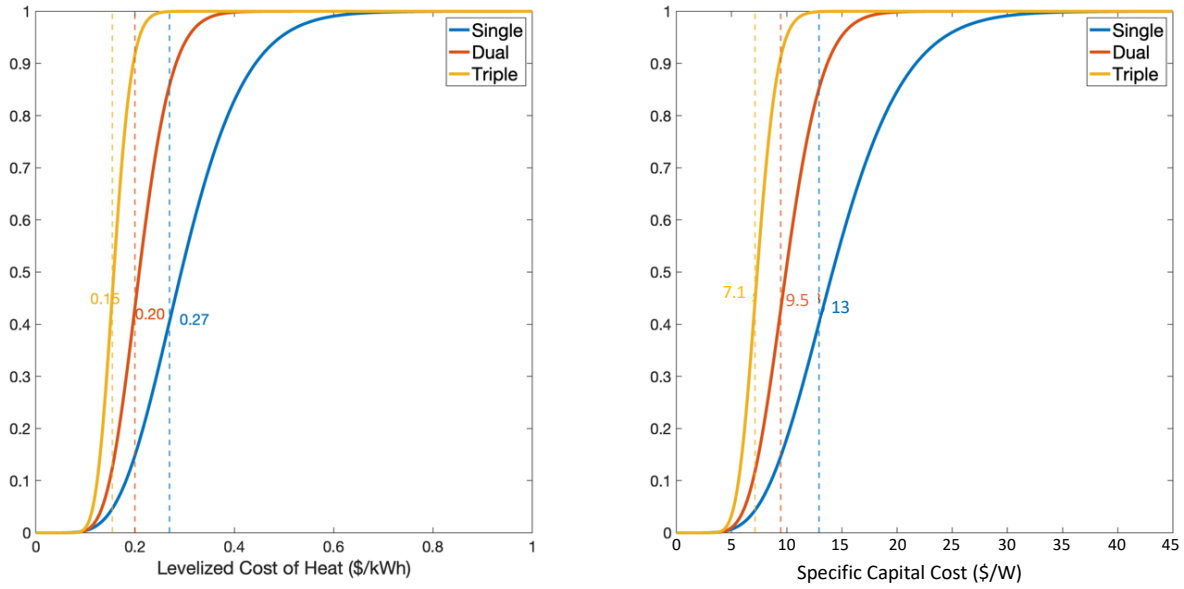

Figure 24: Cumulative Distributive Functions (CDF) of Levelized Cost of Heat ($/kWh) (left) and Specific Capital Costs ($/W) (right) for different lateral well combinations in the LC reservoir. The dashed lines in blue (for single), in orange (for dual) and in yellow (for triple) intersects the distributions at points indicating the most likely values (annotated in the same colors) of the respective parameters for the corresponding well configurations (shown in the legend)

The overall economic feasibility of geothermal projects with different lateral combinations can be evaluated using the two economic metrics: specific capital cost (SCC) and levelized cost of energy (LCOE), here specifically Levelized Cost of Heat (LCOH). Figure 24 shows the Cumulative Distributive Functions (CDF) and the most likely values of LCOH and SCC for single (blue), dual (red), and triple (yellow) lateral wells in the LC reservoir. While LCOH ($/kWh) is a good indicator of the overall cost of energy, considering the lifetime of a project, the specific capital costs ($/W) provide a more direct indication of the present costs of energy generation. The most likely LCOH for the single lateral configurations in the LC reservoir is around 0.27 $/kWh and the SCC is around 13 $/W. The distribution shows a high variability in results as compared to the steeper CDF curves for dual and triple lateral well configurations. For the cases with dual laterals, the most likely LCOH is 0.20 $/kWh and the most likely SCC is 9.5 $/W. For the triple laterals, the most likely LCOH is around 0.15 $/kWh and the most likely SCC is 7.1 $/W, suggesting that the triple lateral well (slim hole) configurations are relatively the most economic case.

4.2.2 Upper Jurassic (UJ)

The histograms below show the distribution of production rates and cumulative energy output (in petajoules, PJ) for different well configurations within the UJ (Malm) reservoirs for the eastern and the western locations:

Eastern wells *(Figure 25)*

In realizations with only single lateral wells, the distribution is positively skewed and concentrated at production rates ranging between 1500 m³/day to 4000 m³/day. The peak is around 2500 m³/day, indicating most of the realizations yield around this rate. Production rates above 5000 m³/day are rare. Corresponding cumulative 20-year thermal energy production for single lateral wells range between

1.5 PJ to 4.5 PJ. The peak of the distribution occurs at around 2 – 2.5 PJ, indicating that most single lateral wells are expected to deliver this amount of energy.

Realizations with two laterals have a broader distribution, with the majority of them producing between 2000 m³/day to 5500 m³/day. The peak of the distribution is at around 4000 m³/day. Very few realizations exceed 6000 m³/day, but beyond this, production rates are uncommon. Dual lateral wells have a broader distribution of energy outputs, ranging from 2 PJ to 6 PJ, with a peak at around 4 PJ. Scenarios with triple lateral wells have the widest spread, ranging from 3000 m³/day to nearly 10000 m³/day, indicating a large variability in production scenarios. The peak is around 4500 - 5000 m³/day, indicating significantly higher production potential. In terms of cumulative thermal energy, the distribution for triple lateral wells is even more wide-spread, ranging from 3 PJ to 10 PJ, with a peak at around 5 PJ.

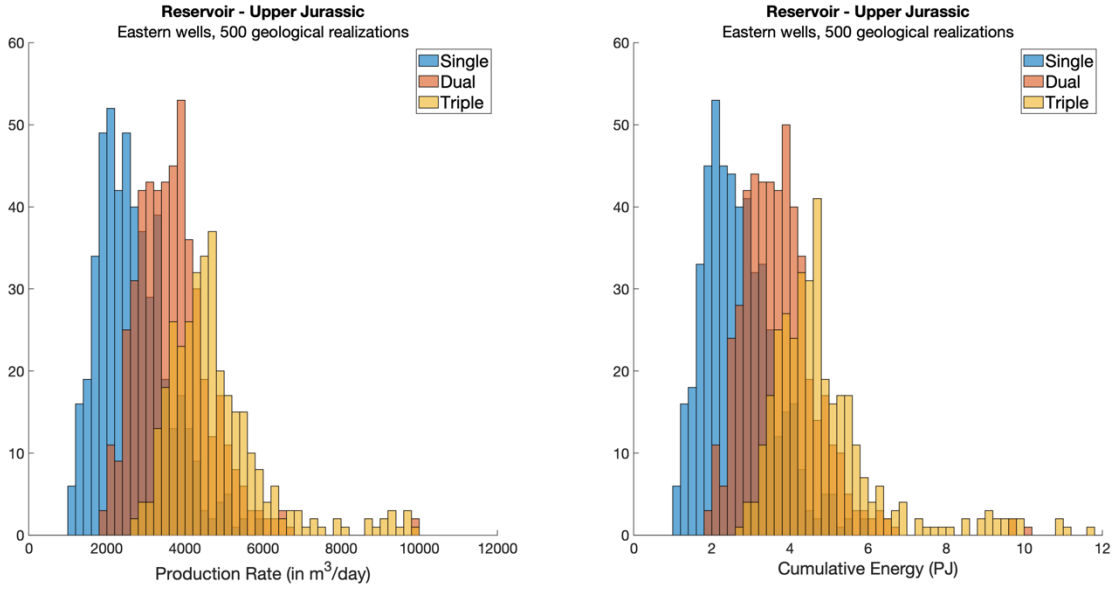

Figure 25: Eastern wells: Left – Production rate from 500 geological realizations at the end of 20 years. Single lateral (in blue) indicates production only from E3; Dual lateral (in orange) includes production from E3 and E4a; Triple lateral (in yellow) includes production from E3, E4a and E4b. Right – Cumulative thermal energy in petajoules (10^{15} joules) at the end of 20 years from different well configurations.

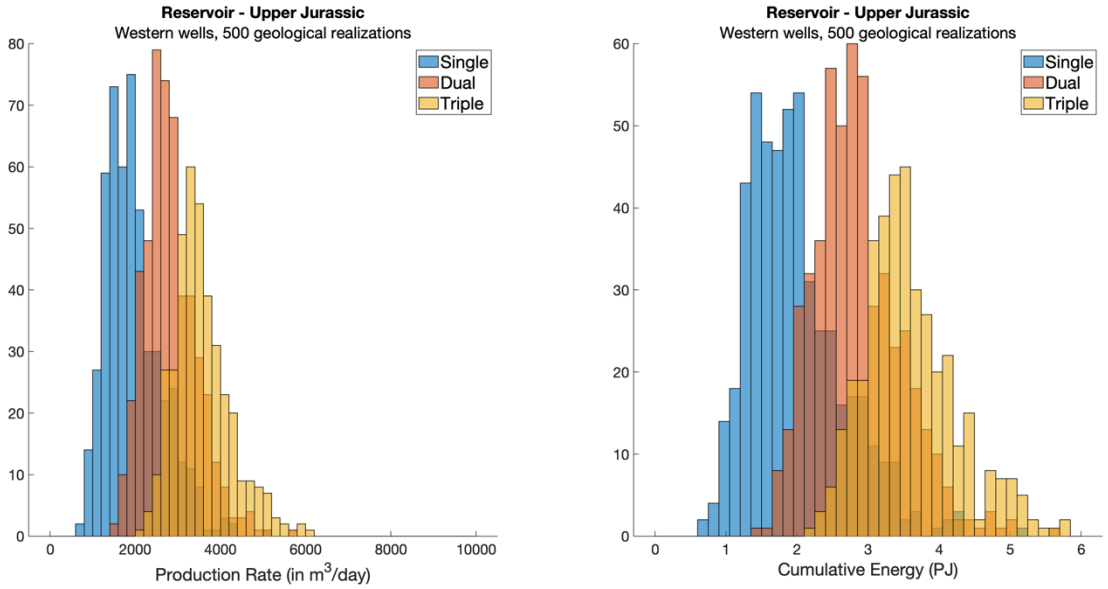

Figure 26: Western wells: Left – Production rate for 500 geological realizations at the end of 20 years. Single lateral indicates production only from W3; Dual lateral includes production from W3 and W4a; Triple lateral includes production from W3, W4a, and W4b. Right – Cumulative thermal energy in petajoules (10^{15} joules) at the end of 20 years from different well configurations.

Western wells *(Figure 26)*

In the western location, production rates from realizations with single laterals range from 1000 m³/day to 4000 m³/day, with the highest frequency around 1800 m³/day (slightly lower than the eastern single lateral). Cumulative energy ranges between about 1 PJ to 3 PJ, with the highest frequency around 1.8 PJ.

The dual lateral wells exhibit a broader distribution, mainly between 2000 m³/day and 4000 m³/day. The mode (most frequent value) is around 2800 m³/day. The dual lateral wells show a broader range of energy outputs, mainly between 2 PJ and 4 PJ, with a peak around 2.5 PJ.

The triple lateral wells show the widest distribution, with production rates spanning 2500 m³/day to 6000 m³/day. The majority of the realizations yield around 3500 m³/day, with very few models reaching higher production rates of up to 6000 m³/day. The triple lateral wells have the widest distribution, with cumulative thermal energy output ranging from 2.5 PJ to 5 PJ, peaking at around 3.5 PJ.

As seen in the LC, the western wells in the UJ also exhibit slightly lower production rates and cumulative thermal energy outputs than the eastern wells. This is likely due to the increased thickness and depth of the stratigraphic units moving towards east, which can increase the overall volumetric heat capacity of the layer as well as the height of the fractures.

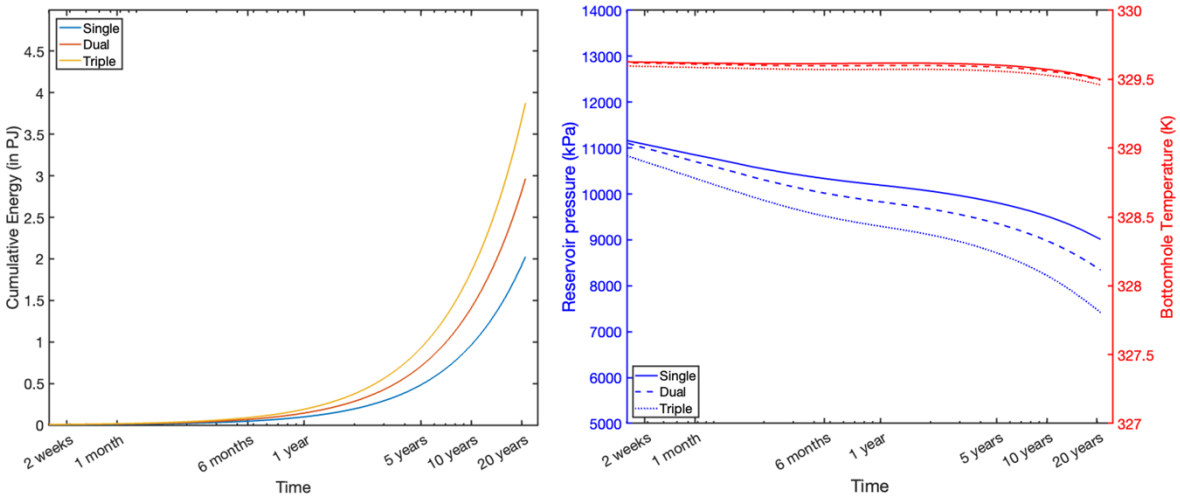

Figure 27: Most likely cumulative thermal energy production (left) and bottomhole temperature (BHT) and reservoir fluid pressure (right) from the UJ (Malm) for a production period of 20 years calculated from 1000 realizations for different well configurations (see legend).

Figure 27 shows the transient behavior over a period of 20 years for the most likely values of cumulative energy production, bottomhole temperature (BHT), and average reservoir fluid pressure for all geological realizations in the UJ reservoir. For single laterals, the most likely production rate is approximately 2200 m³/day, which rises to 3000 m³/day with the addition of a second lateral and further to 4000 m³/day with a third lateral. Correspondingly, the most likely cumulative thermal energy production increases from about 2 PJ for single laterals to approximately 3 PJ for dual laterals, marking a 50% improvement in productivity. With the incorporation of a third lateral, cumulative thermal energy production approximately doubles compared to single laterals, reaching around 4 PJ—a ~100% productivity boost compared to single laterals and a ~30% improvement over dual laterals.

The average reservoir fluid pressure decreases consistently over the 20-year period for all three well configurations, with the single lateral configuration showing the slowest rate of decline and the triple lateral the steepest. The fluid pressure decline (difference between initial fluid pressure and final reservoir fluid pressure after 20 years of fluid production) in the cases of single laterals is around 2000 kPa, while in the cases of dual and triple lateral configurations it is 2700 kPa and 3000 kPa, respectively. It is important to note that the fluid pressure decline in the reservoir is restricted by applying a maximum allowable fluid pressure drawdown as a production constraint. Higher production rates can likely be achieved by increasing the applied fluid pressure differential between the reservoir and the borehole, however, this would lead to larger fluid pressure declines.

The BHT shows only a negligible decrease (< 1ºC) over the 20-year period for all well configurations and maintains a temperature of approximately 329.5 K (~ 56 ºC), suggesting that thermal depletion is not a major concern within the period simulated, which is beneficial for maintaining fluid enthalpy and production efficiency.

Economics

Figure 28 illustrates the average thermal power generated by each configuration and the associated project CAPEX and LCOH for all 1,000 geological realizations in the UJ reservoir. The thermal power for the single lateral configuration exhibits a substantial range, from 1 MW to 8 MW, reflecting the significant variations in volumetric fluid flow rates as a result of variations in geological conditions. The most likely value for the net thermal power is 3 MW, indicating that most of the realizations tend towards this value. The total CAPEX for the single lateral realizations ranges from 7.3 million $ to 9.5 million $, with fluctuations driven by the expense of the heating plant, which depend on the level of thermal power.

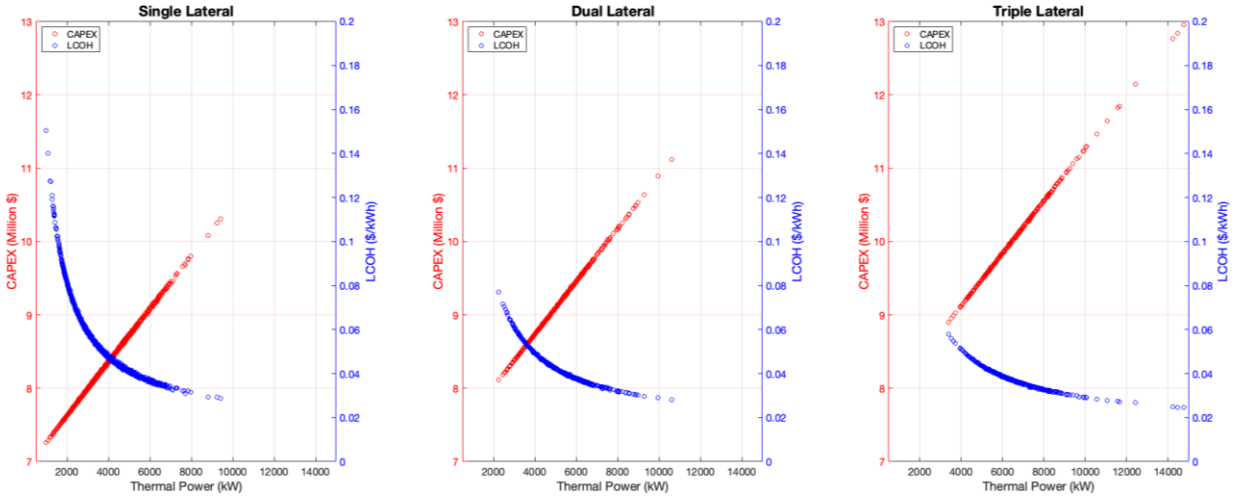

Figure 28: Thermal power (kW) versus total CAPEX ($) and LCOH ($/kWh) for single (left), dual (middle), and triple (right) lateral wells in the UJ (Malm) reservoir.

In the dual lateral scenarios, the net thermal power varies between 2.5 MW and 10 MW across different geological realizations, with a most likely output of approximately 4.6 MW, an increase of almost 50% in the thermal power generation capacity, compared to realizations with single laterals.

Addition of a third lateral further increases the thermal power generation capacity, ranging from 4 MW to 12 MW, with few outliers exceeding 12 MW. The most likely value for the thermal power output for this well configuration is around 6 MW, which is twice the amount (100% increase) produced in the single lateral scenario. Despite these gains in power generation, the total CAPEX, exhibits only modest increases, with the most likely value rising from 8 million $ to 8.8 million $ (10% increase) for dual laterals, and reaching 9.6 million $ (20% increase) for triple lateral configurations.

The right axis in the plots shows the LCOH values with respect to the thermal power. As anticipated, an increase in thermal energy generation leads to an exponential decline in LCOH values across the various well configurations.

Figure 29 shows the cumulative distribution functions (CDF) of LCOH and SCC for various well configurations. In the cases of single lateral well configurations, the LCOH span from 0.025 $/kWh to as high as 0.12 $/kWh, particularly for outlier scenarios, with the most likely value of around 0.053 $/kWh. The distribution is less steep, indicating a broader variation in LCOH across different geological realizations. A few scenarios result in LCOH values exceeding 0.1 $/kWh, which are likely influenced by geological heterogeneity, lower permeability zones, or less efficient heat extraction.

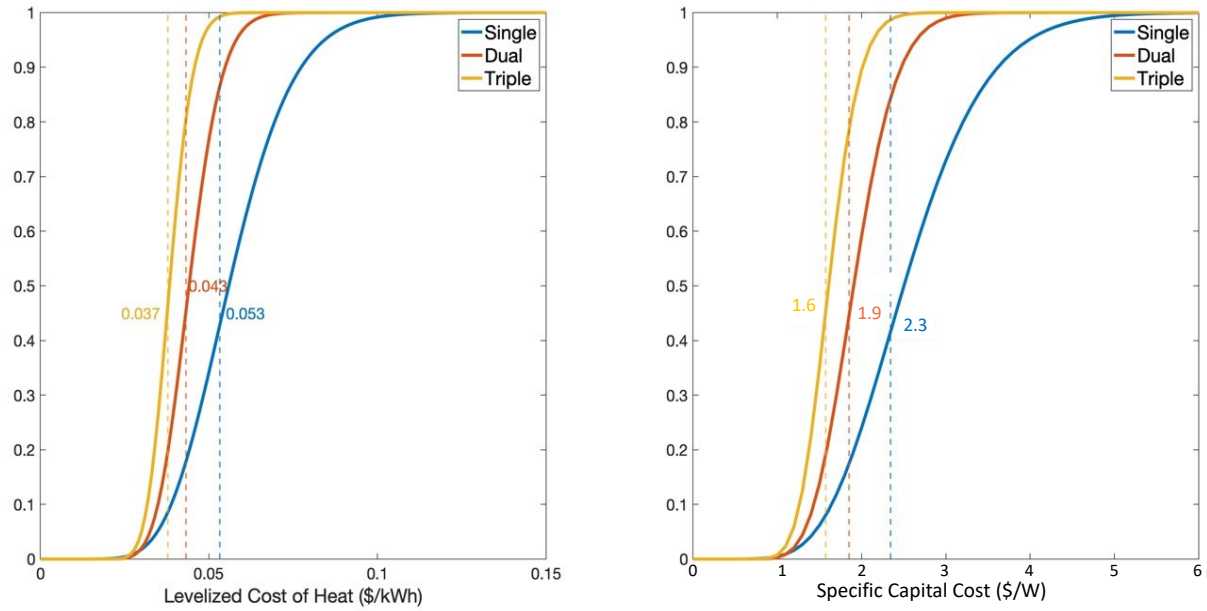

Figure 29: Cumulative Distributive Functions (CDF) of Levelized Cost of Heat ($/kWh) (left) and Specific Capital Cost ($/W) (right) for different lateral well combinations in the UJ (Malm) reservoir. The dashed lines in blue (for single), in orange (for dual), and in yellow (for triple) intersects the distributions at points indicating the most likely values (annotated in the same colors) of the respective parameters for the corresponding well configurations (shown in the legend).

The respective specific capital costs range widely for the single lateral well configuration, varying between 1 $/W to 5.5 $/W, with the most likely value of 2.3 $/W. The gradual slopes for single laterals in both plots indicate greater sensitivity to geological variations, which can lead to cost unpredictability.

In the dual lateral configuration, the LCOH values are reduced significantly, with the most likely value of around 0.043 $/kWh. This configuration's curve is steeper than the single lateral, suggesting more consistent cost estimates across different realizations. The corresponding SCC values are also lower, with the most probable value of 1.9 $/W.

The triple lateral configuration has the lowest LCOH, with the most likely value of 0.037 $/kWh. The steep distribution shows that most of the realizations tend towards lower LCOH, providing the most economically beneficial heating costs consistently. The corresponding SCC for triple laterals is approximately 1.6 $/W, suggesting that this configuration shows the lowest and most stable SCC across different geological realizations.

5 Conclusions

The DEPLOI the HEAT-CH project successfully demonstrated the first ever field trial of the novel DSSD technology in WP2 and demonstrated the potential of slim-hole multi-lateral wells for enhancing the economics and productivity of geothermal energy projects in fractured carbonate reservoirs in WP3. In the following, we provide key conclusions based on the evaluation of the data and numerical results so far.

WP2:

The VSH pilot lasted over four working weeks and with 7 to 13 people continuously on site. The integration of all the hardware into one functional drilling unit required teamwork, trouble shooting, dealing with unfamiliar risks, and the integration of communication systems and data-acquisition systems.

With five nationalities in the team, communication was not trivial and effectively the communication was both in German and English. Despite the challenges, the team made the Directional Steel Shot Drilling system work in an operational setting. The steering capability and the ROP improvement has been verified. Various system improvements for the next DSSD drilling assembly focusing 6-inch wellbores have bene identified. Most importantly, there were zero incidents, no one was hurt and there was no damage to the environment.

In the following, we answer the research questions that were formulated in the P&D proposal to the level possible based on the evaluation of the VSH-trial outcome:

1. *Is the novel, directional steel shot drilling technology capable of drilling a defined wellbore trajectory?*

   A defined wellbore trajectory could be drilled with Canopus' DSSD drilling assembly utilizing the erosive action of the steel shots. A (so-called) dog leg severity (DLS) of 4.0 - 6.5 deg/30m could be realized. The azimuth as well as the inclination of the wellbore was precisely controlled with the DSSD system. Larger DLS could not be drilled as the stiffness of the assembly limited the DLS and the steel shot concentration in the drilling fluid was reduced to adapt the drilling setting to the softer slate formation.

2. *Is the launch system to kick-off the lateral wellbores effectively functioning?*

   The open hole kick-off functionality of the DSSD system could not be tested due to challenges with the electromagnetic (EM) telemetry system. The downlink to the Directional Module (DM) could not be realized when the drilling assembly was in the wellbore and the DM recording delivered reliable data only when the drill string wasn't rotating. Hence, an active steering into a sidetrack was no option during this trial. The telemetry issue is solved with larger versions of the DSSD systems. For the 4-1/8 inch version it wasn't possible to source a mud-pulser to communicate with the DM. The 6 inch version utilized during the Ede trial has the option to deploy standard mud pulse telemetry and hence, the EM communication challenge will be mitigated.

   The creation of very distinct wash-outs / groves in the wellbore whenever the drill bit was rotated at a fixed position (e.g. while making connections), give an indication that the DSSD tool could create an oriented, localized enlargement of the wellbore that will function as open-hole kick-off point for side track drilling. This functionality should be tested in a subsequent trial but is not part of the deployment of the technology in the Ede geothermal well.

3. *Is the current technology capable of geo-steering?*

   The DSSD drill bit shows strong reactions to changes in the hardness of the drilled formation. Whenever a hard quartzite formation has been intersected, the impact on the rate of penetration (ROP) and bit torque could be recorded. These reaction directly at the drill bit can be utilized for geo-steering in case a rock competence contrast is intersected.

   It was planned for this trial to test this bit response when hitting the softer slate overburden after drilling through the full thickness of the hard limestone formation. However, the quarzitic limestone layer had an extension of several meters and the drilling with the DSSD assembly was performed in slate only.

4. *What is the system performance with respect to the rate of penetration (ROP), build radius (DLS), and hole cleaning?*

From the start of the operations, the ROP was higher than expected due to the softer slate formation that has been drilled. The ROP exceeded even 80 m/h. For testing of the DSSD system stable drilling conditions were preferred to be able to assess the response of the directional drilling action. Consequently, the steel shot concentration, the bit hydraulics (pressures) and WOB were reduced to get into a ROP range of 10-30 m/hr.

The ROP enhancement by adding steel shots to the circulation system has been demonstrated. A ROP increase by a factor of 2-4 has been realized in dependence of the steel shot concentration and bit pressure drop.

A controlled DLS > 4 deg/30m has been realized and confirmed by logging even with the reduced concentration of steel shots in the drilling fluid. It is expected that the DLS can be pushed further utilizing a more flexible drilling assembly as well as a higher concentration of steel shots.

Proper hole cleaning has been realized with flow rate of 550 – 600 l/min utilizing water as drilling fluid. This flow rate corresponds to a flow velocity in the annulus of 1.3 m/s which is in the range of expected flow velocities for drilling operations. The steel shots do not pose an extra challenge to the hole cleaning performance while proper wellbore clean out has to be monitored.

5. *What is the operational performance with respect to tool handling, tool control and technology integration into a standard drilling system?*

   The integration of the DSSD system into the drilling operations with the horizontal drilling rig, the integration of the steel shot injection unit (SIU) and the cuttings-steel shot separation system had required several modifications and individual solutions to realize a fully functional DSSD drilling system. This includes the bypass of the high-pressure flow to enable stable steel shot injection or the drum separator that could not be hooked up for continuous steel shot reinjection. The surface systems of the DSSD technology require a dedicated engineering solution to be ready for various wellbore settings and operational drilling environments.

   The wear of the drilling assembly due to steel shot circulation was negligible. Likewise, no wear of surface equipment was identified, nor any problems with making up drill string connections while steel shots have been circulated.

6. *Is the achieved wellbore quality sufficiently high?*

   The softer slate formation required adaptations of the drilling parameters to limit overgaging and washouts during drilling operations. The increase in wellbore quality by parameter modification could be assessed by the logging runs performed in wellbore 2. Further, the composite log (see appendix B) highlights that a perfectly gaged wellbore is produced when harder (quartzite) formation is drilled.

   This dependence of the wellbore quality of the formation strength was pronounced during the trial by the low hydrostatic head that allowed for cavitation at the fluid jets if the pressures aren't tightly controlled. With sufficient hydrostatic head (> 200m), the cavitation is suppressed. Nevertheless, the bit hydraulics and hence, the pressures, flow rates and nozzle diameter should be adapted to the expected formation parameters to mitigate wash-outs due to the jetting action.

7. *Is it possible to complete the lateral structure with a standard well completion system?*

   Completion of lateral structures wasn't focus of the VSH-trial operations. In the remainder of the project, specific completion solutions for DSSD drilled lateral structures will be screened by the project partner and made available as a separate report.

8. *What pressure losses are measured in a lateral structure during production simulation.*

   Compared to the overall pressure losses in the system mainly caused by the nozzles in the drill bit, the pressure losses in the drilled wellbores have been very small and could not be separated. The pressure losses in the drilled wellbores have not been tested with a separate circulation system

WP3:

Stochastic numerical modeling and techno-economic analyses indicate significant productivity improvements with multi-lateral configurations. In particular, the Upper Jurassic (Malm) reservoir shows higher productivity and economic viability due to its greater thickness, higher temperatures, and superior petrophysical properties, compared to the Lower Cretaceous reservoir. Multi-lateral configurations, especially triple-laterals, demonstrated the potential to double energy output compared to single-lateral wells, while maintaining sustainable thermal output over a 20-year period. The techno-economic analysis confirms that the DSSD technology increases the probability of effectively lowering the LCOH and SCC, increasing the likelihood of making geothermal heating projects in Switzerland more commercially viable, compared to not employing slim-hole lateral wells at depth.

Key takeaways/recommendations are as follows:

1. *Target Deeper Reservoirs for Enhanced Productivity:* The thermal power potential of the UJ (Malm) reservoir is significantly higher than that of the LC reservoir as the former exhibits superior petrophysical characteristics, higher temperatures and greater thickness, resulting in higher volumetric heat capacity and potentially longer fracture intersections. Future exploration should prioritize deeper, high-potential reservoirs, such as those located in the Malm, to maximize (the likelihood of) thermal power generation and economic returns.
2. *Enhanced Productivity with Multi-Lateral Wells:* As the number of laterals increase, both production rate and cumulative energy tend to increase. In the UJ (Malm), the addition of a second lateral statistically increases the production by 45 - 50 %, while the addition of a third lateral led to a statistical increase in production by 100 – 125 %. Although single-lateral wells are viable and maintain pressure longer, they tend to have the lowest production rates, making them less efficient for high output needs. Dual and triple-lateral wells tend to significantly increase production rates as these configurations increase the likelihood of intersecting more fracture networks, enhancing fluid circulation and reservoir access. Adopting slim-hole multi lateral well designs might allow efficient utilization of geothermal resources, especially in fractured carbonate formations typical of the Geneva basin.
3. *Leverage novel cost-effective drilling solutions:* The Directional Steel Shot Drilling (DSSD) technology tends to enable multi-lateral drilling at lower SCC and LCOH, compared to traditional lateral drilling. Adding a second DSSD in the UJ reservoir increases the capital costs of drilling by 12% while simultaneously increasing the probability of reducing the SCC and the LCOH by ~17% due to increased thermal energy output. Despite higher CAPEX, triple-lateral configurations show a tendency towards the lowest LCOH, making them likely to be the most economically favorable option for long-term geothermal heating, when averaging over multiple project realizations.
4. *Adopt Sustainable Pressure Management Strategies:* The production from different well configurations is a function of the applied pressure differential. The trade-off between production rate and pressure differential must be considered when designing well configurations, as more aggressive extraction could lead to earlier reservoir pressure declines and reduce well productivity. In this case, the shallow reservoir shows a modest decline in pressure over a period of 20 years (a maximum of 1200 kPa with three laterals producing simultaneously). The deeper Malm reservoir, on the other hand, exhibits higher production rates for all the well configurations and depletes relatively fast as indicated by the pressure decline curves. Applying a maximum allowable pressure drawdown as a production constraint is recommended as it promotes reservoir longevity and production stability. Additionally, pressure management practices, such as reinjection or periodic well rest, should be considered to maintain long-term reservoir sustainability.
5. *Thermal Stability and Reservoir Longevity: The* bottom hole temperature does not show a strong decline after a production period of 20 years. This thermal stability may result from the large

reservoir size and slow heat extraction rates. The stable bottomhole temperature is promising, as it indicates that thermal depletion may not pose an immediate concern, allowing for steady energy production over time.

6. *Expand Geophysical and Subsurface Data Collection:* Newly acquired 3D seismic data in the Geneva basin should be incorporated for generating a more informed/refined geological model and improved understanding of fault/fracture networks. This is of utmost importance for designing the geometry of lateral wells and for improving productivity calculations.
7. *Integrate Advanced Stochastic Modeling in Exploration and Planning:* Economic outcomes are sensitive to geological variations in permeability and fracture distribution. Given the geological uncertainties in the Geneva basin, incorporating stochastic modeling into exploration workflows can improve the prediction of reservoir characteristics by accommodating these uncertainties. In addition, understanding of the likelihood of success and failure can provide valuable assistance while making key financial investment decisions (FID).
8. *Develop Policy and Incentives for Geothermal Energy: Policymakers* should provide incentives to offset high upfront costs and encourage investment in innovative technologies, such as DSSD. Such measures will support geothermal energy development as a sustainable alternative to fossil fuels in district heating.
9. *Further Field Trials and Data Collection:* To validate the scalability of DSSD, additional field trials in varied geological settings are recommended. This will improve reservoir models, refine economic estimates, and better inform reservoir-specific drilling strategies.
10. *Prioritize Long-Term Economic Metrics in Project Feasibility:* LCOH should remain a primary metric for assessing geothermal project viability, especially in the context of district heating, where stable and high operational hours can mitigate high SCC. Projects with higher SCC may still achieve low LCOH if they operate continuously and distribute energy over a large demand base, making the system economically efficient despite higher initial investments.

6 Uncertainty considerations and limitations

This study incorporates uncertainty primarily through the stochastic modeling of fracture properties, which are the key drivers of fluid flow. This approach enables the generation of confidence intervals for production rates, thermal energy, and economic outcomes, offering a quantified range of possible scenarios and enhancing the reliability of predictions. However, several other sources of uncertainty remain unaccounted for. The structural layers of the geological model are deterministic, meaning variations in subsurface geometry and fault structures are not considered. Likewise, thermal and petrophysical properties of the rock matrix are assigned average deterministic values. Well design assumptions are also simplified, whereas real-world deviations in trajectory and completion strategies could significantly impact flow behavior and overall performance. Additionally, production constraints are applied deterministically based on general operational regulations, without capturing potential variations in field operations. While the stochastic fracture modeling provides valuable uncertainty quantification, the study remains constrained by these deterministic assumptions. The confidence intervals provided for flow rates and thermal energy primarily reflect the uncertainty associated with stochastic fracture properties, rather than a comprehensive uncertainty analysis of all influencing factors. Consequently, the predicted Levelized Cost of Energy and specific capital costs should be interpreted within the constraints of these deterministic assumptions, and their validity remains contingent on the acceptability of these predefined parameters.

7 Next steps

Next Step: Ede Field Trial – Demonstrating Full-Scale Potential

The positive outcomes from the Hagerbach trial and ETH Zurich modeling set the stage for a large-scale field demonstration in Ede, the Netherlands. The Ede field trial will be performed under the EU GEOTHERMICA framework:

- Validating operational reliability under real-world geothermal conditions.

- Assessing cost-effectiveness through a 6-inch wellbore scale test.

- Refining directional control strategies using insights from ETH Zurich modeling and Hagerbach operational data.

The Ede field trial will incorporate adjustments based on lessons learned at Hagerbach. These adjustments will improve the telemetry system by utilization of a mud-pulse solution or other means of communication with the downhole sub and will advance the real-time drilling performance monitoring to enable optimization of the hybrid drilling action during the drilling process. Further, the operational procedures during making of connections will be adapted to avoid wash-outs while rotating at constant depth.

8 National and international cooperation

As part of the integration of the Swiss P&D project DEPLOI the HEAT in the Geothermica project 462 DELPOI, the factory acceptance test (FAT1) has been performed by TNO in The Netherlands prior to the deployment of the tools in Switzerland. Likewise, the limestone from VSH underground test site has been cored and tested in TNO's Rijswijk Centre for Sustainable Geo-energy (RCSG) to investigate the expected ROP and ROP enhancement in this competent rock formation.

The results of the work performed at RCSG and by Canopus in The Netherlands were reported in a separate report for the Dutch funding agency. Some results from of the limestone drilling tests performed at RCSG are shown in Figure 30. Figure 30a displays the system changes when the circulation of steel shots in a drilling test is switched on and the related impact on the rate of penetration (ROP). A strong effect can be observed increasing the ROP by almost a factor of 7. While this ROP enhancement is impressive, it is important to mention that the test was performed deliberately at low WOB settings. With higher WOB a stronger effect of the mechanical rock cutting will be superimposed, and the ROP enhancement is expected in the range of 3-4. The bottom hole profiles (Figure 30b) of both drilling methods – mechanical with PDC (left) and erosive with steel shots (right) – are very distinct. The cutters produce concentric circles while the steel shots create a conical hole bottom. With both drilling methods good wellbore quality is produced in competent limestone. A good indication of the impact on the aggressiveness of the rock cutting process can be seen in Figure 30c. The cutting size increases with adding steel shots (top part of the picture) indicating that the bottom hole profile changes with steel shot action and the PDC cutter can remove rock more efficiently.

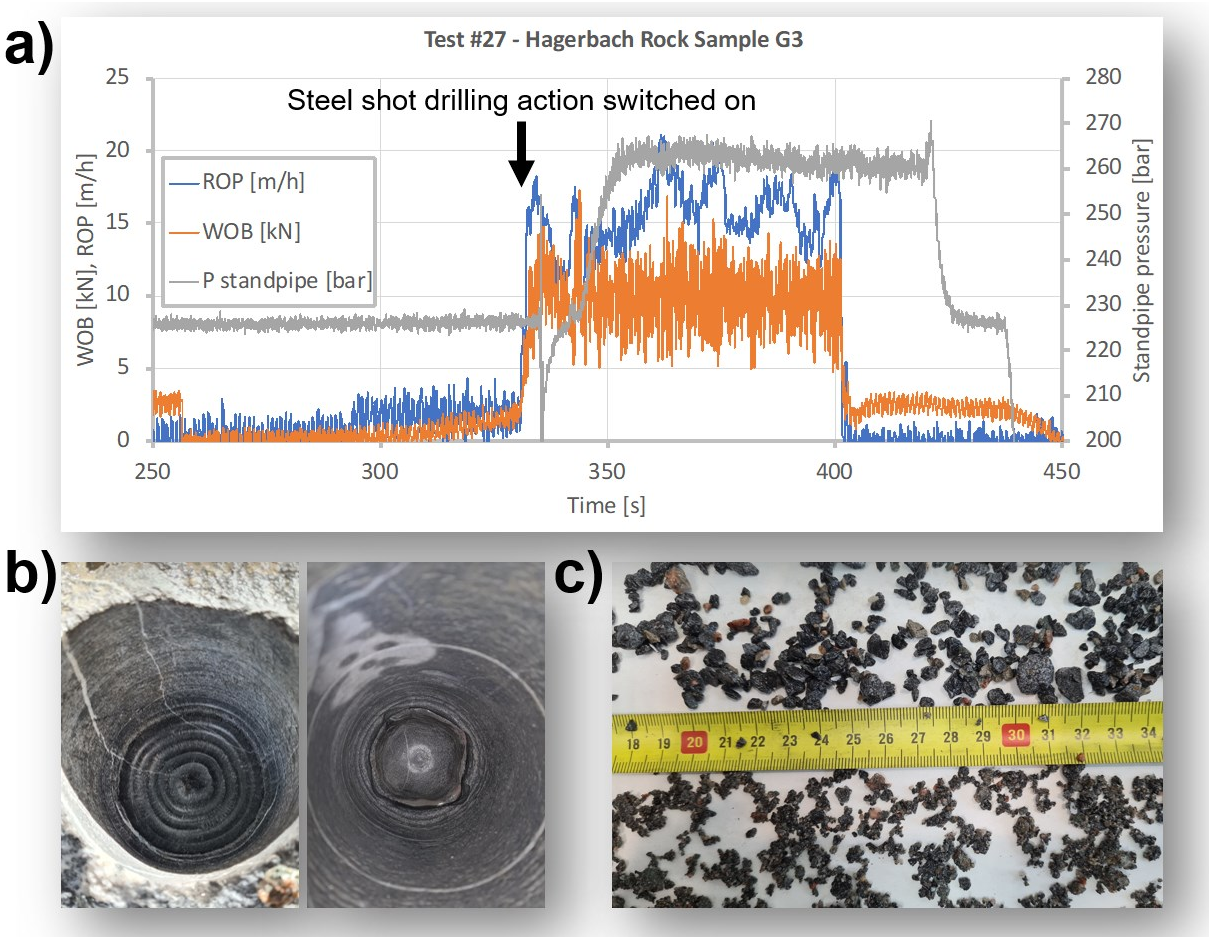

Figure 30: Examples of limestone drilling tests performed at RCSG with the steel shot drilling system. a) An increase of ROP by almost a factor of 7 can be observed in this test scenario when steel shots are added to the fluid circulation. b) PDC cutters (left) and steel shot erosion (right) produce very distinct bottom hole profiles. c) Adding the erosive action of steel shots increases the aggressiveness of the PDC bit and results in larger cuttings (and hence, in higher ROP)

9 WP4: Dissemination / Publications

- 18-20 October 2022 EGC Berlin - Presentation by Jan Jette Blangé (Canopus Drilling Solutions) and Vedran Zikoviç (TNO).
- 16 Feb 2023 - Presentation about Canopus including Geothermica at The Energy Cave in Rijswijk by Diederik Wawoe (Canopus Drilling Solutions).
- 13 April 2023 Geothermie Nederland - Poster presentation by Jan Jette Blangé and Diederik Wawoe (Canopus Drilling Solutions)
- 23-28 April 2023 EGU - Poster presentation in Vienna by Andreas Reinicke, ETH
- June 2023 - 1st Dissemination Workshop during Trial in VersuchsStollen Hagerbach (VSH)
- 21 June 2023 - Presentation by Diederik Wawoe (Canopus Drilling Solutions) (at Delftse Aardwarmte Project (DAP) congress together with RVO and other parties about Deploi the Heat in the context of European subsidy programmes.
- Mid term report and presentation (Sept 2024)
- 04 Sept & 06 October 2023 Pivot 2023 – Presentation by Jan Jette Blangé (Canopus Drilling Solutions)
- 18th October 2023 Der Geothermie Kongress (DGK) Essen, Germany – Presentation by Marcel Knebel (Well Engineering Partners)
- Website launched in Q1 of 2023: www.deploitheheat.eu
- 15th of December 2023 - DEPLOI the HEAT interim report for SFOE
- 14th of November 2024 - 2nd Dissemination Workshop hybrid (ETH & Zoom)
- 2nd of December 2024 - TNO webinar “Novel drilling technology to accelerate the heat transition”
- 31st of March 2025 - DEPLOI the HEAT final report for SFOE
- 20th – 21st of February 2025 – Geotherm Expo & Congress, Offenburg, Germany – Presentations:
    a. Improving Rate of Penetration with Directional Steel Shot Drilling by Jan Jette Blangé - Canopus Drilling Solutions Geothermal
    b. Improving economics of geothermal projects through low-cost side-track drilling by Paromita Deb - ETH Zurich GEG Group
- November 4-7, 2024 - Fifth EAGE Global Energy Transition Conference & Exhibition (GET 2024), Rotterdam, The Netherlands
    a) Multi-Lateral Well Construction by Directional Steel Shot Drilling: Optimisation of the (Mechanical) Specific Energy Utilisation by Andreas Reinicke - TNO
- 4-6 March, 2025 - Presentation and paper at the SPE/IADC International Drilling Conference and Exhibition, Stavanger, Norway

a) Short-Radius Multi-Lateral Well Construction by Novel Directional Steel Shot Drilling: Cost-Effective Solution for Geothermal Production Enhancement (SPE-223789-MS) - A. Reinicke, V. Zikovic, F. v. Bergen, and J. J. Blangé

- Abstract for EGC in Zürich approved (Oct 2025)

10 References

Adams, B.M., Ogland-Hand, J.D., Bielicki, J.M., Schädle, P. and Saar ,M.O. (2021). Estimating the Geothermal Electricity Generation Potential of Sedimentary Basins using genGEO (the generalizable GEOthermal techno-economic simulator). Preprint - https://doi.org/10.26434/chemrxiv.13514440.v1

Blangé, JJ, Zikovic, V., Bergen, F V, Wawoe. D, Heerens, G-J. (2022). Novel Directional Steel Shot Drilling Technology for short radius, long reach multi-laterals. Proceedings European Geothermal Congress 2022. 17 – 21 October 2022, Berlin, Germany.

Bonnet, E., Bour, O., Odling, N.E., Davy, P. , Main, I.,Cowie, P. and Berkowitz, B. (2001), Scaling of fracture systems in geological media, Reviews of Geophysics, 39(3), 347–383, https://doi.org/10.1029/1999RG000074

Chelle-Michou, C., Couto, D D., Moscariello, A., Renard, P., Rusillon, E. (2017). Geothermal state of the deep Western Alpine Molasse Basin, France-Switzerland. Geothermics, 67, 48-65. https://doi.org/10.1016/j.geothermics.2017.01.004

Clerc, N., Rusillon, E., Moscariello, A., Renard, P., Paolacci, S. Meyer, M. (2015). Proceedings World Geothermal Congress 2015. 19 – 25 April 2015, Melbourne, Australia.

Cordero, J. A. R., Sanchez, E. C. M. and Roehl, D. (2019). Integrated discrete fracture and dual porosity - Dual permeability models for fluid flow in deformable fractured media. Journal of Petroleum Science and Engineering, 175, 644-653. https://doi.org/10.1016/j.petrol.2018.12.053

de Joussineau, G. (2023). The geometrical properties of fracture corridors. Tectonophysics , 846, 229637. https://doi.org/10.1016/j.tecto.2022.229637

de Joussineau, G. and Petit, J-P. (2021). Mechanical insights into the development of fracture corridors in layered rocks. Journal of Structural Geology, 144. https://doi.org/10.1016/j.jsg.2021.104278

Guglielmetti, L. 2020. Results of a walk-above vertical seismic profiling survey acquired at the Thônex-01 geothermal well (Switzerland) to delineate fractured carbonate formations for geothermal development. http://dx.doi.org/10.1111/1365-2478.12912

Homuth, S. and Sass,I. (2014). Outcrop Analogue vs. Reservoir Data: Characteristics and Controlling Factors of Physical Properties of the Upper Jurassic Geothermal Carbonate Reservoirs of the Molasse Basin, Germany. Proceedings, Thirty-Eighth Workshop on Geothermal Reservoir Engineering, Stanford University, Stanford, California, February 24-26, 2014. SGP-TR-202.

IRENA, 2023. International Renewable Energy Agency. Abu Dhabi. https://www.irena.org/Energy-Transition/Technology/Geothermal-energy (lastaccessed 27.10.2023).

Kharrat, R.; Ott, H. (2023). A Comprehensive Review of Fracture Characterization and Its Impact on Oil Production in Naturally Fractured Reservoirs. Energies, 16, 3437. https://doi.org/10.3390/en16083437

Laubach, S.E. (1991). Fracture Patterns in Low-Permeability-Sandstone Gas Reservoir Rocks in the Rocky Mountain Region. SPE-21853. https://doi.org/10.2118/21853-MS

Lee, S. H., Lough, M. F., Jensen, C. L. (2001). Hierarchical modeling of flow in naturally fractured formations with multiple length scales, Water Resour. Res., 37(3), 443–455. https://doi.org/10.1029/2000WR900340

Lei, Q., Latham, J-P., Tsang, C.F. (2017). The use of discrete fracture networks for modeling coupled geomechanical and hydrological behaviour of fractured rocks. Computers and Geotechnics, 85,151-176. https://doi.org/10.1016/j.compgeo.2016.12.024

Li, L. and Lee, S.H. (2008). Efficient Field-Scale Simulation of Black Oil in a Naturally Fractured Reservoir Through Discrete Fracture Networks and Homogenized Media. SPE-103901-PA. SPE Res. Eval & Eng 11 (04), 750 – 758. https://doi.org/10.2118/103901-PA

Link, K. and Minnig, C. (2022). Geothermal Energy Use, Country Update for Switzerland. Proceedings European Geothermal Congress 2022. 17 – 22 October 2022, Berlin, Germany.

Maier, C., Schmid, K.S., Ahmed, M., Geiger, S. (2013). Multi-Rate Mass-Transfer Dual-Porosity Modeling Using the Exact Analytical Solution for Spontaneous Imbibition. SPE-164926-MS. Proceedings EAGE Annual Conference & Exhibition incorporating SPE Europec. June 2013. London, UK. https://doi.org/10.2118/164926-MS

Moscariello, A., Guglielmetti, L., Omodeo-Salé, S., Haller, A, D., Eruteya, O.E., et al. (2020). Proceedings World Geothermal Congress 2020. 26 April – 2 May 2020, Reykjavik, Iceland.

Nawratil de Bono, C., Martin, F., Meyer, M. (2020). Geneva Geothermal Program - A Unique Stepwise Approach for Exploring Geothermal Energy and First Success. Proceedings World Geothermal Congress 2020. 26 April – 2 May 2020, Reykjavik, Iceland.

Peaceman, D.W. (1983). Interpretation of Well-Block Pressures in Numerical Reservoir Simulation with Nonsquare Grid Blocks and Anisotropic Permeability. *SPEJ* 23 (03): 531–543. https://doi.org/10.2118/10528-PA

Peters, E., Veldkamp, J.G., Pluymaekers, M.P.D. and Wilschut, F. (2015). Radial jet drilling for Dutch geothermal applications, TNO, Utrecht R10799. http://publications.tno.nl/publication/34620510/4C8joC/TNO-2015-R10799.pdf

Petty, S., Bour, D. L., Livesay, B. J., Baria, R., Adair, R. (2009). Synergies and Opportunities Between EGS Development and Oilfield Drilling Operations and Producers. SPE 121165. https://doi.org/10.2118/121165-MS

Reinicke, A., Deb, P., Saar, M. O., Zikovic, V., V., Lassnig, E., Knebel, M., and Blangé, J. J. (2023). Novel Directional Steel Shot Drilling Technology for Short-Radius Multilaterals – Field Application and Commercial Impact, EGU23-14928, EGU General Assembly 2023, 24–28 Apr 2023, Vienna, Austria. https://doi.org/10.5194/egusphere-egu23-14928

Reinsch T, Paap B, Hahn S, Wittig V, van den Berg S. (2018). Insights into the radial water jet drilling technology – Application in a quarry, Journal of Rock Mechanics and Geotechnical Engineering. https://doi.org/10.1016/j.jrmge.2018.02.001

Rusillon, E., 2018. Characterisation and Rock Typing of Deep Geothermal Reservoirs in the Greater Geneva Basin (Switzerland and France). https://archive-ouverte.unige.ch/unige:105286

Rybach, L. (1992). Geothermal potential of the Swiss Molasse Basin. Eclogae geol. Helv. 85/3, 733-744.

SIG (2019). Services Industriels de Genève, GEo-1 Internal Well Report

Tester, J.W., Anderson, B.J., Batchelor, A.S., et al. (2006). The future of geothermal energy: impact of enhanced geothermal systems (EGS) on the United States in the 21st century. MIT Report INL/EXT-06-11746. Massachusetts Institute of Technology, Cambridge, Massachusetts. https://www1.eere.energy.gov/geothermal/pdfs/future_geo_energy.pdf

(last accessed 27.10.2023).

Yang, Y., Fu, G., Zhao, J., & Gu, L. (2023). Heat Production Capacity Simulation and Parameter Sensitivity Analysis in the Process of Thermal Reservoir Development. Energies, 16(21), 7258. https://doi.org/10.3390/en16217258

11 Appendix

A. Composite log of VSH wellbore 2

B. VSH-trial progress report by Canopus

Depth
1m:40m
Caliper
25 mm 125
Caliper#1
125 mm 25
Bitr
25 125
Bitl
125 25
Caliper - ave from TravelTime-HS
80 mm 140
Caliper#2
80 mm 140
Azimuth
5 deg 15
Inclination
80 90
GR
0 cps 250
Image-HS#1
0° 90° 180° 270° 0°
3D borehole
180°
Centralized TravelTime-HS
0° 90° 180° 270° 0°
Centralized Amplitude-HS
0° 90° 180° 270° 0°

Weekly progress reports VSH pilot DEPLOI the HEAT

Title:	Directional Steel Shot Drilling Pilot
Subtitle:	Part of WP4 of DEPLOI the HEAT
Activity:	Pilot at VersuchsStollen Hagerbach
Document Edition:	Week 1, 2, 3 & 4 - 12 June to 7 July 2023

1. Week one

Preceded by many months of preparation the equipment for the VSH-pilot arrived on location on Monday June 12. That Monday the Bottom Hole Assemblies (BHAs) were unpacked, the drill unit positioned, the flow line set-up, and lots of cables, wiring, hoses and tubing. Also two cameras were installed to monitor out of the control cabin and one more for a time lapse recording of the pilot.

On Tuesday the first drilling assembly was Run In Hole (RIH) for drilling out the first 25 m. That first length is to be used for making up the 20+ m long Directional Steel Shot Drilling assemblies. The first bore hole was also a to be a test of the cuttings transport, the rate of penetration (ROP) and the rock type. The bit was a 4-1/4" Tricone Rock bit IADC 637, selected for the expected hard quarzitic limestone. However, mostly slate cuttings were drilled, and the ROP was higher than expected – about 6 m/hr at relatively low 3,5 tons WOB and 40 RPM of the string. The pump of the drill unit was used for circulating less than 200 L/min water.

The next day, the drilling of the first 25 m depth was finished and still mainly slate cuttings came over the shaker. The bottom hole assembly was Pulled Out Of Hole (POOH) and the first steel shot drilling assembly run in. That first drilling assembly did not contain any electronics, as the purpose of that assembly was to determine the ROP as a function of Weight On the Bit (WOB), string RPM, bit hydraulics and steel shot concentration. This first run with the 'empty' steel shot drilling BHA was also to test the functionality of the Steel shot Injection Unit (SIU).

While RIH the empty assembly the string was found to be blocked by some cavings of slate and only the first part could be RIH. Later on the cavings were circulated over the shaker after connecting the high-pressure pump and circulating at a rate of 400 L/min while RIH. The rig pump does not have a pulsation dampener, so the dampener of the SIU is to be used.
It was also found that the two conveyor belts lined up for transporting the solids to the drum separator did not function as expected. A single, longer conveyor belt was found at Schenk and was prepared for transport to location on Friday.

On Thursday the assembly was POOH, and the bit inspected. The pump pressure had been found to be 90 bar at 400 L/min, whereas only about 55 bar was expected. However, the bit nozzles 8/32 and 9/32 were completely open. The empty assembly could now be RIH. The data-acquisition was also finalized: The data acquisition in the control cabin records the EM-tool data, the SIU of the

On Friday the shaker was repositioned to get closer to the well and to provide room for the new conveyor belt to the drum separator. The lines were inspected to get an explanation of the higher than expected pump pressure at 400 L/min. Plan is to do a circulation test of only the surface system to check for blockages there and to open the SIU valves to make the pump pressure visible on the SIU V1 and V2 pressure gauges.

SUMMARY

- Drill unit operational and data-acquisition of push/pull, Torque left/right, string RPM and ROP sampled at 10 samples/sec and values checked. The data is life recorded on Canopus Laptop 1. Value missing is rotating head position from which the hole depth is to be derived. Will try to resolve for direct matching of setting changes with depth and formation logging with depth.

- Drilling assembly make up and break out in horizontal position has been trained and somewhat optimized but taking considerable time – some 3-4 hrs including rig move out and in. Requires team work of 4 to 5 persons.
- Steel shot return system modified to resolve solids sticking to the belt and its ridges. New belt longer, at reduced slope and without ridges. To be tested at start second week.
- Pump pressure, flow rate and cumulative pumped volume recorded in control cabin (1 sample/sec). The data is exported real time to the Canopus Laptop 1.
- The EM-tool communication has been tested and the electronics of the drilling assemblies have been prepared.
- The rock drilled the first 25 m seems to be primarily slate not limestone. The drilling activities will be reviewed for higher lower mechanical specific energy of the drilling, probably giving somewhat reduced flow rates and lower operating pressures. Obviously, the reduced flow rate should still be sufficient for hole cleaning.

Status at the end of the first week is that all equipment has been installed, procedures tested and the first assembly in the hole. Still to be tested before drilling are the steel shot return system, the pressure testing and the pulsation dampening.

Figure 1. Overview of the drill site (left) and making-up and running-in-hole the 'empty' drilling assembly without electronics (the internal 'jewelry') (right).

2. Week two

The second week started with improving the line up of the stove pipe, shaker, new conveyor belt and the drum separator on **Monday** morning. The set-up was more compact, and was to have less locations where steel shot and cuttings could be dropped. Putting the shaker under the stovepipe return outlet made the flow line redundant, but the anchoring of the rig in the wall had to be moved.

Figure 2. Open ended flow test of the surface system over the shaker

An important test from a safety and also operational point of view was the open flow test of the surface system. Previous flow tests had shown that the pressure drop over the complete surface plus down hole system was 90 bar at 400 L/min whereas 55 bar. This indicated an unexpected restriction in the system. Such a restriction in the surface system would go together with locally high flow rates causing erosion of the hoses or conduits. The surface system was found to require only 3 bar and the pressure reading of the SIU was consistent with the pump pressure.
Consequently, the higher than expected pressure had to be coming from a restriction in the drill string. Indeed, it was found that the nozzles for the drill bits have a flat inlet with a sharp edge making the pass through diameter effectively a little bit smaller – effectively about one nozzle size down. The rest of the BHA was checked and no restrictions were found.

Figure 3. Control room with data acquisition and three camera's

In the first week all rig data and pump data could be acquired and recorded by the data-acquisition system in the control room apart from the rotating head position. The sensor measuring the speed of the rotating head, say the rate of penetration (ROP), could also be used to measure the 'move back up speed' but this was not implemented. For this, a sensor control board was build and mounted on location and wirelessly connected to the control board. Furthermore, all sensors of the rig and the pump were collected in one data file for easier analysis later on. Data recorded: RigPush, RigPull, StringTorqueLeft, StringTorqueRight, StringRPM, RotHeadPosition, RotHeadSpeedUp and -Down, PumpPressure, PumpFlowRate, and PumpCumulativeFlowRate. The SIU is logging independently. As the SIU with its large number of parameters is only active part of the time and is a rather independent functionality it is not very useful for now to integrate these two recording systems. Eventually this will be beneficial.

Figure 4. Pump remote control during the closed-in pressure test at 420 bar

The Monday was concluded with high-pressure testing of the surface system. The Metax high-pressure pump was used for that, which was found to be a challenge due to the limited volume of the surface system, the minimal compressibility of the water and the minimal balooning of the conduits. The operator nevertheless managed to set the closed-in pressures to 50 bar, and thereafter to 420 bar and the closed-in pressure stabilized quickly and within a few % decay. With a safety margin of 1.5 the closed in pressure of 420 bar gives that the system is safe to operate at 280 bar. Second part of the testing concerned the response of the Pressure Relief Valve (PRV). The valve set to 250 bar was installed. The valve responded around that pressure but not fast enough to prevent an overshoot to over 420 bar. The pressure returned to 350 bar within 5 seconds – the data

filtering was the limiting factor for the response time – the actual response time was probably much faster but the pressure overshoot also higher than the 420 bar.
As any PRV will have a response time it was decided to organize PRV only for pressure limitation to 260 bar (for 'slow' regulation) and to set the pump itself, the source of the hydraulic energy, to a maximum output pressure limit of 280 bar.

On **Tuesday** morning the cement of the anchoring of the rig had been hardened. After some final tweaking of the alignment of the shaker, the conveyor belt and drum separator the separation system was also good to go. The SIU was prepared for injecting of a small batch of 50 kg of steel shot and the Canopus bit was run to bottom at 26.5 m hole depth.
Drilling started carefully, without steel shot injection, to test the Canopus bit performance, the cuttings transport in the well and the handling of the cuttings on the shaker. And check the formation type. The ROP was 20 m/nr at 1,5 ton pushing force, 60 string RPM, 350 L/min flow rate and 70 bar pump pressure. Drilling was stable, but cuttings did not come out of the annulus. Upon increasing to 400 L/min (90 bar) some cuttings came out.
At that last flow rate the 50 kg were injected at a concentration of 2%vol. The shot passing the bit produced the expected pressure pulse. This was at a measured hole depth of 30.5 m. The injection rate was not controlled and the steel shot did not get out of the bore hole. Flow rate was increased to 500 and about 25 kg was retrieved by the drum separator. Later on about 20 kg more was found under the first shaker screen which leaked solids. Four things to improve:
1) control of the injection rate by the SIU (pulsation dampening and flow reduction by mounting a by-pass);
2) suppressing the normal Metax triplex pump pressure fluctuations by including a pulsation dampener in the line;
3) use flow rates of at least 500 L/min for hole cleaning;
4) fix the solids leakage of the shaker

Figure 5. Modified shaker screen for suppressing leakage of steel shot underneath the scatter plate

It was found that the screen leaked because the scatter plate on the screen had not been fully effective. Solids could get underneath. This was fixed first on **Wednesday** morning. Also a pulsation dampener was mounted, but it had to be removed immediately and go back to the machine shop for getting a part repaired.
The construction of a bypass for the SIU diverting about 50% of the flow was discussed and missing parts identified. TNO RCSG was happy to provide these parts and shipment organized in the afternoon.

Figure 6. Drill site overview from camera DEPLOI 1

While waiting for the by-pass parts to arrive drilling continued. Objective was to measure a bit performance reference curve without steel shot while varying the operational parameters within the following windows:
Pushing force 1 to 4 daN, string RPM 50 to 70 RPM, Q 500 to 550 L/min, and Ppump 137 to 167 bar. About half of the matrix was measured giving ROP values of 28 up to 60 m/hr while performance and cuttings looked consistently like slate. No indications of any expected quarzitic limestone.

On **Thursday** the matrix was completed, giving ROP from 28 m/hr up to even 80 m/hr. During the final 1.5 m drilled (at the highest bit loading, hole depth 54-56 m) the cuttings suddenly turned predominantly white (quarzite) and the drill rate became unstable and reduced down to 30-40 m/hr – a large reduction. At 3 daN pushing force drilling continued. The transition lasted about 3 m, then the cuttings turned black again and drilling became stable again. Analysis showed we were back in the slate, but the ROP was only 22 m/hr at 3 daN and 60 RPM.

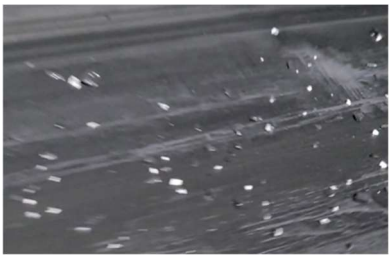

Figure 7. Quarzite cuttings over de running belt.

Figure 8. Core on the VSH site showing a quarzite layers between limestone. Cuttings indicate the Canopus bit ran into a quarzite layer surrounded by slate.

On Friday, the retrieved bit was found to have 4 severely damaged cutters at medium radius. The cutters on the gauge showed a little wear and the four ones in the center minimal or no wear. There were no signs of jet erosion, there was some erosion of abrasive wear on the gauge.
Likely scenario is that the bit ran into a layer of quarzite at a very shallow angle. The bit is rated up to 7 daN weight, but when only a few cutters are exposed to that force they will break down. The cutters at medium radius are most exposed to the pushing force and remove more rock than the inner cutters. With a harder, abrasive layer coming from the side only one or two cutters were likely to be exposed to the full pushing force which may damage them.

Figure 9. Used bit (left) vs an unused bit. The used bit had several cutters at medium radius heavily damaged.

Back to Thursday: Drilling was continued for a few m at 3 daN and 60 RPM while circulating at 600 L/min for hole cleaning. Drilling was stable at about 22 m/hr.

For testing the controlled injection at reduced rate a circulation test 330 L/min was conducted while injecting the retrieved steel shot from the previous test. Injection rate of the SIU was found to be stable at rate settings 1 to 4 and back. Drilling continued slowly at 1 daN pushing force and 60 RPM. Depth between 62 and 64 m. At 330 L/min hole cleaning is insufficient of course and flow rate was increased to 550 L/min while continuing drilling slowly. The drilling on Thursday was concluded by a last joint while circulating at 600 L/min, reaching 72,2 m hole depth. At this flow rate the steel shot came out, but some was found later underneath the shaker screen again.
As the flow rate for good hole cleaning had to be higher at the end than earlier on this is an indication that the hole has been slightly washed out. From about 30 m hole depth onwards it was decided not to reciprocate the string while circulating at full flow rate as the jets (in almost atmospheric, ‘cavitating’ pressures) could wash out the hole. At depths beyond 100 m this would be less of an issue.

Given all the uncertainty on bit damage, hole size and directional behavior of the drilling assembly after these first 72 m of drilling it was decided to POOH.

On **Friday** the last part of the BHA was POOH, revealing the bit damage as described above. A preliminary test was done on running the ETH wireline logging tools and measure hole shape and a directional survey. The hole was logged up to 30 m depth – the wireline was too flexible (+- 10 mm diameter in a >104 mm diameter borehole) to be pushed further. Based on this test a proper logging run is to be prepared with a stiffer propagation string.

Figure 10. Pulling the drilling assembly out of hole.

Figure 11. Making up a connection.

The SIU-bypass and the pulsation dampener were mounted, and the BHA run in hole up to the directional, the EM communication and battery sub-section. These will be RIH after the weekend in order to safe battery life. Based on ROP, the requirements on hole cleaning, the requirements for a stable SIU and the expected pressure loss in BHA loaded with the down hole 'jewelry' it was decided to put the larger 9/32" and 10/32" inch nozzles in the fresh drill bit (no 03).

Figure 12. RIH the BHA up to and including the steering sub

SUMMARY

The second week has been a transition from rigging up and getting the system running to learning how to drill effectively with the integrated system. In bullets:

- Data-acquisition system completed with recording of rotating head position
- SIU requires flow rate of 200-350 L/min for controlled injection, hole cleaning requires 600 L/min. A bypass has been installed to comply with both. To be tested shortly.
- The installation of the pulsation dampener will improve the stable operation of the SIU and will also reduce any fatigue of the HP-conduits. Operational as of Monday.
- A pressure test is to be conducted to check the integrity of the installed bypass and pulsation dampener.
- Drilling through the slate is fast and although the impact of the steel shot drilling onto the ROP will be observed, the steering is to get more focus. Therefor the injected concentration can be reduced and the bit nozzle size increased.
- Performance of the Canopus bit in the slate is good. Dangerous is the event of running at high ROP into a harder rock layer coming in from any side, in our case the quarzite. This causes overloading and damaging some of the PDC cutters in the bit. Would an LWD sensor have prevented this from happening? The erosive jets may mitigate this damage somewhat if carefully positioned for that purpose. During the pilot the drilling preferably is to be done with max 3 daN pushing force (WOB) and 60 RPM.
- Real time monitoring would likely have diagnosed the bit damage while drilling. Rig data to be analysed for that.
- The quarzite at 54-56 m hole depth should probably better be avoided during the sidetracking testing later on in the pilot.

- When running in the next BHA RIH speed should be reduced at the quarzite depth range. Also beyond that depth the hole might be slightly undergauge.
- There are indications of some washouts. The increased flow rate of 600 L/min seems to suffice to clean those as well. Washing/jetting into the wall should be avoided
- The long BHA handling for horizontal drilling is a challenge. The team clearly gets skilled on this, but it remains to be a 4 to 5 person team-operation. Making up the sub with the DM and EM electronics and connecting both the electronics, the internal housings and the external collars is the most challenging. If possible, changing out the BHA, in particular the ones including the down hole electronics, should be minimized.

Assuming the SIU stability and the solids-leaking of the shaker screen can be ticked-off this Monday, the next major subjects to be tested are the steering sub capabilities (actuator, sensors, communication, battery consumption, calibration of tool face control and steering effectiveness) and thereafter the kicking off (control of wash-out on one side by steel shot erosion - depth and direction – and getting the BHA in that pocket).

3. Week three

The third week was a turbulent one. Most importantly we drilled for the first time with the complete DSSD assembly, retrieved the first evidence of the steering action of the steering sub. We had to wait till Friday for that conclusion as we found that the EM communication had been disturbed by the Swiss railways (SSB) powerlines tuned at 16,7 Hz, exactly the same frequency as the EM-tool setting. The data from both the steering sub and the Directional Module (DM) in the EM communication sub could only be downloaded and analysed on Thursday and Friday.

On **Monday**, the complete DSSD assembly was run in hole while regularly testing the electronic functionality. One cable connection at the top of the steering sub had to be fixed and it was found that the power supply to the EM-tool surface kit was just exceeding the rating of the kit – two exchanged fuses and a different adaptor resolved that. The DSSD assembly was run in hole and communication checked.
Before RIH to hole bottom a pressure test was conducted at 50 bar and at 260 bar closed in pressure.

On **Tuesday** morning the bit was run to 30 m depth for a survey and an extensive functionality test of the steering sub – circulation, check sensors, power consumption, actuator functionality. However, the communication was hampered by noise and only surveying data automatically broadcasted to surface could be received at surface. No instructions could be received by the down hole tool. Changing the position of the EM-probes did not resolve the communication. Pulling back to 23 m depth and switching off all surface equipment did restore the communication. And functionality was found to be okay.
RIH again, but S/N increased with depth. As the strength of the signal received by the EM-tool decreases with distance while noise apparently did not many potential causes were reviewed and where possible potential sources at the VSH site switched off. The noise was found to come from a 16.7 Hz source, matching the communication frequency of the EM tool. Further investigation on 167 Hz disturbing sources revealed that five countries in Europe have they railroads powered by 15 kV AC lines at this frequency including Switzerland.

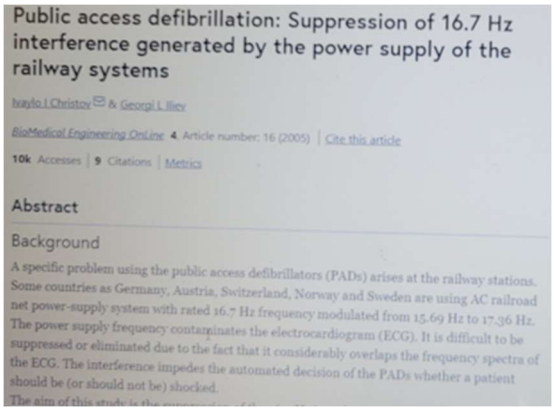
Public access defibrillation: Suppression of 16.7 Hz interference generated by the power supply of the railway systems

Ivaylo I Christov & Georgi I Iliev

BioMedical Engineering OnLine 4 Article number: 16 (2005) | Cite this article

10k Accesses | 9 Citations | Metrics

Abstract

Background

A specific problem using the public access defibrillators (PADs) arises at the railway stations. Some countries as Germany, Austria, Switzerland, Norway and Sweden are using AC railroad net power-supply system with rated 16.7 Hz frequency modulated from 15.69 Hz to 17.36 Hz. The power supply frequency contaminates the electrocardiogram (ECG). It is difficult to be suppressed or eliminated due to the fact that it considerably overlaps the frequency spectra of the ECG. The interference impedes the automated decision of the PADs whether a patient should be (or should not be) shocked.

The aim of this study is the

Figure 13. Example publication of 16.7 Hz noise generated by the Swiss railways

Despite the loss of communication it was decided to continue RIH to bottom at 73 m hole depth. Schenk had provided a Gyro and run the surveying to through the drill pipe to the top of the drilling assembly at 59 m depth. The hole had been dropping from 88˚ down to 83˚ during the first 25 m, but the 'empty' stiff drilling assembly had been climbing slightly back up to 85˚ during the 34 m thereafter.
Tuesday night, the situation with the EM-tool provider Boregyde was set up and the communication could be reolved by changing the communication frequency to another band at 6 Hz. However, this had to be done by re-programming the down hole tool for which it had to be POOH. It was decided to continue testing 'blind' while preparing the EM-software change in parallel for the next BHA.

On **Wednesday** drilling continued and for the first time the complete DSSD system was to be tested. Several batches of steel shot were circulated through the well while keeping the parameters that determine the steering action constant – flow rate and string RPM. As drilling was in slate the pushing force was kept low between 1 and 2 ton (or kdaN) and string

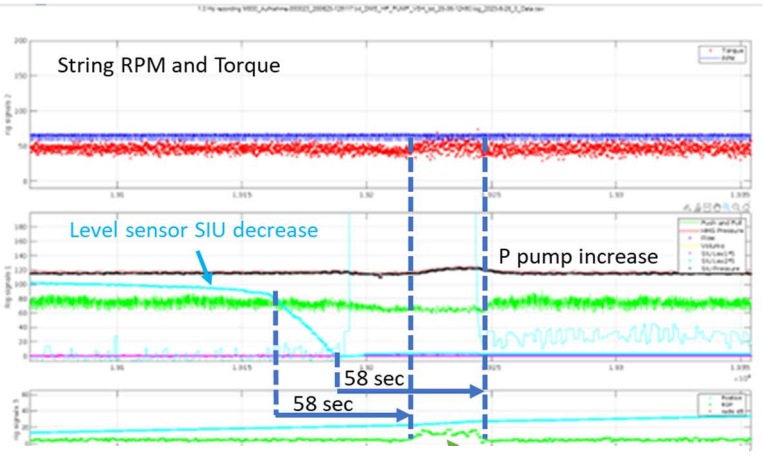

Figure 14. RIg and SIU parameters while circulating a batch of steel shot. The steel shot arrives 58 seconds later at the bit. At that moment the pump pressure increases and the ROP increases.

RPM at 60 and flow rate at 500 L/min.

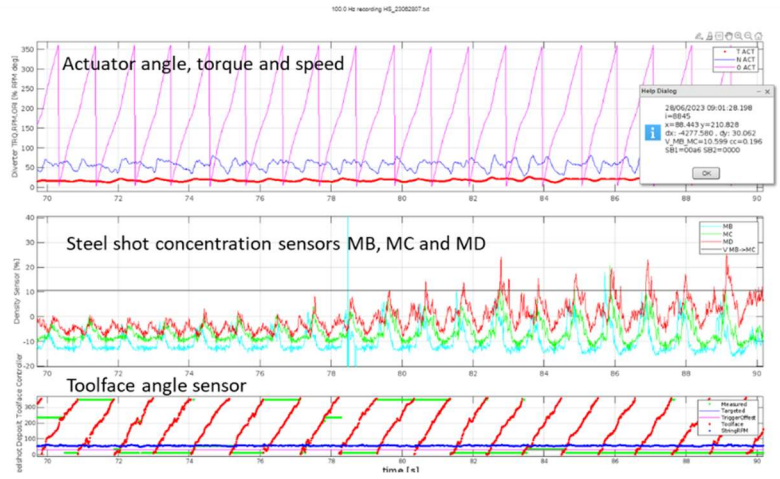

Figure 15. Snapshot of the down hole steering sub data. Sensor MD shows the steel shot concentration at the exit of the steering sub. The MC curve is slightly later than the MB curve as the particles need time to travel from sensor MB to sensor MC.

During 6 batches, a total of 400 kg was circulated at bit depth 80 to 92 m hole depth during six rather short injecting periods. The SIU injection was not very stable and the by-pass valve was readjusted to attempt improving the stability. Both injection vessels were tested. Injection varied between 0.2 and 1.5% by volume. When reaching the bit a clear pressure increase of up to 11 bar was observed about 58 seconds after start injection. Also the ROP went up from 5 m/hr to about 15 m/hr when injecting at 1.5%vol.
On Friday the directional data had been downloaded from the directional module and indicating that in that very same depth interval the azimuth decreased from 3.6˚ to 2.4˚ whereas the inclination increased from 85.5˚ to 87.3˚. So up and to the left. The precision of the measurements were in the range of ±0.2˚. Given the short duration of the steel shot circulation periods this change of direction is realistic but also limited directional effect. The next DSSD, with more steel shot injection and direct directional feedback to surface via the EM-tool is expected to yield a much larger and clearer effect.
On Friday also the steering sub data was downloaded. The sensors had measured the steel shot particles passing by, and also the sensor at the recombined flow contained clear concentration pulses. The velocity in the fast channel was found to be just exceeding 10 m/s at 500 L/min which was a somewhat higher than expected.

Figure 16. Analysis of the EM-downhole memory and the steering sub memory.

Figure 17. Inspection of the steering sub internals: Centralizers (top) and sensors (middle) undamaged. Cable at rotor damaged (bottom).

Eventually the design of the tool can be modified to reduce that velocity to the range of 5-8 m/sec. The toolface detection worked nicely and the actuator control was reasonable. Occasionally the rotor stalled temporarily, but later during the run this became more frequent. Also one of the sensors gave up later on. At disassembly all the cables looked good apart from the location at the height of the rotor. The motor and rotor were free to rotate after removal of the damaged cable.
The next DSSD run we will not have that cable in the assembly and will just change the actuator setting from surface if necessary. Eventually, the tool design can be modified to eliminate the potential contact between rotor and the cable.

The Wednesday was concluded by drilling to 120.9 m hole depth while circulating at 600 L/min. At that rate the cuttings and the steel shot came out of the hole. As previously 450 L/min was sufficient for hole cleaning the hole is likely to have some wash-outs.

Figure 18. Rig repositioned for drilling through stove pipe 2.

On **Thursday** the drilling assembly was POOH and the down hole data from the EM-tool and the steering sub down-loaded. It was also decided to move to the second stove pipe. Because of the expected wash-outs, all the circulation for hole cleaning, and the flow rate and bit nozzle changes in response to the softer rock the second bore hole probably provides better conditions for directional and kick-off testing than the first. The drilling of the first bore hole yielded a lot of understanding of the operation of the drill unit in combination with the steel shot injection, the high pressure pump and the bore hole circulation. The drill rig was repositioned in from of the second stove pipe.

On **Friday** the stove pipe was drilled out up to 26 m depth using the Canopus 4-1/8 inch bit as opposed to the 4-1/4 inch tricone used for the first hole. Reason was the better hole cleaning and in particular the better directional control of the stiffer BHA with the smaller bit. The bit only drilled slate and some quarzite. No limestone cuttings at all.

The BHA was pulled out and the stiff complete DSSD assembly prepared for RIH. The assembly up to the top of the steering sub was run in hole. The rest of the BHA is to be run in hole on Monday – to save battery life.

Figure 19. Replacing the battery (green) for the steering sub in its housing.

The batteries of both the steering sub and the EM-tool were inspected and both had plenty of power content left over. The noise acceptance levels for sleep mode of both tools were increased to be even more efficient on battery consumption. It is expected that the assembly can stay in the bore hole at least 4 days before running the risk of loosing battery power.

Finally, the down hole data is still to be reviewed in detail on whether the steel shot circulation had any impact on the down hole magnetometers. A first glance at the two short periods of 1.5% concentration of steel shot did not reveal any effect.

SUMMARY

In the third week the complete DSSD system was operational for the first time. The assembly drilled to 120 m hole depth and 400 kg steel shot was circulated. In bullets:

- The communication with the EM tool failed because of interference with 16.7 HZ power transmission lines of the Swiss rail road. Communication frequency has been modified to 6 Hz.
- Trigger level for going into sleeping mode has been improved for both the steering sub and the EM-tool. Expected battery life of the next DSSD is expected to be sufficient till the end of the VSH-pilot.
- Steel shot concentration sensors and actuator of the steering sub worked. Steel shot concentration pulses were created synchronized with the bit rotation. Also toolface detection worked.

- Later on, the cable to the sensors hampered the actuator rotation. The sensor data was sufficient for calibration at the operating settings of the pilot. The next DSSD assembly will be without these sensors and their cable to ensure functioning of the actuator.
- The SIU injection rate of both vessels was still unstable. New values for the injection rate timers will be set and the pressure of the pulsation dampener reduced.
- The steel shot concentration can probably be reduced to 0.3%vol concentration for sufficient hole making/steering action. Even at the reduced bit pressure setting of 120 bar instead of 300 bar (to avoid washing out the soft slate) and the reduced WOB of 1 kdaN instead of 4 kdaN (to avoid bit damage when running into quarzite) the steel shot erosion at 0.3% seems more than sufficient.
- The down hole directional data of the first DSSD run indicates a steering action of the steering sub at 500 L/min and 60 RPM. The indicated effect of the steering sub default angle was up and to the left. At this flow rate and RPM an adjustable offset angle can be communicated via the EM-tool.

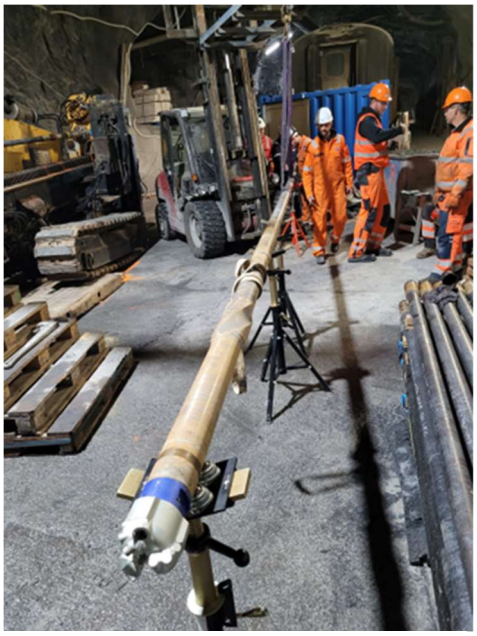

Figure 20. Fresh drill bit and steering sub prepared for running in hole.

The plan for the next (and final) test week deviates from the original plan. Objective is to change the drilling direction, then change into a different direction. Each hole length at fixed steering action should be sufficiently long to have the directional module (10 m behind the bit) to detect the change. Repeat a few times varying angle, steel shot concentration and RPM/flow rate. Requirement is to operate the SIU in a stable manner. Finally, depending on the BHA steering performance and remaining piloting time, the team will pull the BHA back and try to side track with the same stiff BHA or with the more flexible BHA.

4. Week four

The fourth week of the pilot was also the last week. Another stiff bottom hole assembly run was prepared as well as the most flexible assembly. At the end of the third week, the second stove pipe had been drilled out up to 25 m to provide a well defined bore hole to start from. The objective of the final week was to get experience with the complete DSSD system, hopefully to change down hole settings through two-way communication via the EM-telemetry tool and get info on various tool performance settings like power consumption, potential wear zones in the down hole hardware, directional response and identify design & interface improvements and effective operational practices.

On Monday, the batteries of the steering sub and the EM-tool were connected to the stiff assembly and run in hole. The communication with the EM-tool was checked and working. The communication frequency had been readjusted to 6 Hz – as far as possibly away from the 16.7 Hz noise band from the Swiss Railways. Also analogue and digital filter settings had been modified. Still, the EM-tool was still found to have a hard time detecting the broadcasted signal from surface.
At the same time the outlet of the SIU was inspected for erosion as a significant volume of steel shot had been passed through. There were no indications of wear.
In the Monday afternoon, about 500 kg of steel shot were circulated through the well and the hole deepened to 55 m depth.
Later on, the retrieved directional data showed that between 30 and 60 m hole depth the hole made a turn of 3 degrees to the left while holding inclination.

On Tuesday July 4 the down hole EM-tool was found not to receive signals from surface. Further attempts to re-establish connection were not successful. Without two-way communication the steering sub settings could not be changed. Therefore it was decided to pull the assembly out of hole and change to the more flexible drilling assembly. While POOH, the flexible DSSD assembly was reprogrammed such that every hour the steering direction (toolface angle) was automatically changed by 90 degrees.
After pulling the stiff assembly out of hole the hardware was inspected. The bit had no damage, a diode in the actuator motor control had failed because of a construction flaw on that board, the power consumption of the battery diving the steering sub had been minimal – more than sufficient for 4 days of operation - and the toolface detection, control electronics, data storage and process control software in the steering sub were flawless. There was no detected wear of specific steering sub components.

While the flexible drilling assembly was prepared the first bore hole was logged up to 80 m depth. Clear bands of quartzite were visible and the ultrasonic bore hole imaging tools showed zones with good bore hole quality as well as zones with some hole enlargement. The latter confirms that the hole cleaning in the deeper hole required a higher flow rate of up to 600 L/min than earlier on. More details are expected in the full bore hole logging report following the pilot.

The topics of hole cleaning, washing out, and doing side erosion for kicking of are important and closely related. The almost atmospheric down hole ambient pressure will cause the bit jets to cavitate and cause additional erosion of the soft slate formation. The cavitation would be suppressed at depths beyond 100 m, giving room for direction controlled kick off by the steel shot erosion, as opposed to washing out in all directions by the cavitating jets. In the case of limestone the impact of the cavitating jets would have been much less.
In short, uncontrolled wash out with the steel shot jets could lead to hole cleaning issues. But controlled directional erosion of the bore hole wall is key for the steering as well as for the open hole sidetracking.

On Wednesday afternoon, around 15.00 the bit of the flexible assembly had reached hole bottom and had drilled to the next drill pipe connection. DSSD drilling continued till a depth of 73 m while circulating about 440 kg of steel shot.

Thursday July 6 was the last day of drilling. That day about 1100 kg steel shot was circulated through the well and a hole depth of 125 m was reached. Invariably the rate of penetration increased significantly whenever steel shot flew through the drill bit. The variation in the rate of penetration as well as the type of cuttings (quarzite/slate) indicated a very similar rock sequence as for the first bore hole. Flow rate was in the range of 550 to 600 L/min, sufficient for circulating the steel shot out of the bore hole. Pump pressure was very stable and any pump pressure increase a very clear indicator of the concentration of the steel shot flowing through the drill bit. There was no nozzle wear.

Part of the steel shot was reused, but the drum separator could not prevent some of the cuttings to land in the steel shot tank. No effort was taken to achieve better separation as there was plenty of steel shot on site to finish the pilot. An easy measure to improve separation of cuttings from steel shot would have been to direct the solids once again over the drum separator or to change to amount of water flow with the solids of the conveyor belt. The separation efficiency can be optimized further in the lab.

On Friday, the last day of the pilot, the assembly was pulled out of hole and the memory in the EM-tool and the steering sub down loaded for further analysis. Battery consumption had, once again, been minimal. The drill bit had some damage on one or two of the cutters at medium radius, similar to the location of the wear resulting from previous bit runs. The steering sub did not show wear apart from, again, the location where the sensor cables get close to the rotor. This is to be improved for the next steering sub design. As that steering sub will be for 6 inch bore holes, there is more room for putting the wires and the rotor at a safe distance.

Unfortunately, without the two-way communication there was no opportunity to test any open hole side-tracking.

The drilling activities for the VSH-pilot of the DSSD system were finished on 7 july 2023. Remaining activities were the disassembling of the equipment, transport back to their original locations, the completion of the logging of the two bore holes and the analysis of the abundance of surface- and down hole data acquired.

SUMMARY

- A clear directional effect of the steering sub was observed.
- The EM-tool could send data to surface but could not receive commands from surface. The data of the Directional Module was communicated fine with the steering sub.
- No open hole kick-off test could be conducted
- The second bore hole was drilled to a depth of 125 m.
- Overall wear of the drilling assembly was negligible apart from the impact damage of the bit cutters at medium radius and the sensor cable at the height of the rotor.
- A burst disk in the SIU damaged by the shock wave through the SIU when opening the high-pressure valve for activating an injection vessel
- The drilled formation was mainly slate interbedded with some quartzite layers. The bedding plane was at a very high incidence angle with the bore hole direction.
- The steering sub created concentration pulses for steering and the control electronics worked as expected. A soldering construction on the motor controller is to be modified.
- The total steel shot mass circulated during the pilot was 2500 kg. No wear of surface equipment was identified, nor any problems with making up drill string connections.

5. Results acquired after week four

Logging results

Lithology

The cuttings analysis, visual logging and gamma-ray logging all confirmed that both boreholes went through slate with some calcite streaks. The quarzite streaks were clearly visible as clear white bands as well as in the collected cuttings.

Bore hole quality

The caliper run was done with a three arm caliper. Changes in the radial extension of the arms are recorded and plotted in an exaggerated way to clearly visualize the deviation from a gun barrel bore hole.

The caliper log showed interesting results. At a some depths corresponding to a drill break for adding a drill pipe joint grooves were found. At those 'connections' the injection of steel shot was stopped temporarily so apparently the clean water jets were powerful enough to jet the formation. Probably, the almost atmospheric pressure of the made the jets cavitate, which increases the reach of the jets and their erosiveness. The grooves seemed more pronounced at 600 L/min than at 550 L/min flow rate. At 500 L/min the grooves were minor. However, hole cleaning required at least 550 L/min and preferably 600 L/min.

Actually, the bit pressure drop, the nozzle diameter(s), and the ambient down hole pressure that correlate with the occurrence of cavitation and the length of the so-called cavitation flame. Beyond 100m vertical depth the ambient down hole pressure suppresses largely the cavitation. A learning of the above is that if cavitation is to be avoided the bit pressure drop preferably should not exceed 150 bar. In the case the 150 bar bit pressure drop is desired, the TFA is then determined by the minimal flow rate that gives acceptable hole cleaning in a gauge borehole.

At larger depth a clean water jet without solids may also remove rock that is porous and soft like sandstone. In those cases also keeping the bit pressure drop below 150 bar would avoid most of any unwanted wash out.

The Steel Shot laden jets of the DSSD technology also create grooves when stopping ROP for a connection. And that is independent of rock type or hardness. It is therefore important to circulate a steel shot injection break timed with the break or reduce the flow rate just before lifting the bit from bottom, stopping the pumps and the string rotation.

For the directional control and the open hole side tracking the capability of reaming the hole at the right moment and in the desired direction is important. The results above show that this desired reaming capability should be balanced by the suppression of the unwanted reaming. This balance is controlled by the magnitude of the desired steering action, the side-way orientation and diameter of the nozzles in the bit, the hydraulics, the steel shot concentration in the jets, and the best operational practices for, for instance, adding a drill pipe joint.

Bore hole trajectory

The bore hole trajectory was measured by a directional module (DM) in the EM-telemetry assembly as well as by a gyrorun up to 50 m through the drill pipe and by a surveying module in the logging suit ran through the open hole after demobilization of the rig. The EM telemetry only recorded good surveys during string rotation breaks while adding a new joint. The DM-measurements could have been hampered by a steel shot bed in the bore hole at the location of the sensors. The gyro run through the drill pipe could only reach the top of the drilling assembly and required some operational time. The logging run was continuous but the logging tool had to be pushed through the horizontal open hole with some bore hole irregularities.
Together the tools provided a reliable overview of the two bore hole trajectories. The gyro run confirmed the measurements of the DM in the drilling assembly. The potential presence of the steel shot on the low side of the horizontals apparently did not impact the magnetometer detection of the earth magnetic field.

The survey runs were continuous with depth but the logging tool could not be pushed further than 92 m into the horizontal hole. The runs showed that crossing the quartzite layers at small incidence angle did not have an impact on the directional drilling trend.

The directional data showed three turns that correlate well with the circulation of the steel shot. In the first bore hole two small turns while injecting steel shot were made and one long section without any steel shot injection

To determine the directional tendency of the bottom hole assembly without any steering action a hole length of 28.3m was drilled **without steel shot injection**. The inclination was found to be constant at 87.1 deg and the azimuth constant at 2.5 deg. All surveys every 3m deviated less than 0.2 deg in both azimuth and inclination. Therefore the drilling direction of the assembly straight within a directional change, the so-called dog leg severity (DLS), smaller than **0.3 deg/30m**, and the precision of the measurements better than 0.2 deg.

Directional results with steel shot injection in the first bore hole:

- 0.7 deg up over 3m -> 6.6 deg/30m DLS
- 0.9 deg to the left over 3 m -> 9.0 deg/30m DLS

Directional results with steel shot injection in the second borehole:

- 3.0 deg to the left over 15.3m -> 6.6 deg/30m DLS
- 5.6 deg to the right over 30.5m -> 5.5 deg/30m DLS

In advance, the drilling assembly had been modelled to be angle holding without steering action and to be able to turn with at least 5 deg/30m DLS. Both have been confirmed.

Additional comments: The SIU operation was more stable and continuous while drilling the second bore hole than the first. Also the operational efficiency of the steering sub actuator was limited due to a motor controller board issue during one run and disturbance of the rotor by the sensor cable during two other runs, see the analysis of the computational fluid dynamics modelling below.

Demobilization

The demobilization of the Vermeer 55 rig, drill pipe and Metax high pressure pump was rather straightforward. The SIU, drilling assemblies, the down hole equipment provided by Well Guidance and the HP tubulars of TNO were shipped back to their owners. Also the EM communication tools were shipped back to the rental company in Los Angelos via the Netherlands. As the documents for temporary import (so-called T1-form) had not been arranged upfront the import taxes had to be corrected which was an administrative hassle. Apart from the latter point the demobilization went smooth.

Most importantly, as during the mobilization and the execution of the trial no safety incidents occurred and nobody was injured.

Results of the computational fluid dynamics analysis of the steering sub

Canopus had a detailed analysis of the steering sub executed with Ansys CFD. In short, the results relevant for the pilot were as follows

1. At 500 l/min flow rate the pressure drop over the steering sub was 8 bar over the section up to and including the first concentrator and 3 bar over the second concentrator. The pressure drop over the dual tube section was minimal.
2. The calculated fluid velocity in the internal channel was up to 17 m/sec, whereas the steel shot velocity was measured to be around 11 m/s. These results are in agreement taking into account that the particles travel slower due to, for instance, particle-wall collisions, particle rotation and acceleration time. The velocity is higher than necessary and can be reduced by adjusting the dimension of the channels.
3. The calculated separation of the particles into a high concentration flow and a low concentration flow was very effective: 999 out of 1000 tracked particles travelled through the port for the high-concentration.
4. The fluid through the port for the low concentration downstream the first concentrator was found to be bouncing off on a ridge on the rotor thereby creating a high velocity stream impacting the inner wall of the outer channel – exactly the location where the cable of the sensors was mounted. The movement of the rotor through that high velocity stream must have created

strong pulling and pushing drag force on that cable for every rotation. This likely caused the unexpected wear of the sensor cable at that location and eventually the hampering of the movement of the rotor. Several straightforward design modifications have been identified that should avoid the creation of the high velocity jet stream and/or the interaction of that stream with the rotor.

Impact of the steel shot erosion on rate of penetration (ROP)

The standard practice when starting drilling after adding a new drill pipe joint to the drill string was to first start the circulation to a modest flow rate, then rotate the bit to bottom, and then drill gently at a low weight on bit of about 1 kdaN. And then increase the flow rate to the desired setting. After drilling in this stable mode the steel shot injection was turned on after which it took about 30 sec for the particles to arrive at the bit. The down hole arrival of the steel shot made the pump pressure increase by up to 14%.

At a volumetric concentration of 1% the high density of the steel shot particles of 8 SG make the SG of the drilling fluid (water) go up by 7%. Towards the end of the pilot the injection rate was better controlled at a value of 0.3% giving a pressure increase of 2% or 3 bar at 150 bar pump pressure. Therefore, at injection rates of 0.3% or higher the arrival of the steel shot at the bit could easily be detected by monitoring the pump pressure.

Apart from the pump pressure increase, the arrival was also invariably observed by the driller who found that the ROP had to be increased to keep the weight on bit constant. The ROP impact was large and at one moment informed the control cabin that the bit might have drilled into a cave. This was about 30 sec after the injection unit had briefly lost injection control and briefly released particles into the drilling fluid at its maximum injection rate of about 2% of the flow rate.

The recorded data includes ROP, WOB, string RPM, string torque, Pump pressure, flow rate and injection rate. From this data the combined action of the PDC-bit cutters and the steel shot erosion can be investigated. This is beyond the scope of this report, but the indication of the impact on ROP is the following. At 60RPM, flow rate 500L/min, pump pressure 117 bar, and WOB 1 kdaN, the circulation of 1.0% of steel shot made the ROP increase from 4 m/hr to 15 m/hr. Later, at similar operational settings, the ROP increased from 7,5 m/hr to 20 m/hr at 1.2%. And at 550 L/min, 195 bar, WOB 1 kdaN and 40RPM an increase of 10 to 20 m/hr at 0.7% steel shot concentration. At these settings, the steel shot erosion does easily increase the ROP by more than a factor two. Reliable extrapolation to performance at larger depth and at higher WOB and higher bit pressure drop is, but the pilot does qualitatively confirm the large ROP increase when combine PDC drilling with DSSD.

6. VSH pilot summary

The VSH pilot lasted over 4 working weeks and with 7 to 13 people continuously on site. For all team members at least one major component of the set-up was completely new. The integration of all the hardware into one functional drilling unit required team work, trouble shooting, dealing with unfamiliar risks, and the integration of communication systems and data-acquisition systems. With 5 nationalities in the team, communication was not trivial and effectively the communication was both in German and English. In spite of these challenges, the team made the Directional Steel Shot Drilling system work in an operational setting, verified the steering capability and the ROP improvement, identified various system improvements for the full scale DSSD for 6 inch diameter bore holes and - most importantly – nobody was hurt and there was no damage to the environment.

The Detailed Drilling Plan described the objectives of the pilot in a few categories. The following provides the results and recommendations these categories.

System integration

Setting up the Canopus DSSD system and connecting to the Vermeer 55 horizontal drilling unit of Schenk was done with limited effort and worked, but a few things had to be resolved. These things concerned the following:

- the shaker was found to leak some steel shot which had to be fixed.
- The set-up of the shaker and the steel shot return system required some modifications for good solids handling. The separation of steel shot and cuttings was okay but can be improved: some cuttings ended up in the steel shot catch tank.
- The high pressure pump, SIU, surface high pressure conduits, swivel and drill pipe worked well. There were no indications of wear due to the steel shot handling. Pressure and circulation testing were fine, but it was hard to do the pressure control with the high-pressure pump.
- It was found that the pulsation dampener was important for injection stability, but mounting the dampener and adjusting its pressure setting were harder than expected.
- Running in hole and pulling out of hole of the 25 m long drilling assembly took a full working day. It required team work of 5 people including hoisting and fork lift operation. On site training helped to speed up the operation slightly. Therefor the exchanging bottom hole assemblies was kept to the minimum required.
- The data-acquisition system worked and rig data and pump data could be recorded at 10 samples per second. However, the an improvised solution was required to get the rotary drive position recorded, and the pump pressure data was found to be filtered for frequencies higher than 1 Hz.
- A high-pressure by-pass had to be mounted to reduce the flow rate through the SIU to about 250 L/min. At higher flow rates the injection rate could not be controlled. It is recommended to mount an adjustable by-pass valve and use a stronger magnetic injection rate control valve.
- Despite some overgauge drilling hole cleaning was reasonable at 550 L/min and okay at 600 L/min flow rate. Making up connections was not hampered by steel shot.

The drilling performance

- The control of the hole making was done by the driller who actively tried to keep the pushing force (WOB). In case of a change in, for instance, rock strength or steel shot erosion, the driller would adjust the displacement rate (ROP) to stabilize the pushing force. After some practice this worked well, although procedure includes a human response time to any changes, of course. The change in ROP as a response to the arrival of the steel shot particles at the bit was found to be up to a factor three. A smooth start up and shut down of the steel shot injection does help the driller to follow the changing rate of penetration and keep the mechanical loading of the drill bit constant during steel shot concentration changes.
- From the start of the pilot till the end the ROP was much higher than the expected 10 m/hr. Drilled cuttings and the formation log confirmed the rock was slate with an occasional quartz layer. Slate is much softer than quarzitic limestone and therefore the high rates of penetration that even exceeded 80 m/hr were not surprising.
  For the testing of the DSSD system stable drilling conditions were preferred to be able to test the response of the directional drilling to the steel shot the bit hydraulics and WOB were reduced to get into a range of 10-30 m/hr.

- The telemetry was done by an EM-telemetry device in the BHA. Whenever the strong rotation stopped, the EM-sub measured down hole the drilling directional and communicated the data to the steering sub and to the surface via EM-waves. This all worked fine. However, the team could not get the EM-tool to receive the EM-commands from surface. Consequence was that commands requesting specific parameters or modification of steering sub settings could not be communicated. This was a limitation concerning making directional changes. Also because of the time required to exchange bottom hole assemblies a kick-off operation was not tried.
- The down hole battery consumption of both the EM-tool as well as the steering sub was found to be low. The bottom hole assemblies were found to run at least 4 days on a single battery module. Identified design and control improvements indicate that this good longevity can be improved further.
- The BHA was inspected after each run and down hole memory of both the EM-tool and the steering sub downloaded. The near bit stabilizer looked green apart from some limited wear on the down hole side. The drill bit was repetitively found to have impact damage on the medium radius cutters. During circulation the pressures were higher than calculated. All parts of the assembly and the surface HP-system were inspected for unexpected restrictions and the eventually it was found that the bit nozzles had a simple cylindrical entry channel instead of a smooth or at least conical entry shape which causes a reduced nozzle coefficient and with that the increased pump pressure. Obviously, it is recommended to improve the bit design to mitigate the medium radius cutter impact wear and the nozzle design to improve the nozzle coefficient.
- The bottom hole assembly was designed such that it would have no directional tendency without any steering action. In the case of steering action it was expected to have a directional capability of at least 5 deg per 30 m bore hole length. Both were confirmed: directional stability better than 0.3 deg per 30 m; directional changes between 5 and 10 deg per 30 m.

7. Management summary of the VSH pilot

The VSH pilot lasted over 4 working weeks and with 7 to 13 people continuously on site. For all team members at least one major component of the set-up was completely new. The integration of all the hardware into one functional drilling unit required team work, trouble shooting, dealing with unfamiliar risks, and the integration of communication systems and data-acquisition systems. With 5 nationalities in the team, communication was not trivial and effectively the communication was both in German and English. In spite of these challenges, the team made the Directional Steel Shot Drilling system work in an operational setting, verified the steering capability and the ROP improvement, identified various system improvements for the full scale DSSD for 6 inch diameter bore holes and - most importantly – nobody was hurt.

The below summarizes the results per aspect of the pilot and concludes with recommendations on the follow up of the DEPLOI the HEAT project.

1. Safe operations, no damage
2. Integration DSSD with drilling rig no issues
3. Two horizontals drilled, each 125 m long
4. Up to 3x faster with steel shot through the bit
5. Tangent section straight within 0.3deg/30m
6. Four turns 5-9deg/30m while circulating steel shot, consistent with stiffness of the drilling assembly
7. Hole cleaning okay at 600 L/min. Risk of wash-outs at connections or while reciprocating.
8. Normal flow rate. Pressure could be reduced to 150-200 bar range
9. Stable injection of SIU requires pulsation dampener and a by-pass
10. The DSSD works at a steel shot concentration of 0.5%, which is the injection capacity of the existing SIU for 6 inch drilling. In hard rock or at large depth, a higher concentration would be attractive for increasing the rate of penetration and increase bit longevity
11. Concerning the steering sub: The actuator, sensors, down hole communication, and control unit worked as desired. The steering sub created concentration pulses and the solids handling was as expected. To prevent wear of the sensor cable: Modify the mount of this cable.
12. The power consumption of the steering sub was as low as expected. An assembly can run for at least 100 hrs on a single standard down hole battery module.

Recommendations

1. Upgrade SIU with a regulated by-pass
2. Upgrade the automatic control of the SIU with automating the steel shot return system
3. Increase the strength of the magnetic regulator for the injection rate and make it fail-close
4. Modify the bit design for 6 inch bore holes to provide more support of steel shot erosion to the medium radius cutters and/or place more cutters at that radius
5. Modify the mount of the sensor cable in the new steering sub for 6 inch drilling
6. Modify the actuator control for reducing power consumption and to make the steel shot concentration variation smoother.
7. Test the rate of penetration as a function of hydraulic hole bottom pressure in limestone and sandstone
8. Test the control of directional washing out of the bore hole in the drill test facility of TNO
9. Upgrade the pulsed concentration control for a more balanced steel shot erosion while rotating
10. Reduce the flow rate in the fast channel thereby shortening the steering sub
11. Implement telemetry into the steering sub while adding pressure sampling >10/sec for uplinking
12. Test DSSD on a small vertical drilling rig in hard rock at 100-1000 m vertical depth. If possible build to at least 20 deg inclination and test open hole side tracking.